# REGULATION OF CRANIOFACIAL BONE HEALING USING NOGGIN

by

Gregory M. Cooper

B.S., B.A., University of Pittsburgh, 1997

Submitted to the Graduate Faculty of

School of Engineering in partial fulfillment

of the requirements for the degree of

Doctor of Philosophy

University of Pittsburgh

2006

UNIVERSITY OF PITTSBURGH

SCHOOL OF ENGINEERING

This dissertation was presented

by

Gregory M. Cooper

It was defended on

December 1, 2006

and approved by

Mark P. Mooney, Ph.D., Professor, Departments of Oral Medicine and Pathology,

Anthropology, Orthodontics, and Surgery

Kacey G. Marra, Ph.D., Assistant Professor, Departments of Surgery and Bioengineering

Partha Roy, Ph.D., Assistant Professor, Department of Bioengineering

Dissertation Director: Johnny Huard, Ph.D., Professor, Departments of Orthopaedic Surgery,

Molecular Genetics and Biochemistry, and Bioengineering

**REGULATION OF CRANIOFACIAL BONE HEALING USING NOGGIN**

Gregory M. Cooper, PhD

University of Pittsburgh, 2006

In cases of craniosynostosis, defined as the premature fusion of the cranial sutures, there is a need to inhibit bone formation in small calvarial defects to avoid the occurrence of postoperative resynostosis. Similarly, reconstruction of bone in the craniofacial skeleton following injury or tumor resection necessitates controlled bone regeneration to avoid bone overgrowth. Bone morphogenetic proteins (BMPs) are potent bone inducing growth factors that are expressed during normal bone healing. Noggin is an extracellular antagonist to BMPs. This work studied the use of Noggin to prevent postoperative resynostosis in a rabbit model of human nonsyndromic craniosynostosis via protein therapy. A mouse model of a healing suturectomy was also developed. This model was used to study the effects of Noggin ex vivo gene therapy on the inhibition of postoperative resynostosis. Finally, the ability of Noggin to inhibit bone overgrowth and improve BMP4-induced bone formation was tested. The work presented here demonstrates that a single dose of Noggin protein is capable of inhibiting resynostosis and improving craniofacial growth after surgery to correct craniosynostosis in rabbits. Noggin delivered through ex vivo gene therapy was able to inhibit bone formation in a novel mouse model. Also, the implantation of Noggin expressing cells along with BMP4 expressing cells reduced ectopic bone formation and improved bone density. These results suggest that Noggin therapy may be useful for the inhibition of postoperative resynostosis in children with craniosynostosis. Furthermore, by recreating naturally occurring expression patterns (for example, both Noggin and BMP4), we may be able to control the size, shape and quality of bone formed by biologically-driven therapies.

## TABLE OF CONTENTS

## LIST OF TABLES

## LIST OF FIGURES

# PREFACE

I would first and foremost like to thank Dr. Johnny Huard for being my mentor and dissertation director. He supported me through both failure and success. He was able to teach me many things about experimental design, getting "the point" across, and grant writing. For these things, I will be forever grateful.

I would also like to thank Drs. Mark Mooney, Kacey Marra, and Partha Roy for their advice and support as members of my dissertation committee. They represent diverse academic fields and have helped be gain a better understanding and appreciation of the complexity of tissue engineering. Thank you also to the Department of Bioengineering that afforded me this opportunity.

I would especially like to thank Dr. Mark Mooney. He hired me as a technician and fostered my initial development into a researcher. I offer my deepest thanks to him for always treating me like a colleague and a friend.

I would like to thank Dr. Joseph Losee for his faith in my abilities and his faith in our shared vision of the future.

Dr. Huard's Stem Cell Research Center has been a pleasure to work in. I cannot thank every member of this team whom I have conversed with, developed studies with, and collaborated with. However, each conversation and situation has been appreciated. I would like to thank Arvydas Usas for all of his assistance with the long hours of animal surgery and data

collection. Also, Anne Olshanski's work on creating the retroviral vectors that were used in these experiments is greatly appreciated.

This work was financially supported in part by a grant to Johnny Huard from the NIH (2 R01 DE 013420-06), by the William F. and Jean W. Donaldson Chair at Children's Hospital of Pittsburgh, and by the Henry J. Mankin Endowed Chair for Orthopaedic Research at the University of Pittsburgh.

Most importantly, I would like to thank my family. My parents, Mel and Judy, have always supported me and there is no way to describe how much they have given me. My sister, Nicole, was always able to give me the advice that only a sister could give. I would like to thank Ann and Steve for their support of me and my family.

To my wife, Christina, for whom this work is dedicated. You are my guide, my companion, and my love. Without you, none of this would have been possible.

And finally, to my beautiful daughter, Adaline. I hope that someday you may know the happiness that you have brought to me.

# 1.0 INTRODUCTION

## 1.1 CLINICAL STUDIES OF CRANIOSYNOSTOSIS

### 1.1.1 Occurrence of Craniosynostosis

Craniosynostosis (CS) is a pathological condition defined as the premature fusion of the sutures of the skull—i.e., fusion happens before cessation of brain growth which, in 90% of humans, occurs by 6 years of age [1]. CS has been reported in Asian-, African-, and European-derived populations [2], and the birth prevalence of the condition is estimated to be 300–500 cases per 1,000,000 live births [2]. CS involves the overgrowth of bone at the osteogenic fronts of the developing cranial bones. Normally, where osteogenic fronts meet each other, a region of tissue between the fronts remains undifferentiated. This region of non-bony tissue (the suture) allows for prenatal and postnatal brain growth. In CS, bone growth is accelerated (hyperostotic) at the osteogenic fronts, and the region between the fronts differentiates into bone and obliterates the suture, leading to a bone-filled joint between osteogenic fronts (synostosis). Sagittal suture synostosis is the most common type (approximately 55% of total cases), followed by coronal suture synostosis (approximately 24%), multiple suture synostosis (approximately 10%), metopic suture synostosis (approximately 7%), and lambdoidal suture synostosis (approximately 4%) [2]. Approximately 72% of sagittal cases are sporadic, with a male preponderance of 3.5:1. No paternal or maternal age effects have been reported. The 6% of cases that are familial usually are

inherited as an autosomal dominant condition with 38% penetrance. Sporadic coronal cases account for approximately 61% of all cases, with a female preponderance of 2:1 and an advanced paternal age effect. More coronal synostosis cases than sagittal synostosis cases are familial. Ten to 14% of nonsyndromic coronal cases are inherited as an autosomal dominant condition with 60% penetrance. Most autosomal dominant CS syndromes involve the coronal suture. When CS is a symptom of a syndrome, it usually is associated with facial, limb, ear, or heart malformations (**Figure 1**) [2, 3].


**Figure 1: Photographs of Patients with Craniosynostosis.**

**A**) Crouzon Syndrome. **B**) Apert Syndrome. **C**) Pfeiffer Syndrome. **D**) Jackson-Weiss Syndrome. Notice that the child with Apert Syndrome (**B**) has a fusion of the coronal suture, causing the skull to grow shorter, but also taller and wider. From Jabs et al., 2002 [3].

### 1.1.2 Management of Craniosynostosis

Premature suture fusion leads to secondary deformities in the cranial vault, cranial base, and midface [4-14]. Such skeletal deformities often result in significantly elevated intracranial

pressure [15-22], altered intracranial volume [20, 23-25], and dilation of the subarachnoid spaces [26], events that may result in optic nerve compression, papilledema, and, if left uncorrected, optic atrophy, blindness [27], cognitive disabilities, and mental retardation [16, 20, 27-30]. Such severe craniofacial growth, ocular, and neural abnormalities pose extensive, costly, and (often) recurrent clinical and surgical management problems [4, 28, 31-37].

The goals of current therapy for and surgical management of CS include the following: 1) to provide adequate intracranial volume for normal brain growth and development, 2) to re-establish normal intracranial fluid pressure dynamics, and 3) to correct the progressive cosmetic skeletal deformity [2-4, 28, 31-44]. The timing and sequence of these procedures vary according to the number of affected sutures, the severity of the secondary deformities, and the functional and psychological needs of the patient. Surgical management typically comprises the following actions: 1) surgical release of the synostosed suture, cranial vault decompression, and upper orbital reshaping and advancement (during infancy at approximately 3–12 months of age); 2) surgical correction of midfacial deformities (during childhood at approximately 4–12 years of age); and 3) orthognathic surgery to correct jaw discrepancies (during adolescence at approximately 14–18 years of age) [2-4, 28, 31-33, 38, 41-44].

### 1.1.3 Postoperative Resynostosis

Although these techniques have enabled clinicians to achieve the goals stated above, the suturectomy site frequently reossifies very rapidly (in 30%–100% of reported cases and, in some cases, as early as 6 months after surgery) [28, 38, 44-52], particularly in cases involving the use of simple suturectomies or linear craniectomies [38, 52]. Pancraniosynostosis (fusion of all of the cranial sutures) has even been reported after surgical correction of single suture synostosis [53].

This rapid resynostosis can increase intracranial pressure, further restrict the growing brain and cranial base, and alter craniofacial growth [4, 5, 54]. To overcome such reossification problems, researchers and clinicians have devised and used a number of clinical strategies [28, 34, 35, 37, 55]. Initial attempts at preventing previously released stenosed sutures from reclosing involved wrapping the intact bony margins with a barrier. However, new bone rapidly overgrew the barrier and reossified the suturectomy site, necessitating the performance of additional invasive surgeries [56]. New suture formation was never observed by clinicians using this method. Alternatively, other clinical investigators have used techniques designed to chemically damage the dura and reduce its osteogenic potential [55, 57, 58]. The frequency of resynostosis decreased with the use of these techniques, but seizures and neurological problems typically resulted, probably due to the toxic effects of the chemical adjuvants used in the technique [28, 55]. Yet another approach involves extensive surgical intervention and radical repositioning of the calvarial bones, performed in part to keep the margins of the craniectomy sites from physically reapproximating and resynostosing [4, 28, 31-33, 35, 38, 41-44, 55, 59]. Although sutural reossification is less of a problem with the aforementioned techniques, the rates for other complications resulting from these high-risk procedures range from approximately 15%–25% and include osseous relapse and instability, severe intraoperative blood loss, convulsions, infections, conjunctival chemosis/facial swelling, and soft tissue necrosis [28, 32, 44, 49, 51, 55, 60, 61]. Major complications can require additional surgical procedures to correct (with reoperation rates ranging from 6%–27%) [60, 61], which in turn increase patient morbidity and mortality.

These findings suggest that much more research is necessary to improve the clinical and surgical management and the eventual quality of life for infants born with craniosynostotic

defects. The importance of developing biologically-based therapies that could be combined with earlier and less radical surgical interventions is evident. This approach must prevent postsurgical resynostosis, re-establish the normal intracranial fluid pressure dynamics, improve craniofacial and neurocapsular growth, and obviate the need for multiple surgeries for neonates with various synostotic conditions.

## 1.2 GROWTH FACTOR REGULATION OF BONE AND SUTURE MORPHOGENESIS

At the present time, the literature contains only a few abstracts and full-length reports describing the phenotypic characteristics of osteoblasts from and protein expression profiles within craniosynostotic calvaria [62-71]. This paucity of information is related, in part, to the scarcity of homogeneic human tissue available for biochemical analysis (because tissue from craniosynostotic and normal control human neonates is difficult to obtain) and, until recently, the lack of a genetic animal model of CS.

Although researchers have proposed numerous theories to account for premature suture closure in craniosynostotic patients, there is sufficient evidence to suggest that abnormal amounts of growth regulatory proteins are at least partially responsible for the osteogenic changes. In normal bone, certain proteins (e.g., transforming growth factor-beta1 [TGF-β1] and insulin-like growth factor 1 [IGF-1]) are known to enhance osteogenesis [69-77], whereas other proteins (e.g., interleukin-1 [IL-1] and tumor necrosis factor-alpha [TNF-α]) exert negative effects by directly inhibiting collagen and bone formation [72, 78, 79]. In addition, IL-1α, IL-1β , IL-6, and TNF-β all stimulate osteoclastic activity, but TGF-β1 inhibits it [72, 80]. In light of the

knowledge that growth factor induction is genetically controlled and that these osteogenic factors play a major role in bone development [72, 76, 81], it is reasonable to suggest that the enhanced osteogenesis noted in craniosynostotic individuals is at least partially attributable to alterations in growth factor production or regulation [38, 39, 63, 72, 81].

### 1.2.1 Transforming Growth Factor Beta

Several recent studies have demonstrated that normal suture maintenance and eventual fusion require soluble, heparin binding, growth factors secreted by the dura mater [62, 82-89]. The TGF-β isoforms constitute one such group of local growth factors that control osteogenic processes in cranial sutures [62, 65, 68, 72, 81-83, 86, 90, 91]. Three closely related TGF-β isoforms are present in mammals: TGF-β1, TGF-β2, and TGF-β3 [65, 72, 92-94]. TGF-βs are potent growth regulatory molecules that influence craniofacial development during early embryonic stages and subsequent stages of mesenchymal cell differentiation. The three isoforms are regulated by latency-associated proteins 1–3 (LAP1–3) and latent TGF-β binding proteins 1–3 (LTBP1–3) [65, 95, 96]. When combined with LAP and LTBP, the growth factors are bound to the bone extracellular matrix (ECM) and are inactive. Plasmin cleaves LTBP from the ECM, and the LAP-TGF-β inactive complex binds to the cell membrane. At this point, TGF-β is released from LAP and becomes active [65, 95, 96]. The activated isoforms are particularly important in suture biology because they mediate the proliferation and differentiation of osteoblastic suture cells and effect fusion in vivo [62, 65, 72, 82, 83, 86, 90, 91].

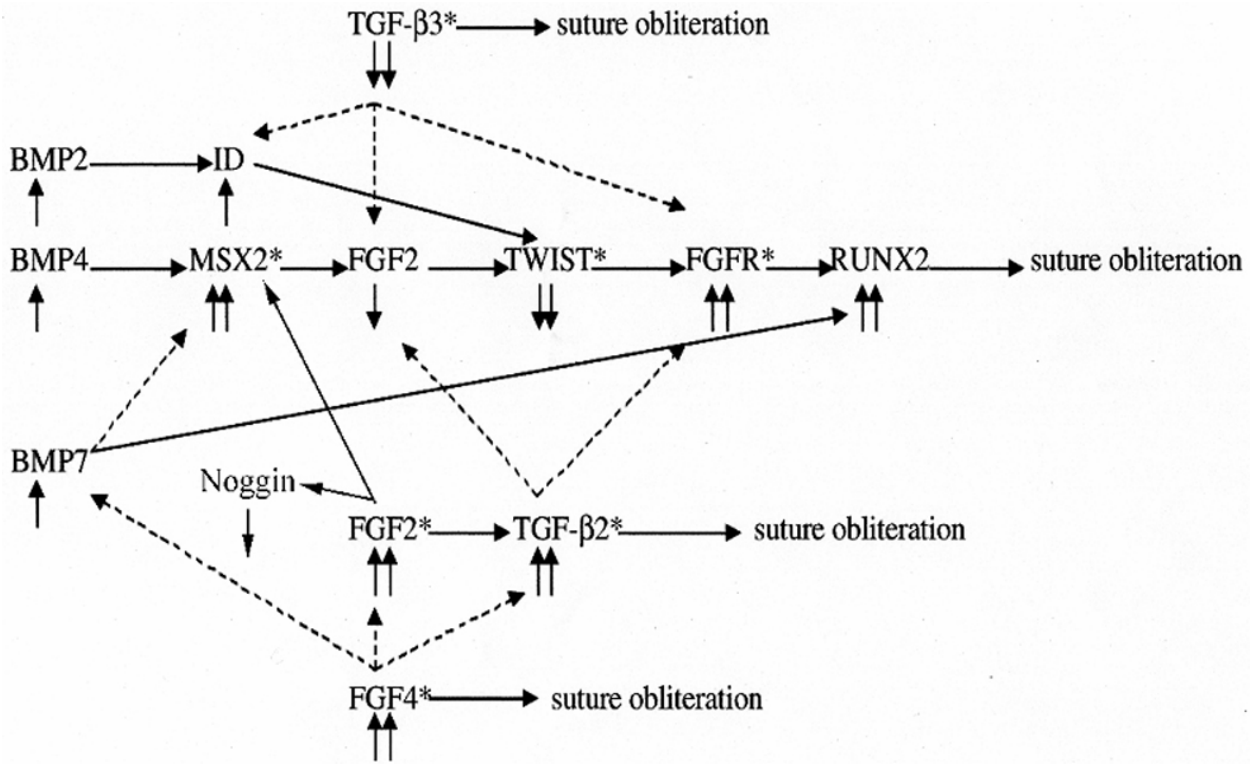


**Figure 2: Diagram showing molecular interactions surrounding suture fusion.**

Modified from Opperman et al., 2002 [81].

Researchers have reported differential distribution gradients of TGF-β1, TGF-β2, and TGF-β3 in developing, patent, and fusing calvarial sutures and the dura mater in rodents and humans [62, 68, 82, 83, 97]. Such distribution gradients may be responsible for the regulation of normal suture morphology and for the various suture alteration zones observed histologically in sutures that fuse prematurely [81, 86, 90, 91, 98, 99]. Coordinated functional regulation of the TGF-β isoforms in these areas may be important because calvarial osteoblasts and sutures in craniosynostotic individuals exhibit accelerated bone formation rather than reduced bone resorption [18, 54, 64, 70, 71, 98-101]. Researchers also have demonstrated differential actions by these isoforms. TGF-β isoform–null mice show distinct craniofacial and somatic phenotypes depending on which isoform is knocked-out [102]. The inhibition of TGF-β2 by using

neutralizing antibodies will prevent suture obliteration, whereas the inactivation of TGF-β3 will induce fusion in sutures that normally remain patent [81, 91, 101, 103-105]. Thus the TGF-β isoforms appear to perform distinct biological functions, and differing distributions of these isoforms may play an important role in premature suture fusion.

### 1.2.2 Fibroblast Growth Factors

Several recent publications have associated certain mutations in FGF receptors with human developmental syndromes associated with prematurely fused sutures [3, 106, 107]. Because FGF-induced mitosis in osteoblasts precedes mineralization [108-110] and TGF-β1 synergistically increases FGF-induced osteoblast mitogenicity [111], TGF-βs in the sutural region likely regulate the expression of FGFs or their receptors (**Figure 2**). Because mutations in FGF receptor 3 cause the most common form of dwarfism, achondroplasia [112], and a mutation in a TGF-β superfamily member causes a phenotypically similar defect in limbs and limb joints [113], a multifactorial system involving the FGFs and members of the TGF-β family may regulate suture development, function, and fusion.

### 1.2.3 Transcription Factors

The expression of FGFs, FGFRs, and TGF-βs also may be regulated by members of the Msx homeobox gene family [107, 114-119]. The human analogs of the *Drosophila* muscle-segment homeobox genes, Msx1 and Msx2 (previously HOX7 and HOX8), are expressed in an overlapping pattern during embryogenesis and organogenesis. Because their temporal and spatial patterns of expression are highly conserved in mammals and birds, they likely play a fundamental role in development. The human Msx2 gene is located in chromosome region 5q34-

q35. After Muller et al. mapped a gene for "Boston type" CS to this region [120], Jabs et al. [115] identified a mutation in the homeobox domain of Msx2 (missense: His→Pro7) in the same disorder. Msx2 overexpression also has been observed in the perisutural tissues of 25-day-old craniosynostotic rabbits when compared with age-matched wild-type rabbits (unpublished data from Dr. MP Mooney). Msx2 is expressed in differentiating cells at the margins of the skull bones. Under the control of local factors, these cells grow at the margins but do not normally fuse until completion of skull growth.

Mutations in Msx2 may cause CS by allowing the premature differentiation of these Msx2-expressing cells [121] and the migration of cranial neural crest cells that form the calvarial bones, the mesenchyme of the sutural spaces, and the dura mater [114, 116, 122]. Recent experimental studies [116, 123] have induced CS by using a transgenic Msx2 mouse model. Researchers conducting these studies have suggested that Msx2 caused CS through a dominant gain-of-function effect, possibly by affecting TGF-β signals emitted from the dura mater, thus permitting the inappropriate growth of the calvarial bones that, in turn, resulted in premature sutural fusion [3, 116, 123]. CS also has been elicited by researchers using a transgenic FGF mouse model with a retroviral vector inserted 6 kb upstream of FGF4 between the tandem of FGF3 and FGF4 genes. Although the effect of the retrovirus on the expression of FGF4, FGF3, or both is not yet fully understood, this is the first craniosynostotic mutation found to involve a ligand in the FGF/FGFR transduction pathway [106]. FGFRs have been shown to coexpress with Msx2 at a variety of sites in the developing mouse embryo [114, 124, 125]. Also, TGF-βs have been shown to modulate Msx2 expression in the oral epithelium and the hindbrain [126, 127]. Consequently, it is possible that TGF-βs, FGFRs, and Msx2 might function together (possibly in the same epistatic pathway) to regulate the temporal sequence of suture development and help

coordinate the growth of the skull and that of the brain (**Figure 2**) [72, 107, 114, 116, 118, 128]. These findings suggest that, although research has elucidated a part of the normal chain of events leading to suture morphogenesis, the complex pathogenic mechanism(s) causing accelerated bone formation and CS remains poorly understood [39, 63].

### 1.2.4 Noggin and Craniosynostosis

Recently Warren et al. [129] have shown that the interaction between FGF receptor activity and CS is mediated by the BMP antagonist Noggin. These investigators used the mouse posterior frontal suture as a model for CS. The mouse posterior frontal suture generally undergoes fusion within the first 45 days of life, whereas all other sutures remain patent throughout the lifetime of the animal. After culturing cells obtained from the dura mater underlying the posterior frontal, coronal, and sagittal sutures, Warren et al. observed that the dural cells from underneath the posterior frontal suture, unlike those from underneath the coronal or sagittal sutures, exhibited reduced expression of Noggin concomitant with FGF-2 protein expression. The investigators were able to delay the fusion of the posterior frontal suture in vivo by using adenoviral transfection to increase Noggin expression. This dissertation attempts to investigate the ability of Noggin to inhibit bone formation in the craniofacial skeleton.

In the developing embryo, Noggin protein is expressed in the Spemann organizer and was initially characterized by its ability to induce dorsal structures in *Xenopus* embryos [130]. Noggin is now known to antagonize the activity of BMP2, BMP4, and BMP7 by binding directly to the proteins and making them inactive [131, 132]. Because Noggin expression is reduced only in the dura mater underlying fusing sutures, researchers have postulated that BMP activity contributes to normal suture fusion. Because Noggin acts by binding to and inactivating BMPs,

Noggin's effect on delaying suture synostosis suggests that the BMP signal may be involved in cranial suture fusion. Rice et al. [133] have demonstrated that the addition of BMP2-soaked agarose beads to the calvarial suture mesenchyme in mice up-regulates the expression of Msx2 in the tissues surrounding the beads. As discussed above, gain-of-function mutations in Msx2 lead to CS [106, 107, 116]. The data from these studies enable us to propose a pattern of protein expression and interaction that may be involved in the fusion of calvarial sutures (**Figure 3**).


**Figure 3: Proposed pathway of protein expression and interaction during suture fusion.**

Recent advances in our understanding of the molecular events that occur during normal suture fusion and craniosynostosis [30, 81], when combined with novel techniques developed to engineer craniofacial tissues [134-136], may enable us to design therapeutic strategies to enhance the current surgical treatment of craniosynostosis, thereby decreasing the complications inherent in current surgical procedures [38, 54, 81, 83, 101, 106, 129, 137]. A minimally invasive surgery, when assisted by a molecular therapy, may allow for normal brain growth patterns, restore normal intracranial volume and intracranial pressure, and alleviate the need for extensive craniofacial reconstruction.

## 1.3 PROGRESS TOWARD THE IMPROVEMENT OF BONE HEALING

Less than optimal healing after bone damage is a common problem encountered by reconstructive surgeons. Although most bone defects heal well, difficulties such as delayed union or non-union can be devastating. To treat non-unions, clinicians often use autologous bone-

grafting techniques. A recent review reports that approximately 1.5 million bone-grafting operations are performed each year in the United States [138]. Autografting, which uses bone grafts taken from other bones within a patient, is the current gold standard for care. Unfortunately, donor site morbidity [139], the lack of available harvest sites (especially in the pediatric population), and the high risk of suboptimal outcomes have all lowered the appeal of autografts [140]. Consequently, there is intense interest in improving fracture treatment through the use of allografts, defined as bone substitutes obtained from sources other than the patient.

Synthetic materials currently used for bone reconstruction include metal prostheses, calcium phosphate-based ceramics and pastes, methyl methacrylate constructs, and polymers [141-144]. These materials are useful to varying degrees; their overwhelming shortcomings are their inability to integrate with surrounding tissues, their inability to become vascularized, and their inability to remodel. For these reasons, many investigators have begun to study the effectiveness of using tissue engineering techniques (biologically enhanced allografts, cell-based therapies, and gene-based therapies) to treat bone defects.

### 1.3.1 The Use of Biological Factors to Improve Bone Healing

Research results continue to support the important role of biologic factors in fracture healing. Many biologic interventions are designed to either improve osteoconduction or osteoinduction. Osteoconduction is defined as a graft's ability to act as a scaffold for the ingrowth of native bone, which incrementally replaces the graft structure. Osteoinduction is the recruitment of osteoprogenitor cells into an osseous defect by bioactive proteins. Typically, osteoinduction occurs through the osteogenic differentiation of pluripotent stem cells or through the proliferation of already committed pre-osteoblasts. The refinement of currently available

treatment modalities will likely rely on improving clinicians' ability to influence these biologic activities.

No topic in bone healing currently receives more scrutiny than the use of osteoinductive agents such as BMPs. The seminal work in this area is Urist's 1965 demonstration of the ability of demineralized bone to induce ectopic bone formation [145]. Since that time, many of the proteins responsible for bone induction (including BMP2, BMP4, and BMP7) have been characterized, cloned, and made available as recombinant human proteins. Recombinant human BMPs (rhBMPs) can induce bone formation in many animal models [146-157], particularly when allograft substances are delivered along with the BMPs [158-168]. Recombinant BMP use is already challenging the gold standard of autologous bone grafting in terms of the ability of recombinant BMP to improve bone healing in several human trials involving tibial fracture treatment and spinal fusion [169-171]. The widespread use of rhBMP, however, is hampered by the large volume of protein required to induce healing comparable to that attained through the use of autografts.

### 1.3.2 Bone Tissue Engineering

To improve bone healing after surgical interventions, trauma, or congenital insults, many investigators have begun to use gene-based tissue engineering techniques to administer different BMPs [172-180]. Many of the reported studies have involved the direct addition of genetic material to the bone defect site, a process referred to as "in vivo gene therapy". When using in vivo therapies, researchers must choose the transgene that will evoke the desired effect. Ex vivo gene-based therapies involve the addition of genetic material to cells in vitro and the subsequent implantation of the genetically altered cells within the defect. The use of ex vivo gene-based

therapies necessitates selecting the optimal transgene, choosing a cell population to use, and selecting an appropriate scaffold to deliver cells at the site of desired activity. Investigators have used many different cell populations in ex vivo gene-based therapies designed to promote bone healing, including bone marrow stromal cells [181-187], adipose tissue-derived cells [178, 188-194], fibrous tissue-derived cells [195, 196], and skeletal muscle-derived cells [172, 197-205].

## 1.4 SIGNIFICANCE

The scientific understanding of the process of bone healing was greatly advanced by Urist's discovery of the bone forming BMPs [145]. Since then, many researchers have been focused on means to improve bone healing, often by inducing increased bone volume or by reducing the time it takes for bone to form. Although this research has led to some improvements in the treatment of large bone defects, there has been little work to translate this research to a clinically relevant treatment. Furthermore, as in cases of craniosynostosis, there is a need to develop strategies that will inhibit bone formation and avoid rapid reossification of surgical sites. In this series of studies, we tested the general hypothesis that the ability of Noggin to inhibit BMPs could be used to control the formation of bone within craniofacial defects. The work presented here was intended to further the understanding of the regulation of bone formation following injury. A more complete understanding of the molecular pathways that can be manipulated to inhibit bone formation may also offer insight into means of enhancing bone formation.

# 2.0 NOGGIN INHIBITS RESYNOSTOSIS IN CRANIOSYNOSTOTIC RABBITS

## 2.1 INTRODUCTION

Craniosynostosis is the term given to the premature fusion of one or more of the cranial sutures and occurs with an estimated birth prevalence of 300-500 per 1,000,000 live births [2]. Primary craniosynostosis causes secondary deformities in the cranial vault, cranial base, and in the midface [6, 9, 12, 14, 206] that can cause increased intracranial pressure [15-17, 20, 23, 50] and altered intracranial volume [20, 23-25] that can lead to blindness, cognitive deficiencies and mental retardation if left uncorrected [16, 20, 27, 29]. Current surgical management involves the extirpation of the fused suture along with extensive cranial vault reshaping [31, 33, 41, 43, 44].

Although current surgical strategies often allow for normal brain growth and development, re-establish normal intracranial volume and pressure, and correct cosmetic deformities, the suturectomy site frequently reossifies very rapidly after surgery (in 30%-100% of reported cases and as early as 6 months after surgery). Reossification of the suturectomy site leads to the reapproximation of the osteotomy margins and the refusion of the extirpated suture, termed “resynostosis” [28, 38, 44, 45, 47, 48, 52]. Such resynostosis can lead to a secondary increase in intracranial pressure and further restrict craniofacial growth [4, 5, 54], necessitating additional surgical procedures [61] and increasing the risk of patient morbidity and mortality.

The molecular mechanisms underlying resynostosis are poorly understood, though we believe that, through an understanding of normal bone healing events, we may be able to

successfully inhibit resynostosis following surgical correction of craniosynostosis. The healing of bone fractures and surgically created defects has been rigorously investigated. Several bone morphogenetic proteins (BMPs) have been extensively studied for their ability to induce bone formation, including BMP2, BMP4 and BMP7 [138, 160, 169, 207]. More importantly, BMPs have been shown to be expressed during normal bone healing, suggesting their involvement in the healing process [208, 209].

Since BMPs seem to be involved in normal bone healing events, the inhibition of BMP signaling may lead to the inhibition of bone formation. Noggin has been identified as an extracellular antagonist to BMPs [131, 132] and has been shown to be expressed along with BMP4 during normal bone healing [210]. Furthermore, Noggin has been shown to inhibit ectopic bone formation when delivered either systemically [211] or locally [212], and has been used to inhibit membranous bone healing [213].

In an attempt to develop an adjunct to standard surgical techniques that improves postoperative outcomes, we hypothesized that local application of Noggin to the suturectomy site would inhibit resynostosis in a well-described rabbit model of human, nonsyndromic coronal suture synostosis [9-11, 18, 22, 24, 54, 100, 214].

## 2.2 HYPOTHESIS

It was hypothesized that Noggin protein treatment would inhibit postoperative resynostosis and improve postoperative outcomes in a rabbit model of human nonsyndromic craniosynostosis.

## 2.3 MATERIALS AND METHODS

### 2.3.1 Sample

Thirty-one New Zealand White rabbits with bilateral coronal suture synostosis (**Figure 4A**) were obtained from an ongoing breeding colony of craniosynostotic rabbits housed at the University of Pittsburgh [9, 215, 216].

The rabbits were randomly assigned to three groups as follows: Group 1) Suturectomy with no treatment, which served as the surgical control group (n=13); Group 2) Suturectomy with non-specific, bovine serum albumin (BSA) in a slow release collagen vehicle, which served as the protein control group (n=8); and Group 3) Suturectomy with Noggin protein in a slow release collagen vehicle, which served as the treatment group (n=10). This protocol was approved by the Institutional Animal Care and Use Committee at the University of Pittsburgh.

### 2.3.2 Surgical Technique

Following diagnosis of bilateral coronal suture synostosis, the synostosed coronal sutures were extirpated in 10 day old rabbits using a strip suturectomy procedure described previously [54, 101]. All rabbits were anesthetized with an intramuscular injection (0.59ml/kg rabbit body weight) of a solution containing 91% Ketaset (ketamine hydrochloride, 100mg/ml) and 9% Rompun (xylazine, 20mg/ml). The scalps were then shaved, depilated, and prepared for surgery. The calvaria were exposed by a midline scalp incision, and the skin was reflected laterally to the supraorbital borders. Each synostosed coronal suture was identified and a cutting burr was used to extirpate a 3mm–wide strip of frontal and parietal bones, including the entire length and width

of the coronal suture, in one piece (approximately, 3x15mm defects). Care was taken to preserve the meningeal (fibrous) layer of the dura and the regional vascularity.

In rabbits in the suturectomy control group, only the suturectomy was performed; nothing was injected. The periosteal and skin incisions were closed with 4-0 vicryl suture. In rabbits in the vehicle/protein control group, a 26G needle was used to inject collagen (0.1ml/suture) that was mixed with BSA (Sigma) into the suturectomy site (10µg BSA per defect) (**Figure 4B, C**).

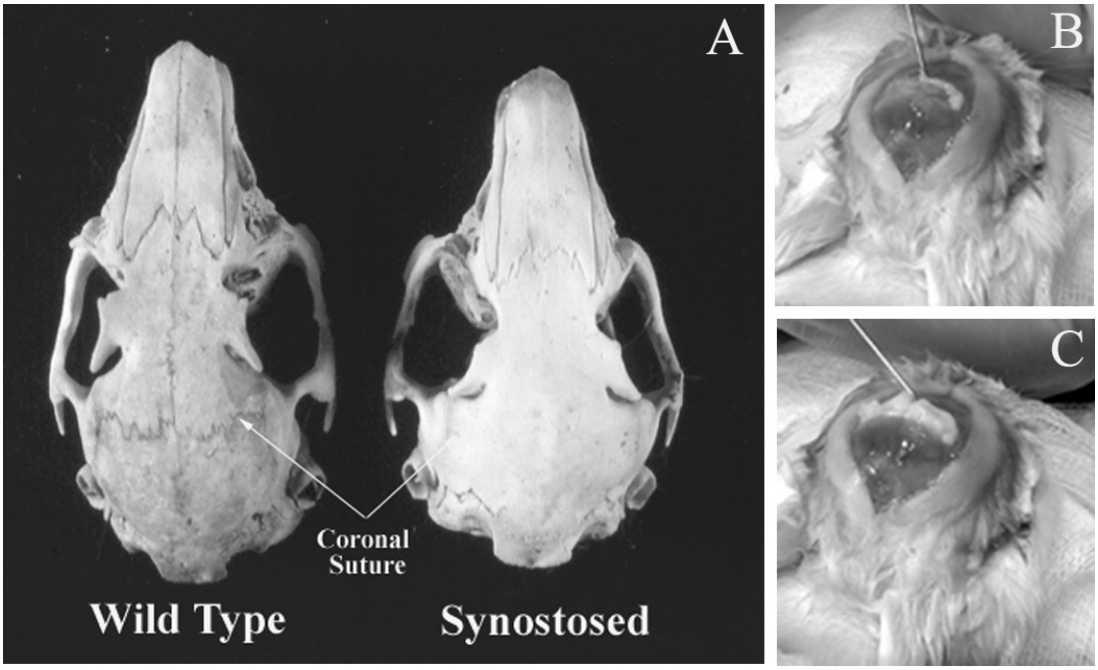


**Figure 4: Animal model of craniosynostosis and surgical intervention**

**A**) Photograph showing the skulls of a normal, wild type rabbit (right) compared to a rabbit with complete bilateral coronal suture synostosis. Both skulls were from 84 day old rabbits. Note the lack of a coronal suture in the synostosed rabbit (arrow). **B**) Intraoperative photograph showing the defect resultant from the suturectomy and the initial placement of the collagen gel. **C**) Intraoperative photograph showing the final placement of the injectable collagen gel that was either mixed with BSA or Noggin. Note: the injectable nature of the gel allowed for precise placement of the treatment within the defect site.

The third group of defects was injected with collagen mixed with Noggin protein (Sigma) for a final concentration of 10µg/defect. Next, a fine dental burr (0.5mm) was used to make holes

in the periosteum and bone for radiopaque amalgam markers. The holes were placed in quadrants, 2mm anterior and posterior to the coronal, frontonasal, and lambdoidal sutures and 2mm lateral to the sagittal and interfrontal sutures. These holes were packed with silver dental amalgam to serve as radiopaque markers for the radiographic analysis of postoperative craniofacial growth. All animals received postoperative intramuscular injections (2.5mg/kg of rabbit body weight) of Baytril (Bayer Corp., Shawnee Mission, KS).

### 2.3.3 Data Collection

#### 2.3.3.1 Somatic and skeletal growth

Longitudinal somatic (body weight), skeletal (third right metacarpal length from radiographs), and cephalometric growth data was recorded for all rabbits at 10, 25, 42, and 84 days of age. At 84 days of age, approximately 90% of calvarial [5, 6, 9, 217, 218] and 90% of brain growth [214, 219] are completed in rabbits. Lateral and dorsoventral radiographs of the head and front right paw were taken with the rabbits tranquilized with an IM injection (10 mg/kg) of Ketaset (Ketamine hydrochloride, 100 mg/ml). The heads were immobilized in a specially designed cephalostat and a Phillips Oralix 70 dental x-ray unit was used at an exposure of 50kV, 7mA, a .17 to .50 second exposure time, and a tube-to-cassette distance held constant at 152 cm. Lateral and dorsoventral radiographs of the head were viewed on a light box, and the amalgam markers and landmarks under study were identified and traced. Craniofacial growth in a number of dimensions was assessed, including: amalgam marker separation at the coronal suturectomy site; craniofacial length; and cranial vault shape. All measurements were taken blind as to rabbit group identity and intra-observer, repeated measurement reliability was calculated ($r=0.901;p<0.01$) on a randomly drawn sample (10%) of rabbit cephalographs.

#### 2.3.3.2 Suturectomy site healing and intracranial volume

Serial computed tomographic (CT) scans of the rabbit heads were obtained at 10, 25, 42, and 84 days of age. A GE HiSpeed Advantage Scanner (DFOV = 24.0-18.0cm; mA = 120–150; kV = 120) was used at a thickness of 1mm to scan heads in the sagittal plane. The boundaries of the suturectomy sites were automatically traced, the healing defect site reconstructed in three dimensions, and the defect areas calculated. The endocortical boundaries of the cranial vault cavities were also traced both automatically and manually and reconstructed in three dimensions. Finally, the indirect intracranial volume (ICV) of each animal at each time point was calculated. All calculations were performed with Allegro Software (ISG Technologies, Atlanta, GA) on a Sun Workstation. All measurements were taken blind as to rabbit group identity and intra-observer, repeated measurement reliability was calculated ($r=0.936;p<0.01$) on a randomly drawn sample (20%) of the rabbit 3D-CT scans.

### 2.3.4 Statistical Analysis

Means and standard deviations for suturectomy site areas, ICVs, body weights, third metacarpal lengths, and the craniofacial measurements were calculated and compared among groups using a 3 x 4 (group by age) two-way analysis of variance (ANOVA) with an unweighted means analysis. Significant intergroup differences at each age were assessed using the Least Significant Differences multiple comparison test. The relationship between defect area and ICV at different ages was also assessed using Pearson product moment correlations. All data were analyzed using SPSS 12.0 for windows (SPSS, Inc., Chicago, IL). Differences were considered significant if $p < 0.05$.

### 2.3.5 Histological Analysis

At 84 days of age, all rabbits were euthanized by intravenous injection of pentobarbital (300mg/kg rabbit body weight), and the defects harvested for histological examination. The specimens were fixed, demineralized in 10% EDTA, and processed for paraffin sectioning. The specimens were then sectioned in a sagittal plane in the middle of both the right and left coronal sutures at a thickness of 5μm. Sections were stained with hematoxylin and eosin for qualitative histological description.

## 2.4 RESULTS

### 2.4.1 Somatic Growth

Mean body weight in all three groups changed in a linear fashion across age (**Figure 5A**). Significant group ($F=5.83;p<0.01$) and age ($F=586.54;p<0.001$) main effects were noted. No significant group x age interaction effects ($F=1.20$;NS) were seen. Multiple comparison tests revealed that BSA treated rabbits were significantly ($p<0.05$) heavier than the other two groups at 42 days of age (**Figure 5A**). Mean metacarpal length increased in a curvilinear fashion in all three groups (**Figure 5B**). A significant age main effect ($F=161.42;p<0.001$) was noted. No significant group ($F=1.83$;NS) or group x age interaction effects ($F=0.61$;NS) were seen.

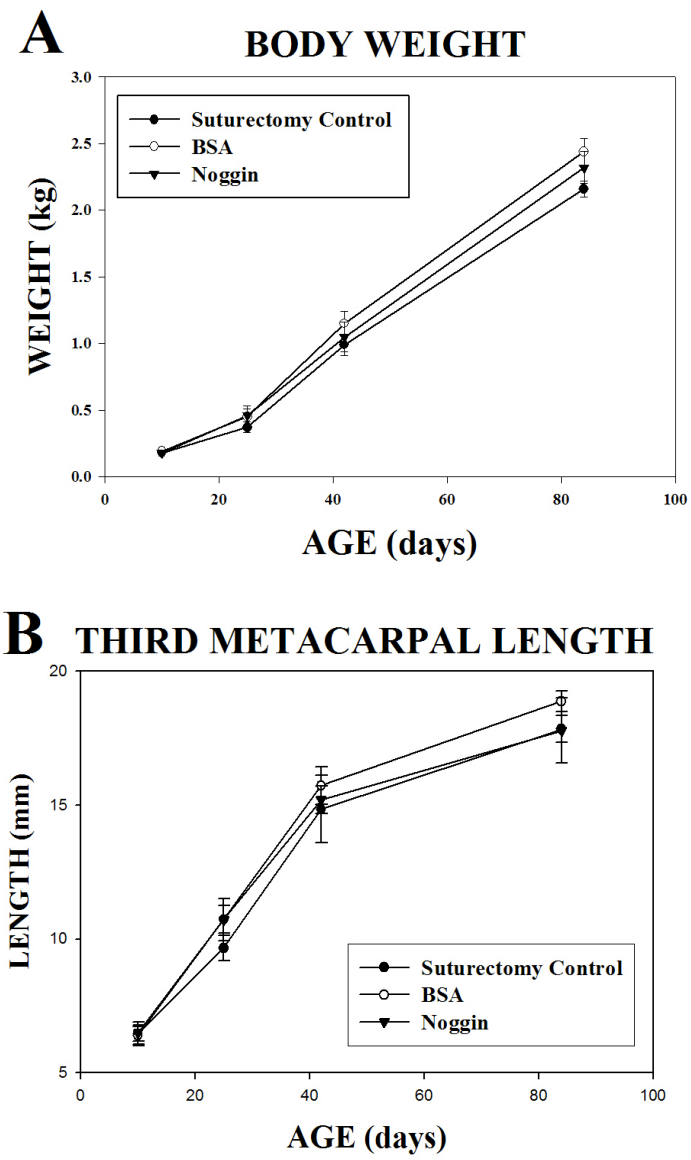


**Figure 5: Somatic growth results**

**A**) Graph showing the changes in body weight over time (±SEM). Note: there were no significant differences in body weight. **B**) Graph showing third metacarpal length over time (±SEM). No significant differences were found between groups.

### 2.4.2 Cephalometric Analysis

Lateral cephalographs at 84 days of age show still patent suturectomy sites, widened coronal suture amalgam markers, and slightly altered craniofacial skeletons in Noggin treated rabbits compared to the two other groups (**Figure 6**).

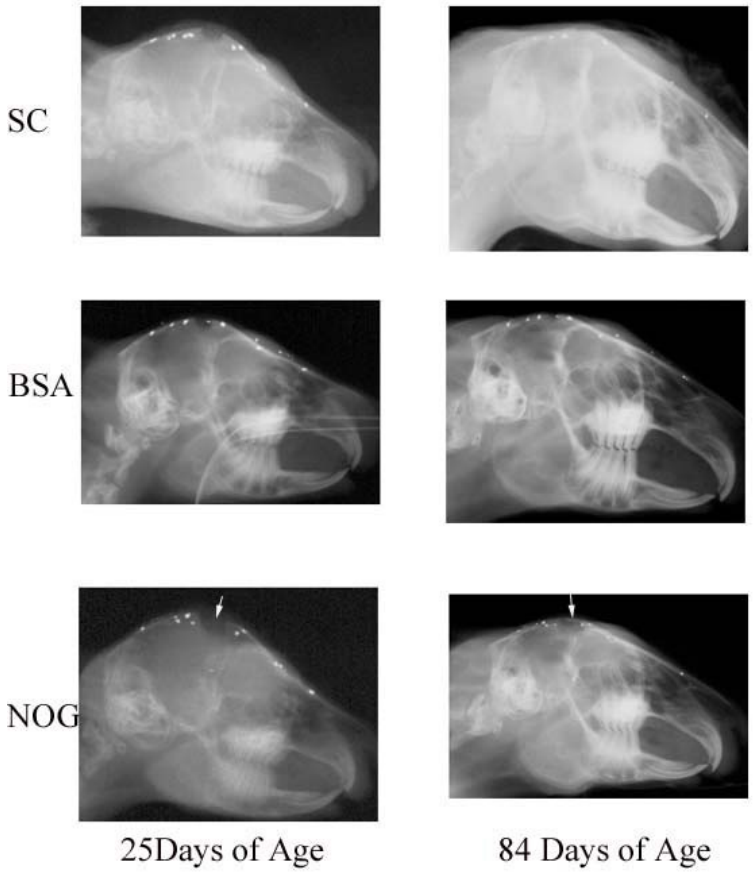


**Figure 6: Lateral cephalographs of select rabbits**

Lateral cephalographs were used to measure the separation of radioopaque markers placed in the calvaria at the time of suturectomy (10 days of age). Note that the Noggin treated (NOG) rabbits showed large areas of radiolucent defects even at 84 days of age (arrows) compared to suturectomy control (SC) and BSA-treated (BSA) animals.

Analysis of mean coronal suture marker separation revealed that Noggin treated rabbits had greater marker distances at all postoperative intervals compared to both control groups (**Figure 7A**). Statistical analysis revealed significant group ($F=7.00;p<0.001$) and age ($F=23.38;p<0.001$) main effects. No significant group x age interaction effect was noted ($F=0.98$;NS). Multiple comparison tests revealed that coronal suture marker separation in Noggin treated rabbits was significantly ($p<0.05$) greater than suturectomy controls or BSA treated control rabbits at all three postoperative ages (**Figure 7A**). No significant difference in mean marker separation was noted between suturectomy controls or BSA treated rabbits at any age. Mean craniofacial length in all three groups changed in a curvilinear fashion across age (**Figure 7B**). Significant group ($F=2.39;p<0.05$) and age ($F=369.73;p<0.001$) main effects were noted. No significant group x age interaction effect ($F=0.81$;NS) was seen. Multiple comparison tests revealed that Noggin treated rabbits had significantly ($p<0.05$) greater craniofacial lengths than suturectomy controls or BSA treated rabbits only at 84 days of age (**Figure 7B**). Mean cranial vault shape indices decreased in a curvilinear fashion in all three groups over time (**Figure 7C**). Noggin treated rabbits showed greater indices than the other two groups at all three postoperative times. However, only a significant age main effect ($F=23.72;p<0.001$) was noted. No significant group ($F=0.59$;NS) or group by age interaction effects ($F=0.70$;NS) were seen.

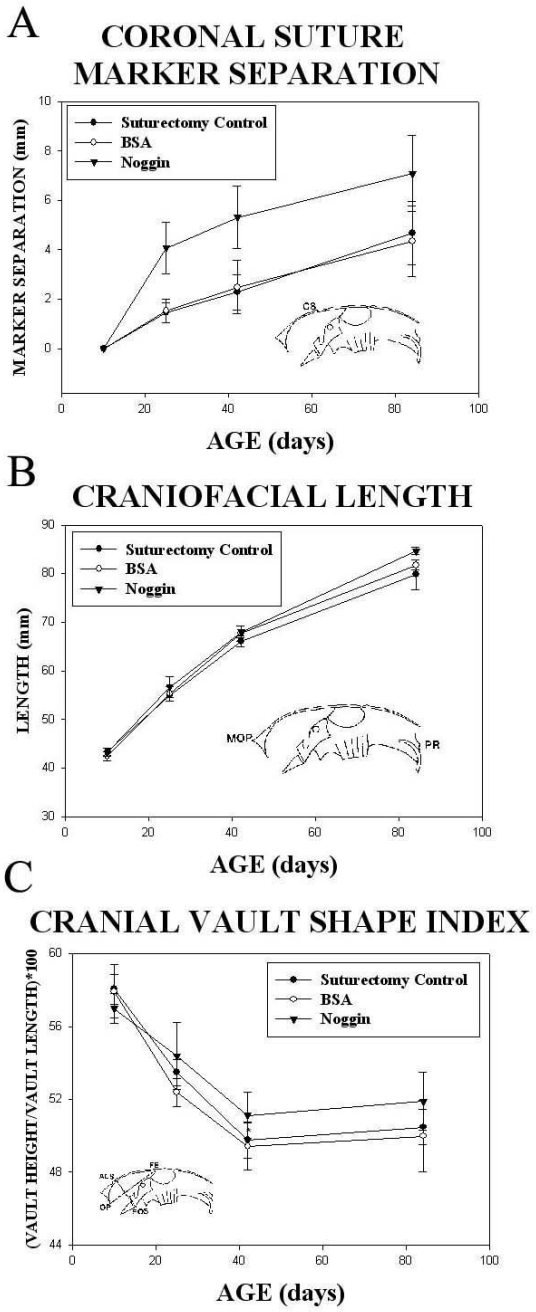


**Figure 7: Cephalometric data**

**A**) Coronal suture marker separation (±SEM) shows that Noggin treated defects allowed for significantly increased marker separation compared to suturectomy and BSA treated defects. **B**) Mean craniofacial length (±SEM) was increased in Noggin treated animals at 84 days of age compared to suturectomy and BSA treated controls. **C**) Cranial vault shape indices (±SEM) were found to be greater in Noggin treated animals. Analysis revealed that the differences were not significant.

### 2.4.3 Computed Tomographic Analysis

Suturectomy sites in both suturectomy control rabbits and rabbits treated with BSA showed rapid reossification through 84 days of age, as seen on the 3D-CT scan reconstructions (**Figure 8A**). In contrast, suturectomy sites in rabbits treated with Noggin increased in size at 25 days of age and were more patent at 84 days age (**Figure 8A**). Mean suturectomy site area in both suturectomy control rabbits and rabbits treated with BSA showed similar reossification rates which decreased to approximately 30% of the original defect area by 84 days of age (**Figure 8B**). In contrast, mean suturectomy site areas in rabbits treated with Noggin increased to approximately 120% of original defect size at 25 days of age and had approximately 60% of the original defect area remaining at 84 days of age (**Figure 8B**). It is interesting to note that suturectomy site areas in Noggin treated rabbits paralleled the two other control groups from 25 to 84 days of age (**Figure 8B**). Statistical analysis revealed significant group ($F=23.29;p<0.001$) and age ($F=31.75;p<0.001$) main effects. No significant group x age interaction effect was noted ($F=0.19;NS$), showing that defect area was changing in a parallel fashion among groups over time between 25 and 84 days of age. Multiple comparison tests revealed that Noggin treated defects were significantly ($p<0.05$) larger than suturectomy controls or BSA treated control defects at all time points after surgery (**Figure 8B**). No significant differences in mean defect area were noted between suturectomy controls or BSA treated rabbits at any age.

ICV in all three groups showed similar curvilinear changes from 10 to 84 days of age (**Figure 8C**). Noggin treated rabbits had greater ICVs from 25 to 84 days of age (**Figure 8C**). Statistical analysis revealed significant group ($F=5.15;p<0.01$) and age ($F=180.74;p<0.001$) main effects. No significant group x age interaction effect was noted ($F=1.30;NS$), showing that ICV was changing in a parallel fashion among groups over time. Multiple comparison tests revealed

that ICV in Noggin treated rabbits was significantly ($p<0.05$) greater than suturectomy controls or BSA treated control rabbits only at 84 days of age (**Figure 8C**). No significant differences in mean ICV were noted between suturectomy controls or BSA treated rabbits at any age. The relationship between percent defect area and ICV was assessed within groups at all three postoperative ages. Noggin treated rabbits had positive correlation coefficients at 25 ($r= 0.30$;NS), 42 ($r=0.68$;$p<0.05$), and 84 days of age ($r=0.33$;NS). In contrast, suturectomy controls (25 $r= -0.48$;NS, 42 $r=-0.45$;NS, and 84 days of age $r=-0.33$;NS) and BSA treated rabbits (25 $r= -0.35$;NS, 42 $r=-0.61$;NS, and 84 days of age $r=-0.03$;NS) had negative correlation coefficients at all three postoperative ages.

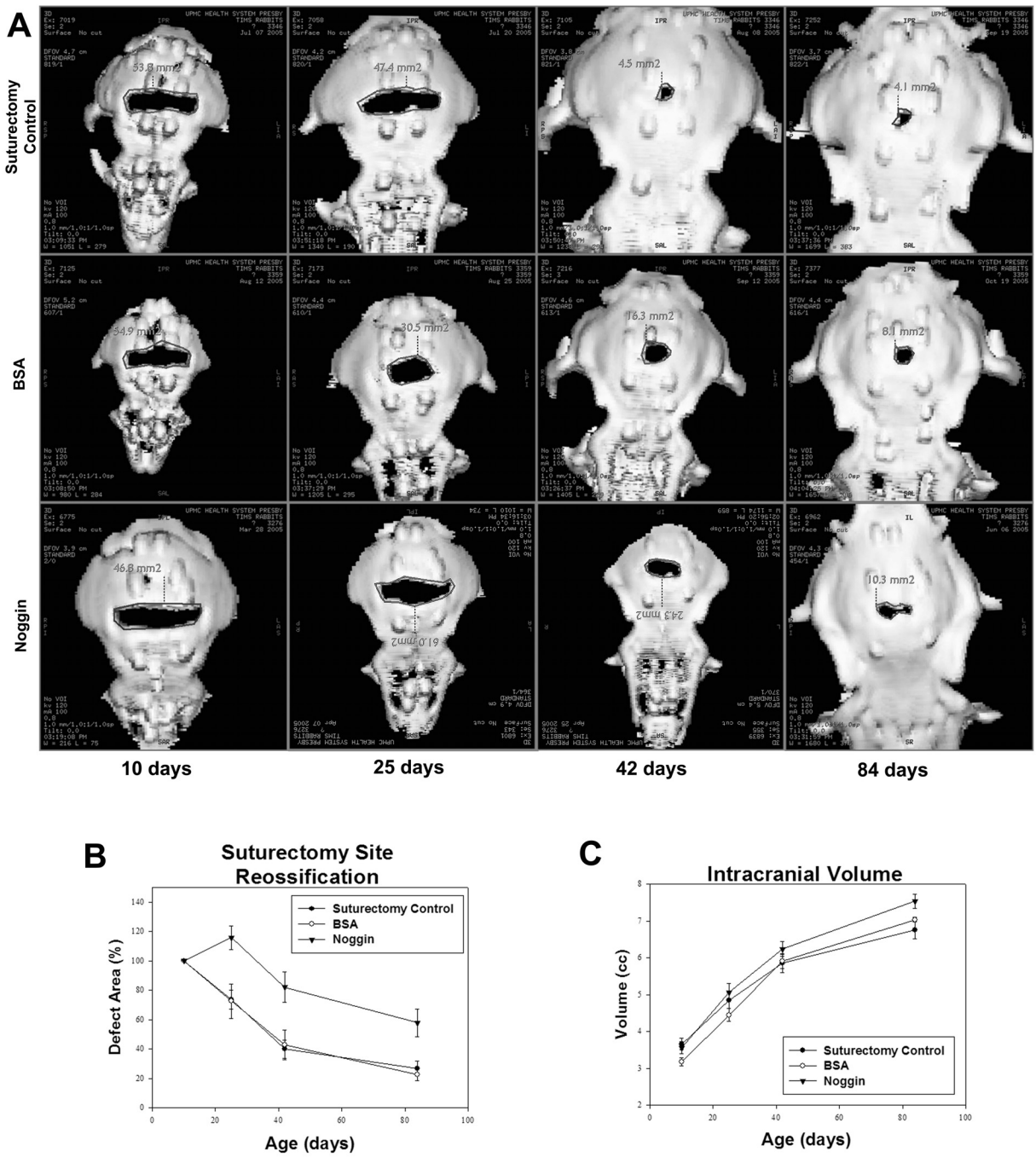


**Figure 8: CT reconstructions and defect healing data**

**A**) 3D reconstructions of serial CT scans performed on suturectomy control, BSA treated, and Noggin treated rabbits at 10, 25, 42, and 84 days of age. Noggin seemed to inhibit healing of suturectomy sites. **B**) Analysis of defect area (±SEM) showed that Noggin treated defects were significantly larger at every time point after surgery (25, 42 and 84 days of age). **C**) 3D analysis of intracranial volume (±SEM) showed that Noggin treatment increased intracranial volume significantly at 84 days of age.

### 2.4.4 Histological Analysis

Qualitative microscopic analysis revealed that, at 84 days of age, the suturectomy control group had nearly complete wound healing, with extensive reossification and resynostosis of the suturectomy sites (**Figure 9, Suturectomy control**). In this control group, most of the original suturectomy sites were completely obliterated (**Figure 9, Suturectomy control**). The BSA treated defects showed incomplete wound healing with some bony bridging. Most sections demonstrated some fibrous tissue within the suturectomy site (**Figure 9, BSA**). The Noggin treated defects showed incomplete wound healing, with large regions of fibrous tissue within the defect (**Figure 9, Noggin**).

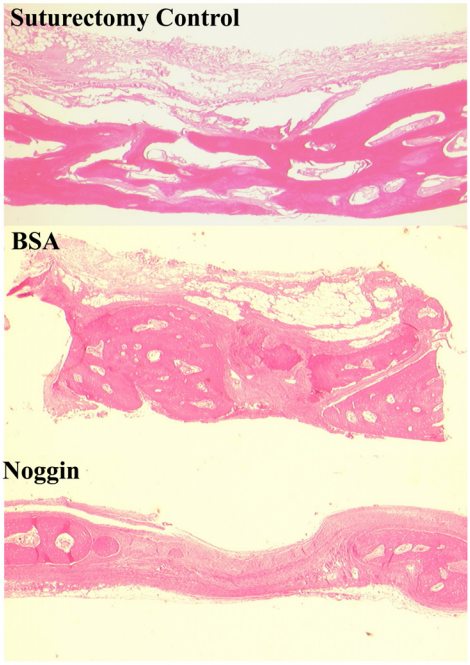


**Figure 9: Histology at 84 days of age**

Histological analysis revealed that suturectomy control and BSA treated defects showed almost complete defect healing at 84 days of age, whereas Noggin treated defects showed large areas of fibrous tissue within the defect at 84 days of age. This qualitative data supports the radiographic data showing larger, unhealed defects in the Noggin treated group compared to the other groups.

## 2.5 DISCUSSION

Craniosynostosis can result from several identified genetic mutations, including *FGFR1*, *FGFR2*, *MSX*, and *TWIST*. For the nonsyndromic craniosynostoses, the genetic and/or epigenetic causes remain largely unknown. Much of the recent research in craniosynostosis has centered on the elucidation of the molecular mechanisms that lead to either normal [82, 87, 97, 220, 221] or premature [62, 68, 98, 222] suture fusion. This line of research has led to a better understanding of the complexity of the molecular interactions that regulate bone formation and suture development and maintenance, though it has not, as yet, been used to develop biologically-based therapies to reduce the occurrence of postoperative resynostosis or to improve surgical outcomes.

One correlate that is common to all types of craniosynostoses, regardless of genetic or environmental cause, is an overgrowth of bone. Normal sutures remain patent, or devoid of bony bridging, to allow for the growth of the developing brain. The fusion of sutures occurs by the ossification of the normally patent suture through the process of osteogenic differentiation. We believe that the regulation of bone overgrowth should be the target of any therapy developed to improve treatment of craniosynostosis if a single therapy is to be useful to all patients presenting with craniosynostosis. Because BMP2, -4, and -7 have been found to be potent bone-inducing proteins that are expressed during normal bone healing [209], we hypothesized that BMP function may be instrumental in the occurrence of resynostosis in a rabbit model of human non-syndromic craniosynostosis. Noggin was chosen to test our hypothesis because of its ability to inhibit the activity of BMP2, -4, and -7 [131, 132, 223].

We found that Noggin treatment was effective in inhibiting bone healing and delaying suturectomy site resynostosis in the rabbit model, evidenced by the long-term persistence of defects in the calvaria up to 84 days after treatment. The data also suggest that Noggin, delivered

once, within a slowly resorbing collagen gel, can have long term effects on craniofacial growth in this model. There was an initial increase in the size of the suturectomy site in the Noggin treated group. We believe that this increase is because, after the surgical release of the fused suture, the brain begins to expand in the anteroposterior direction. Though this brain expansion may also be occurring in the BSA and untreated control groups (evidenced by the similar ICV measurements at 25 and 42 days of age, **Figure 8C**), the amount of bone healing obscures this fact.

The inhibition of bone healing by Noggin therapy occurred primarily in the first 15 days after surgery (up to 25 days of age), followed by the resumption of bone healing at rates similar to control defects. Notice that the graph of reossification (**Figure 8B**) shows that lines connecting 25, 42, and 84 days in the Noggin treated group closely parallel the lines in the two control groups. The only difference between these lines is that the Noggin treated group shows an increase in defect size between 10 and 25 days of age, starting their normal healing from a different defect size than the two control groups. We believe that the resumption of normal healing after 25 days of age in the Noggin treated group reflects the loss of Noggin function due to its release from the collagen gel over time. Although the protein was added to a slowly resorbing collagen gel, we believe that most of the protein releases from the gel over the first two weeks in vivo. This would account for the normal healing that is noticed after 25 days of age (15 days after surgery). This hypothesis regarding the 15 day duration of Noggin activity is also supported by the marker separation data. We find that the markers in the Noggin treated group are significantly farther apart at 25 days of age compared to the control groups, and not significantly different at the later time points. We believe that the marker separation data reflects

the occurrence of resynostosis (healing) along the lateral aspects of the defects, causing a reduction in the rate of marker separation.

Although the protein may have had limited temporal activity, the data presented here show that a single dose of Noggin can have lasting effects on defect healing and improve ICV and craniofacial growth in synostotic rabbits almost to levels similar to wild-type rabbits. In rabbits, 90% of the total brain growth is completed by 84 days of age [214, 219]; whereas, in humans, it takes nearly 6 years to complete 90% of brain growth [1]. Therefore, therapies developed for use in humans must have a much longer period of effect than those studied in our rabbit model of simple, nonsyndromic craniosynostosis. For this reason, our group is working on testing several delivery mechanisms for protein-based and gene-based therapies.

We believe that Noggin-based therapy may represent a particularly useful means for the inhibition of postoperative resynostosis for two reasons. First, Noggin therapy, similar to any biologically-based adjunct to surgery, may improve surgical outcomes while at the same time allow for minimal surgical intervention. We envision that small craniectomies, placed where sutures normally exist, will be able to remain patent by inhibiting bone formation in that region using Noggin-based therapies, thus allowing for more normal brain and craniofacial growth postoperatively. Second, by targeting BMP signaling, we may be able to sidestep the direct molecular cause of the original synostosis. BMPs are potent inducers of bone formation. Interruption of BMP signaling should inhibit the osteogenic differentiation of cells regardless of their genetic background. Though much work needs to be done with respect to understanding the role of BMPs in craniosynostosis, their role in bone healing is well understood. We feel that the inhibition of BMP signaling may be the upstream event that can nullify many of the downstream events that are associated with the known mutations that lead to craniosynostosis. Most

importantly, this study showed that Noggin treatment may have some effect on the abnormal healing patterns that are exhibited by individuals (both rabbit and human) with craniosynostosis.

# 3.0 DEVELOPMENT OF A MODEL FOR CRANIOFACIAL BONE REGULATION

## 3.1 INTRODUCTION

The second chapter of this dissertation showed that a therapy using a natural inhibitor to BMPs can have lasting effects on surgical outcomes. This work was undertaken to try and reduce the occurrence of the clinically relevant problem of postoperative resynostosis in craniosynostotic children. The results of the protein therapy in craniosynostotic rabbits showed that mixing Noggin protein with a slowly resorbing collagen gel had an approximate 15 day temporal effect. Though the Noggin therapy had long-term effects on the intracranial volume in treated animals, the defects seemed to heal normally after about 15 days after surgery. Therefore, the effect of this type of "one-shot" treatment was shown to be about 15 days.

In order to better understand the possible effects of long-term Noggin treatment on bone healing, we had two choices. The first was multiple dosing of the rabbits with Noggin. Repeated injection of Noggin at different times after surgery would allow for a determination of the effects of extended Noggin exposure on defect healing. Such a strategy would, however, necessitate multiple surgeries on each animal and run a higher risk of infection (multiple interventions). Therefore, we decided to utilize a tool developed by Dr. Hairong Peng in the laboratory of Johnny Huard [212] to test the effects of longer-term Noggin treatment on calvarial defect

healing through the transduction of muscle-derived cells with a retroviral vector encoding Noggin expression.

The vast majority of the research that has been done on bone healing and bone formation relates to the improvement of large defect healing. In order to pursue the study of bone regulation, it was necessary to identify a reliable animal model. The goal of this aspect of my research was to test the effects of Noggin treatment on the regulation of normal bone healing in a mouse model. It was necessary to create a model of bone healing in the rodent that would simulate the molecular events that occur during resynostosis following surgical intervention to correct craniosynostosis. This model would need to have three key characteristics: 1) it would be a calvarial bone defect; 2) it would heal reproducibly; and 3) it would show significant healing within a short period of time.

There are very few standardized calvarial defect models. The most widely used and well-defined is the critical size defect, or CSD. A CSD was defined by Schmitz and Hollinger as "the smallest size intraosseus wound in a particular bone and species of animal that will not heal spontaneously during the lifetime of the animal" [224]. This animal model of human bone defect nonunion was proposed as a way to standardize research models for bone repair materials [224, 225]. Since the introduction of the term, CSDs have been used routinely in many laboratories to test the osteogenic capacities of different bone repair techniques (for review, see Mooney and Siegel, 2005 [226]). We believed that a minor modification of the CSD would yield new model for craniofacial bone healing.

## 3.2 STRATEGY

### 3.2.1 Defect Size

Mouse calvarial CSDs are defined as 5mm round defects [199, 226, 227]. The first variable that we manipulated to try and create a non-critical size defect was the defect size. We were confident that defects smaller than 5mm in diameter would consistently heal in a relatively short period of time because CSDs were defined as the "smallest" defects that would not heal. To test this hypothesis, we created sub-critical size defects using 1.8mm outer diameter trephines (Fine Science Tools), in 10 week old normal (C57BL-6J, Jackson) mice. At the time of surgery, the trephines were used to make unilateral, bicortical, mid-parietal defects. The 1.8mm trephine was chosen because it was the smallest commercially available trephine. We analyzed healing of these mice radiographically using 2-dimensional defect area analysis 6 weeks after surgery (**Figure 10A**), expecting to find that the calvarial defects we created were significantly healed. However, in the 10 animals in this study, we found large defects still remaining with an average of approximately 43.3% healing after 6 weeks (**Figure 10B**)

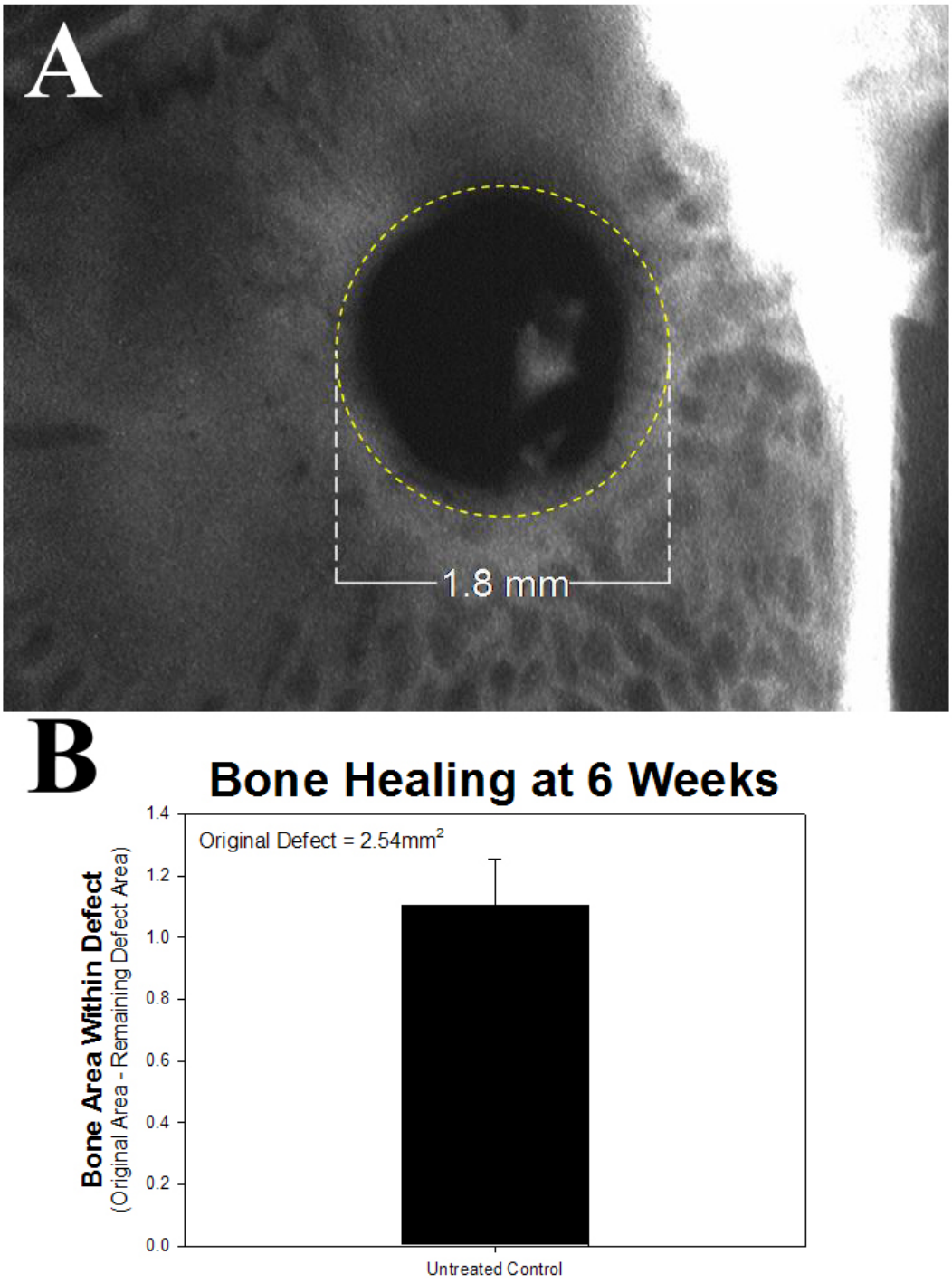


**Figure 10: Analysis of untreated mouse 1.8mm calvarial defects 6 weeks postoperatively**

**A**) Radiograph showing remnant defect in mouse calvaria 6 weeks after creating a 1.8mm outer diameter defect. Yellow dashed circle shows the outline of the original defect. **B**) Graph showing the 2D measurement of bone formation (±SEM) within the defect after 6 weeks.

This data demonstrated that defects much smaller than critical size do not readily heal in the adult mouse calvaria. One possible reason for this inability to heal was the technique. The trephine burr is known to easily damage the underlying dura mater as soon as it cuts through the endocortex of the calvaria (anecdotal evidence). The next most logical variable to manipulate was the surgical technique used to make the defect.

### 3.2.2 Surgical Technique

It is well known that the dura mater plays a significant role in the healing of calvarial defects [47, 228-232]. The dura mater seems to be both the primary source of osteogenic cells and the source of osteoinductive factors during calvarial wound healing [233]. The surgical technique employing a trephine may have damaged or destroyed the dura mater underlying the defect, thereby inhibiting defect healing.

In order to eliminate the possibility of dural damage, a set of experiments was designed with the assistance of Dr. Joseph E. Losee, a pediatric craniofacial surgeon who performs similar surgery routinely in infants with craniosynostosis. This experiment compared the healing among three groups of animals with defects created in different ways. In the first group of animals, we used a trephine to create the bicortical defect, paying particular attention to preserving the dura mater ("trephine" group). In the second group of animals, we used the trephine, but deliberately damaged the dura mater to ensure disruption of the dural component ("dural damage" group). In the third group, we performed surgery a bit differently. First, we used the 1.8mm trephine to score the parietal bone and cut through the ectocortex and some of the endocortex. A small otoelevator was then used to break through the remaining endocortex and to remove the bone from the defect ("elevator" group). This technique allowed us to preserve the dura mater (**Figure**

**11A**) and create a defect that was 1.8mm in diameter at the ectocortex; however, the technique also led to a defect with a variable diameter along the endocortex, because the bone was fractured instead of cut in this region (**Figure 11B**).

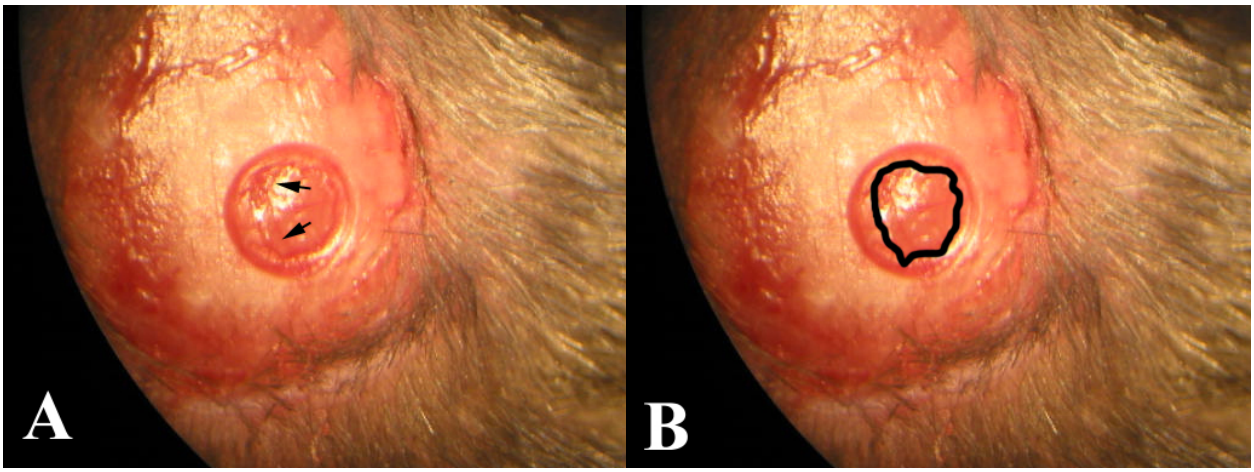


**Figure 11: Intraoperative photograph of defect created using the "elevator" technique**

**A**) Photograph of defect created by fracturing through the endocortical layer of the parietal bone. The undamaged blood vessels within the defect (arrows) demonstrated that the dura was left intact. **B**) Same picture as in **A** with an outline of the endocortical defect margin. Notice that the margin is not uniform because of the fracturing technique that was used in the elevator group.

Animals in this study were killed 4 weeks, 8 weeks, and 1 year after surgery and healing of the parietal defects was assessed radiographically. Defect area was calculated using Northern eclipse software and statistical analysis was performed with SPSS. Statistical analysis showed that the elevator group healed more than the trephine group at both 4 (**Figure 12A**) and 8 weeks (**Figure 12B**) after surgery. Analysis of radiographs after 1 year of healing (**Figure 12C,D**) showed that defects created using the elevator technique were 52% filled by bone, whereas the trephine and dural damage groups healed no more than 35% of the defect (p=.257).

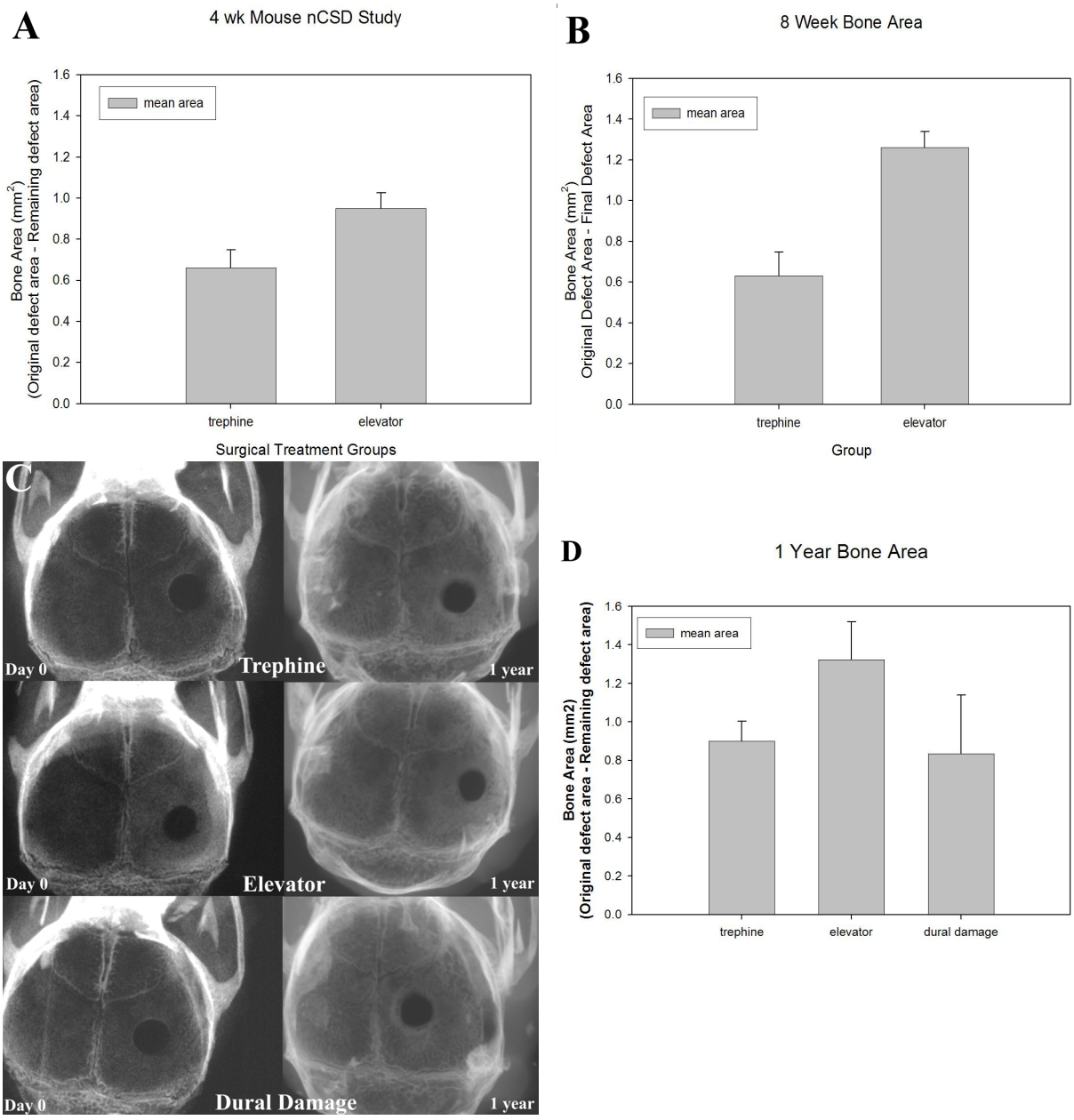


**Figure 12: 2-Dimensional radiographic analysis of surgical technique effect on defect healing**

**A**) Graph showing the mean (±SEM) area of new bone formation within defects 4 weeks after surgery. The trephine group healed approximately 26% while the elevator group healed approximately 35% after 4 weeks. **B**) Graph showing defect healing 8 weeks after surgery at which time the trephine group had healed approximately 25% compared to nearly 50% healing in the elevator group. **C**) Radiographs showing the initial defects (day 0) and healing at 1 year for all groups. **D**) Graph showing the mean (± SEM) of defect healing in all groups 1 year after surgery. After 1 year, the trephine group only healed about 35% of each defect, and the elevator group healed approximately 52%. As shown in **D**, dural damage group healed similarly to the trephine group at all times (not shown).

These results suggest that the surgical technique alone did not significantly influence the healing of small parietal bone defects in normal mice. Specifically, our hypothesis that the lack of significant healing could have been due to damage to the dura mater during surgery was not supported by this data. The presence of intact, undamaged dura mater in these 1.8mm defects did improve the defect healing, but not significantly, and did not lead to complete healing in any animal tested. Therefore, we focused on the effect of animal species on the healing of small calvarial defects.

### 3.2.3 Model Species

The rat calvarial model is larger than the mouse, and the critical size defect for the rat is 8mm [224]. We used a 2.3mm outer diameter trephine to make small calvarial defects in adult Sprague-Dawley (SD) rats and allowed the rats to heal for 6 weeks. This experiment was used to test the hypothesis that a small calvarial defect created in rats would heal completely in a short amount of time. Six weeks after surgery, we killed the rats, removed the brain from the skull, and tested defect healing using radiographic analysis.

Radiographs showed that 2.3mm defects in the parietal bone of SD rats did not heal completely after 6 weeks (**Figure 13A**). In fact, analysis showed that defects healed approximately 36.9% (**Figure 13B**).

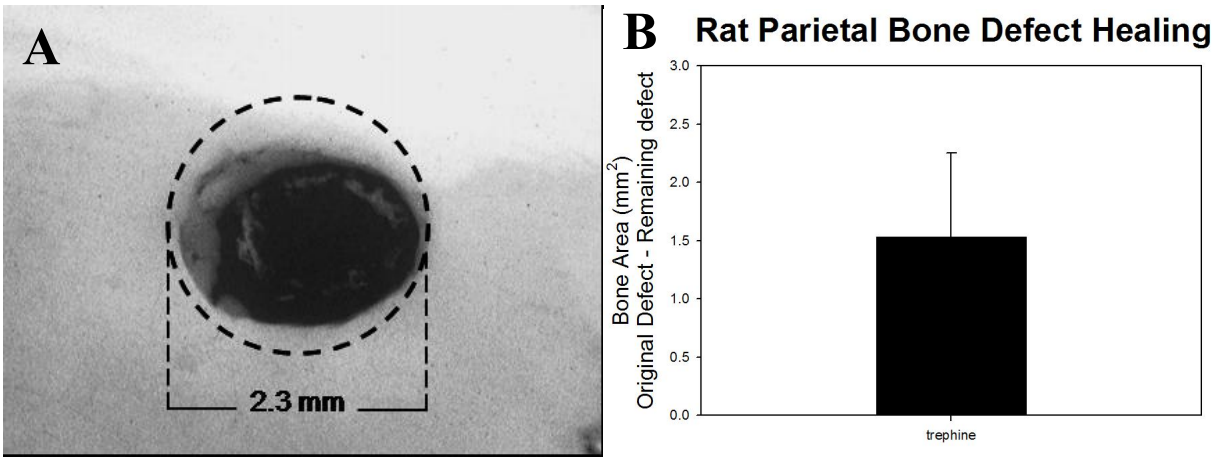


**Figure 13: Rat parietal bone defect healing 6 weeks postoperatively**

**A**) Radiograph showing the defect remaining after 6 weeks of healing. Notice that most of the healing occurred around the perimeter with small islands of bone forming within the defect. **B**) Analysis of remaining defect area (±SEM) determined that these defects healed approximately 37% of the original defect area (2.3mm diameter = 4.155mm$^2$ area) after 6 weeks.

These data show that we were unable to achieve the large-scale, rapid healing of a small calvarial defect by changing the species to rat. We hypothesized that the choice of strain of rat may effect healing. A small study was performed by creating 2.3mm defects in the parietal bones of SD, Lewis, and Fischer 344 rats. That study showed that none of the defects in any of the strains was able to heal significantly in 6 weeks.

Although the rat was believed to be a robust bone-forming animal model, the data presented above shows that small defects made in the rat parietal bone do not meet the criteria that we needed for a new model of craniofacial bone healing.

### 3.2.4 Defect Placement

The data presented above show that we were unable to create a model of normal craniofacial bone healing by decreasing the size of the defect below the "critical" size, by changing the

surgical technique to ensure the preservation of the dura mater, or by changing the animal species from mouse to rat. Another variable that we could manipulate to try and create the desired model was the placement of the defect on the skull. All of the defects described above were made within the parietal bone. Identification of an optimal site for creating a defect would increase the likelihood of defect healing.

In addition to more rapid defect healing, we also hoped to model resynostosis following suturectomy surgery in craniosynostotic patients. The perfect model for postoperative resynostosis is the rabbit model of human, nonsyndromic craniosynostosis as described above [9, 11, 24, 25, 54, 100, 137, 215, 216, 234]. However, the rabbit model is more expensive to breed and to house and the occurrence of bilateral coronal suture synostosis in this model is low enough that large-scale studies (<50 animals) may take a few years to complete. Furthermore, it would be extremely difficult to test the effects of a regenerative strategy for rabbits that included using multipotent cells because very little work has been done on the characterization of rabbit stem cells or their use for gene-based therapies.

The most logical site to make a defect that may model resynostosis is at a fused suture. A defect created in a naturally fused suture would model the removal of the prematurely fused suture (suturectomy). In rodents, there is only one suture that fuses normally early in life. It is the interfrontal suture [84-88, 235]. The interfrontal suture has been shown to fuse by 55 days of age in mice and by 35 days of age in rats (**Figure 14**) [84-88, 235].

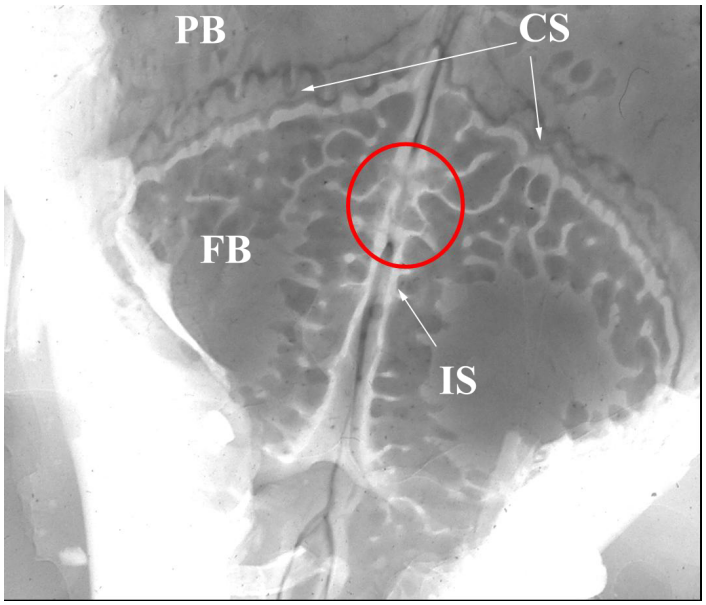


**Figure 14: Radiograph of 10 week old mouse calvaria**

Radiograph showing parietal bone (PB) and frontal bone (FB) with intervening coronal suture (CS) in a 10 week old C57BL/6J mouse. Between right and left frontal bones is the interfrontal suture (IS). The region of the interfrontal suture circled in red represents the naturally occurring fusion of the right and left frontal bones.

In addition to testing the placement of the defect, we also wanted to model a small-scale surgical intervention, so we hoped to create the smallest defect possible. We used a cutting burr with a much smaller diameter (0.5mm) than any trephine that was available (1.8mm) attached to a hand engine (set to 2000 rpm) to create a defect in the posterior interfrontal suture region (the region that is fused) in 10 week old C57BL/6J mice (Jackson, USA). We compared these defects (n=12) with defects made with the same cutting burr in the middle of the parietal bone to control for technique. We killed mice for radiographic analysis immediately postoperatively (n=3), 6 weeks (n=3), or 12 weeks (n=3) after surgery.

Immediately after surgery, the interfrontal defects were highly variable in their size and shape as evidenced by radiography (**Figure 15, Day 0**). Three and 6 weeks after surgery, marked healing was evident in all the defects (**Figure 15**), but small defects still persisted in most of the

animals. However, by 12 weeks after surgery, we found that all three of the defects analyzed were completely healed (**Figure 15**). Most importantly, we found that there was no evidence of new suture formation in the defect region. This type of healing seemed to model the events that occur during resynostosis; namely, a fused suture that was surgically removed healed completely and resynostosed.

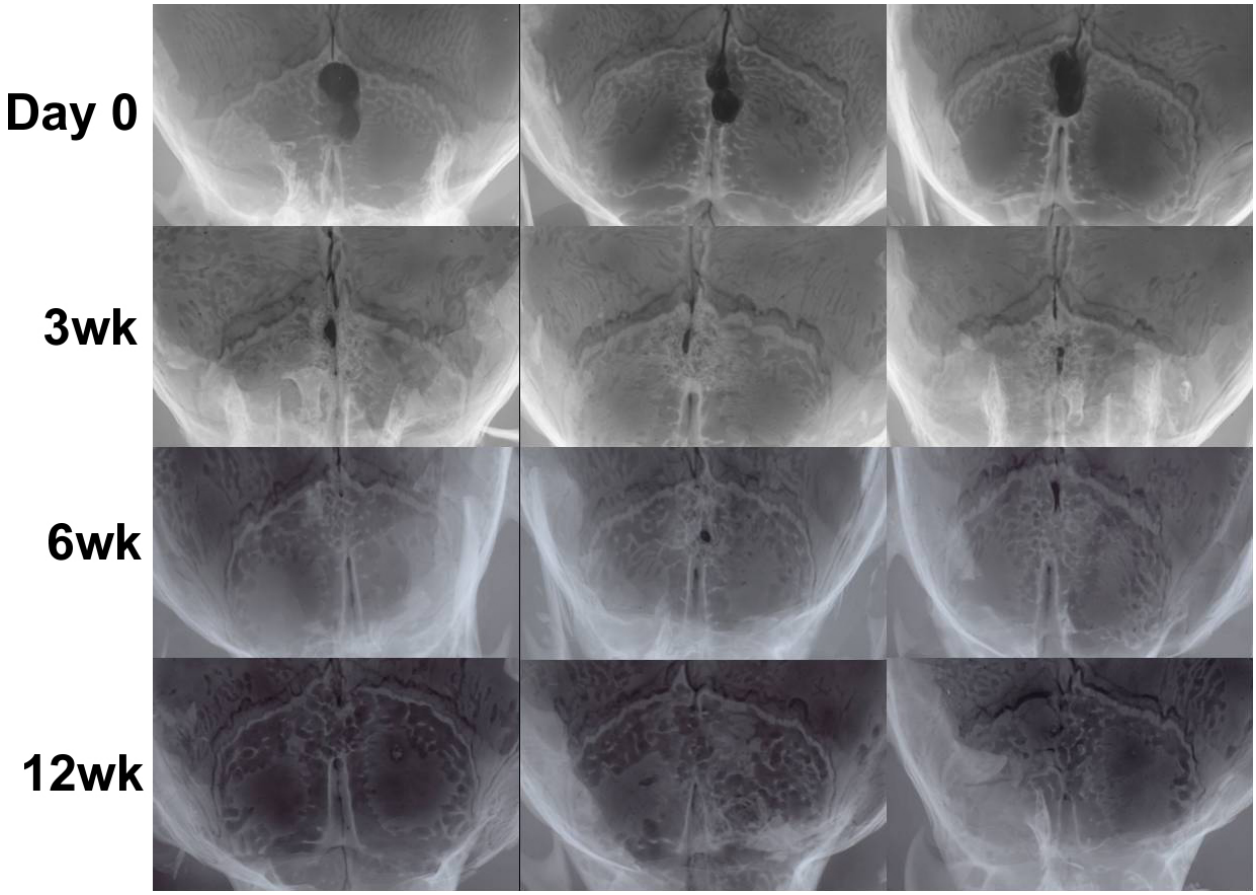


**Figure 15: Radiographs of calvaria after novel interfrontal suturectomy surgery**

Radiographs taken of mouse calvaria after animals were killed and the brain removed, anterior is toward the bottom of the page. The radiographs show that the initial defect (Day 0) is variable in its size, shape, and area (n=3). All defects analyzed 3 (n=3) and 6 weeks (n=3) after surgery showed some level of healing. By 12 weeks after surgery, all animals showed complete healing of the defect with no evidence of new suture formation (n=3).

We also tested the healing of linear defects created in the parietal bone using the same 0.5mm diameter dental burr to test whether the healing we observed was simply due to the smaller size of the defect. We observed incomplete healing of the small 0.5mm width defect even after 12 weeks postoperatively (**Figure 16**). These data suggest that the healing of small defects is dependent on the placement of the defect, rather than the initial size of the defect because small defects created in the interfrontal suture tended to heal, while defects created in the parietal bone did not heal well.

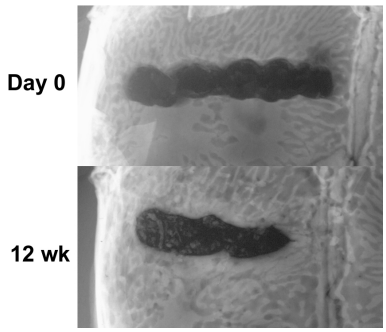


**Figure 16: Radiographs of 0.5mm parietal defects**

Radiographs showing an initial parietal defect (Day 0) and a defect after 12 weeks of healing (12 wk). Note the incomplete healing even after 12 weeks.

This data represents the first evidence that we were able to create a small calvarial defect modeling a suturectomy that would heal well and model postoperative resynostosis.

## 3.3 DISCUSSION

### 3.3.1 Critical Size Defects

#### 3.3.1.1 The original "critical size defects"

Despite great strides in our understanding of the molecular and mechanical mechanisms behind bone wound healing, very few changes have been made to the clinical treatment of large bone defects. Research on bone replacement and bone regeneration has shown that a therapy involving an osteoconductive scaffold, osteogenic cells, and an osteoinductive factor (often delivered via gene therapy) can impact healing [236]. In general, most of this research is interested in creating the largest amount of bone in the shortest amount of time. Unfortunately, in cases of bone overgrowth, such as craniosynostosis, it is necessary to control bone formation. For this reason, there is a need to develop means to regulate the amount of bone that regenerates following surgical damage. To test such regulatory strategies, it was necessary to develop a model of normal bone healing.

The concept of the critical size defect (CSD) was created as a model of nonunion that could be used by researchers to test bone replacement materials (BRM) in a consistent manner [224, 225, 237]. The need for such a standardized defect came from the practice of researchers using many different surgical procedures to test their BRM of interest [224]. CSDs were used for two decades to test BRMs, cellular therapies, and other bone replacement strategies. Because CSDs were the only standard craniofacial bone defect model, we hoped to use it as a basis for the development of a novel model of craniofacial bone healing.

The CSD, at its inception, was defined as "the smallest size intraosseus wound in a particular bone and species of animal that will not heal spontaneously during the lifetime of the

animal" [224]. CSDs were developed to model fibrous nonunions in humans. These nonunions are not capable of healing without medical assistance. Therefore, the goal was to create a defect in animals that would be "shut down" and unable to heal, similar to human nonunions.

In an attempt to define the difference between "in the process of healing, but not healed yet" and "shut down and never going to heal," Schmitz, et al. attempted to characterize the pattern of healing within rat critical size defects by comparing the temporal microscopic healing of the CSD (8 mm) over 4 weeks [237]. As a control, the microscopic healing of 3mm and 4mm defects was observed. In that study, "no differences in patterns of bone formation and fibrous scar tissue formation were observed between the smaller and larger defects" and "none of the defects healed completely during the experimental period" [237]. Schmitz, et al. did not find any differences between CSDs and smaller defects at 4 weeks other than finding more bone in the smaller defects. This study also did not look at the healing of the defects at the end of the animal's natural lifetime. Since there was no microscopic differences observed between "shut down" CSDs and "not healed yet" smaller defects, there may be no difference at all, save the fact that one is larger than another.

There is an intuitive difference between the biology of a bone defect that is healing but has not completely healed and the biology of a defect that has filled with fibrous tissue and will never heal. Clinically, the term "nonunion" is given to a defect that is not healed within 8 months of injury [238], but the decision to intervene surgically is mainly up to the individual clinician. This clinical definition that employs an 8 month "cut-off" point can be altered, based on the discomfort of the patient. A surgeon can initiate intervention or wait longer to see if a bone defect will heal, depending on whether the patient is in pain or debilitated. It is important to notice that the definition of a CSD, which is supposed to be a model of human nonunion, is

based on the size of the defect that will not heal within the lifetime of the animal. There is no direct clinical correlate to the CSD defined in this way because such a definition would depend on outcomes measured at the death of the patient.

More importantly, there seems to be no clinical relevance to the CSD not healing. In orhopaedic reconstruction, after a nonunion is diagnosed, surgery is performed to debride the defect and create, basically, a new bone defects that can be treated by whatever means the surgeon deems useful, usually bone autograft. At no point is the nonunion or the fibrous tissue that fills a CSD treated directly. In reconstruction of the calvaria, the dura mater underlying the defect often becomes scarred and calcified. This tissue cannot be disturbed to avoid causing a dural tear. Though the translation of a defect that is "shut down" does seem to apply to the clinical reality of calvarial defects, no research has yet been performed to test therapies to heal CSDs that were already filled with fibrous tissue. Because of the weak clinical applicability, and the lack of experimental backing for the biological relevance, the definition and use of CSDs must be amended.

#### 3.3.1.2 Re-defining "critical size defects"

A few researchers have found that the original definition of CSD is not really functional. Gosain et al. stated that "A critical-size defect is one that will not heal within the lifetime of the animal. However, because most studies are of limited duration and do not extend over the entire life of the animal, the critical-size defect in animal research refers to the size of a defect that will not heal over the duration of the study" [239]. This new definition dropped the idea of "smallest interosseus defect" and the dependence on the "lifetime of the animal."

There are several theoretical issues with altering the definition of "critical size" that have not been discussed in the literature. First, Gosain et al. state that "the critical-size defect in

animal research refers to a defect that will not heal over the duration of the study" [239]. In fact, critical size defects are only defined in animal research. The clinical term is nonunion, and is defined as stated above [238]. Therefore, it is incorrect to state that critical size is defined differently for animal research than for an animal model.

Second, this re-definition undermines the attempt to standardize bone healing research. When employing the new definition of critical size as not healing within the duration of the study, the definition hinges on the length of the study, not the surgical model. If someone creates a very small fracture or defect, and looks for healing in a very short time (one hour, for example), should the small defect be considered critical size? If the answer is yes, then there is no point to defining "critical size defects" in order to standardize research practices because each researcher can utilize his or her own defect to test bone healing strategies.

Third, the CSD theoretically models the nonunion by simulating a defect that is "shut down" and will never heal. By changing the definition to a defect that will not heal over the course of the study, we lose the concept that the biology might be different for non-healing defects than it is for normally healing or slowly healing defects. Therefore, this re-definition also undermines the attempt to model human nonunions.

#### 3.3.1.3 Technology and "critical size defects"

Analytical techniques go hand-in-hand with the choice of model. Our means to analyze bone growth and regeneration are improving through technological advances. Our use of experimental models must change to utilize the new technologies. Common techniques to analyze bone formation include histological bone area measurement or assessment of radiographic area or radiodensity measurements. These techniques are useful for the identification of bone formation but are less useful when comparing different treatments (to obtain a quantitative measurement of

bone formation) due to the fact that these analyses change three dimensional data into two dimensional data. Radiodensity can be used as a general indicator of the *mass* of the formed bone in that more bone in a region will be more opaque. However, high radiographic density may be caused by the superimposition of poorly organized bone. Therefore, it is difficult to interpret the quality of bone formation from radiographic evidence.

Similarly, histological analysis can only consider the quantitative measurement of bone area within a 2-dimensional cross section and the qualitative morphology of the bone. Area measurements cannot be directly compared between treatment groups because the morphology must be considered. For example, a region of many small trabeculae may have a larger measured bone area than a thin sheet of cortical bone. It is difficult, with this information, to determine which one is "better." Gosain et al., after re-defining critical size, attempt to assist researchers to more accurately measure the amount of bone that forms within a critical size defect [239]. Their suggestion was to measure the area of bone within the defect through histological evaluation, rather than a linear measurement if defect healing. Fortunately, technology has improved to allow for the accurate quantification of the volume of bone within a defect. Bone volume is much more accurate than a gross estimation of 2-dimensional bone area taken from a histological cross-section, the area of which is dependent on the angle of the bone when the slide is cut.

Bone volume and its complimentary defect volume can be measured in live animals using micro computed tomography (μCT). Because of the limitations of traditional analytical techniques, many investigators are utilizing computed tomography to improve their analyses[166, 174, 179, 182]. CT analysis allows for the quantification of bone mineral density [179, 240, 241] and bone mineral content [174, 242] within the newly formed bone. The use of CT for these types of analyses allows investigators to quantify the opacity of bone in thin slices

of the area of measurement (often 1mm) versus a radiographic, 2-dimensional, picture that encompasses the entire bone mass. With the advent of micro computed tomography (μCT), investigators are able to make the same measurements of bone density and mineral content from extremely thin slices through the region of interest (5-100 μm). Also, by using any type of CT, one can generate 3-dimensional images of the newly formed bone. Similar to the use of histology to assist radiographic analysis, μCT-generated morphological data can be used to strengthen interpretations of the quality of bone formation (see **Figure 17**).

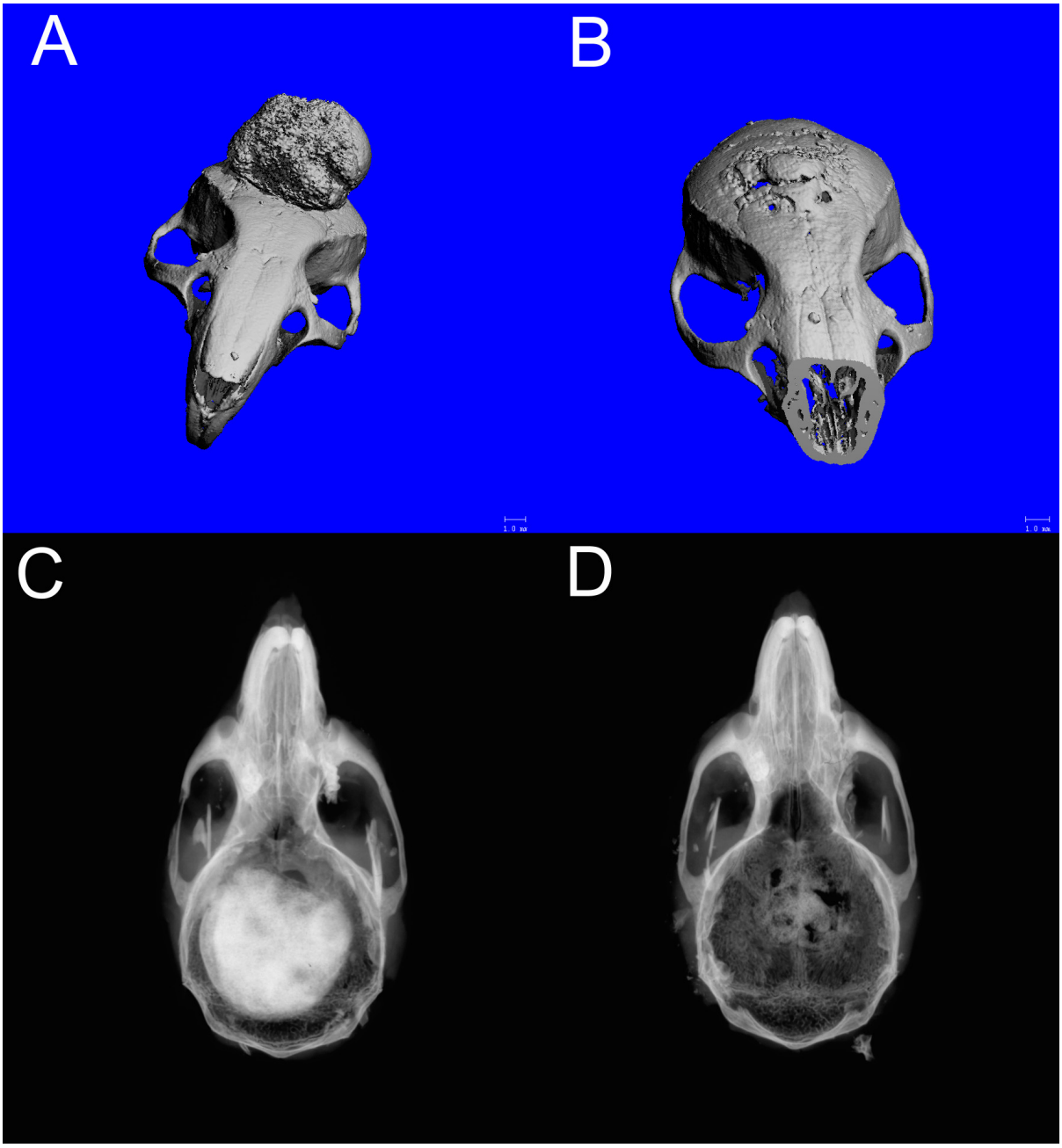


**Figure 17: Comparison between radiographic and µCT images**

Three dimensional reconstructions of micro-computed tomography (µCT) scans (**A,B**) and radiographs (**C,D**) of mouse skulls after treatment to repair 5mm calvarial defects. The large bone formation in the µCT (**A**) is seen as a region of radio dense tissue in the corresponding radiograph (**C**). However, the trabecular nature of the regenerated bone indicated by µCT (**A**) is not conveyed by standard radiographic analysis (**C**). Normal size and shape of regenerated bone (**B**) with the corresponding radiograph (**D**). A radiographic comparison of the two samples would interpret sample **C** being better than sample **D**. However, with µCT analysis, sample **B** shows optimal bone formation. µCT allows for more accurate determination of the quality of the regenerated bone.

#### 3.3.1.4 The future of "critical size defects"

Since critical size defects were arbitrarily defined rather than experimentally generated, and researchers have found problems with the definition, we have three choices: 1) we can use the term "critical size defect" as defined by Schmitz et al. [224] and strengthen it by analyzing the healing of defects of all sizes at the end of the animals' lifetimes to experimentally determine the smallest defect that will not heal in the lifetime of the animal; 2) we can re-define the CSD as any defect that does not heal over the duration of the study and have no standardization or good clinical correlate to the model; or 3) discontinue the use of the term "critical size defect."

Of these choices, the most logical is to discontinue the use of the term "critical size defect." The model has only a limited clinical applicability and currently only serves to standardize the research methodology. However, through the use of μCT, we can more accurately define the size of our initial defect in live animals and more accurately measure the amount (volume) and quality (density) of formed bone. Such quantifiable measurements allow each researcher to design a surgical defect model that most closely resembles their area of clinical interest. Technology is enabling us to quantify small differences in the amount and quality of bone formation within small defects and more readily create useful animal models of human disease. The future of bone research will lie in the development of treatment modalities that are tailored to specific clinical applications. This strategy necessitates the use of appropriate animal models and technological advances and minimizes the need for a critical size defect model.

### 3.3.2 A New Model for Postoperative Resynostosis

This chapter presents data that led to the development of a new model of postoperative resynostosis in an adult mouse. We needed to develop a model to allow us to test strategies to control bone growth and inhibit resynostosis after surgery to correct craniosynostosis. Because CSDs were defined as the smallest defect that would not heal, we were confident that any defect smaller than critical size would readily heal. The work presented here shows that simply making smaller defects is not sufficient to achieve reproducible healing. In fact, while we were testing defect sizes, Cowan et al. demonstrated (in their supplementary online data) that sub-critical size defects did not heal within 12 weeks after surgery [243]. We also found that surgical technique aimed to ensure the maintenance of the dura mater underlying the defect did not help small defects heal consistently up to 1 year postoperatively (**Figure 12**). Finally, we found that small defects made in a reputedly osteogenic (rat) parietal bone did not heal completely (**Figure 13**).

Cowan et al. showed that very small, 0.8mm diameter, defects made in the parietal bones of mice were able to heal completely within 12 weeks after surgery [243]. Knowing that defects had to be that small, we sought to create a model that was more appropriate for our intended clinical use. We therefore used a small 0.5mm diameter cutting bur to perform a suturectomy on the posterior interfrontal suture that undergoes non-pathological synostosis early in the mouse life. Defects created in this way were shown to heal completely within 12 weeks of surgery. More importantly to our model, the interfrontal suture resynostosed as it healed.

We believe that this model can be useful to test therapies targeted to inhibit the formation of bone within small calvarial defects. Furthermore, we believe that the use of μCT technology will strengthen the use of such models with respect to the non-uniformity of the initial defects.

# 4.0 THE EFFECTS OF NOGGIN GENE THERAPY ON POSTOPERATIVE RESYNOSTOSIS

## 4.1 INTRODUCTION

Craniosynostosis is the term given to the premature fusion of one or more of the cranial sutures [1] and it occurs with an estimated birth prevalence of 300-500 cases per 1,000,000 live births [2]. Craniosynostosis causes secondary deformation of the cranial vault, cranial base, and the midface often leading to increased intracranial pressure, and altered intracranial volume [15-24]. Currently, the surgical intervention to correct craniosynostosis involves release of the synostosed suture, cranial vault decompression, and extensive craniofacial bone reconstruction [2-4, 28, 31-33, 38, 41-44]. Although such strategies have improved the long-term outcomes of surgical intervention, the suturectomy site often reossifies, causing increased intracranial pressure, restricting brain growth, and altering craniofacial growth [4, 5, 28, 38, 44-52, 54]. The detrimental effects of postoperative resynostosis necessitate secondary surgeries and increase patient morbidity and mortality [60, 61]. Because of the failures of current surgical interventions and the desire to avoid secondary surgeries, further work must be done to improve the outcomes for children presenting with craniosynostosis.

The genetic mutations that lead to a handful of the syndromes involving craniosynostosis recently have been elucidated [40]. Unfortunately, the occurrence of syndromic craniosynostosis

only accounts for approximately 11% of all cases of craniosynostosis [2]. The vast majority of craniosynostosis cases are nonsyndromic and have no known genetic basis. Because of the unknown causes of nonsyndromic craniosynostosis, it surely will prove difficult to develop molecular therapies that can be tailored to specific individuals or specific cases.

Bone morphogenetic proteins (BMPs) are members of the transforming growth factor beta superfamily of proteins that were initially characterized by Urist in 1965 [145]. Several BMPs, including BMP2, BMP4, and BMP7 have been shown to be potent inducers of bone formation and are expressed during bone healing events [209, 244]. Noggin is an extracellular antagonist that binds directly to and inhibits the activity of BMP2, -4, and -7 [131, 132, 223]. Noggin has been shown to inhibit BMP induced bone formation in several different models [211-213, 245]. Noggin's ability to inhibit BMP-induced bone formation may be useful in inhibiting postoperative resynostosis.

Previous studies have shown that Noggin protein therapy was capable of inhibiting bone formation and resynostosis in rabbits. However, the data also show that Noggin seemed to exert its effect in the first 15 days after implantation. One means of achieving longer-term exposure of the injury site to a therapeutic protein is through gene therapy. Gene therapy can be defined here as the genetic manipulation of cells to produce a desired effect. In this case, the desired effect is the production of exogenous Noggin protein.

There are two strategies for the delivery of genetic material for therapeutic purposes. The direct application of vectors containing genetic material to the cells, tissues, or organs of interest within the living organism is termed in vivo, or direct, gene therapy. The use of in vivo gene therapy is hampered by the inability to control the type of cell that is infected by the vector being added. Any cell that comes into contact with the vector can potentially uptake the vector and

become altered. Also, it is extremely difficult to control the number of cells that are altered after the material is implanted in the body, making dosage difficult to control. The second strategy for gene-based therapies involves the implantation of genetically altered cells to deliver a protein of interest. This strategy is termed ex vivo gene therapy. Ex vivo approaches allow control of the cell type that will be altered and the number of altered cells that can be delivered to the injury site. For either in vivo or ex vivo approaches, it is important to choose the correct vector to introduce transgenes, the DNA that will cause the expression of the protein of interest.

### 4.1.1 Gene Therapy Vectors

#### 4.1.1.1 cDNA plasmids

Plasmids are safe vectors used for short-term transient transfection of cells. The drawback of plasmid vectors is the low transfection efficiency whereby only a small percentage (usually around 30%) of cells receives the transgene and produces functional protein. Also, when cells are successfully transfected, they will only express the exogenous protein for a few days (usually 3-5 days). Recent reports using cDNA plasmids for bone regeneration attempt to increase the uptake of the plasmid by adding cationic liposomes [246] or poly(ethlenimine) (PEI) [247]. These authors chose to deliver the plasmid by hydroxyapatite scaffold [246] or by poly(lactic-co-glycolic acid) (PLGA) scaffold [247]. The addition of plasmids to scaffolds that slowly degrade and release the plasmid is a promising direction for developing safe gene-based bone therapies.

#### 4.1.1.2 Adenoviral vectors

Transduction of cells using adenoviral vectors leads to longer expression than plasmid transfection. Some recent reports have used luciferase activity to analyze expression patterns in

vivo and found that adenoviral vectors can cause expression of protein for anywhere from 10 [176] to 14 days [180]. Many investigators have recently used adenoviral vectors to induce expression of BMPs or VEGF using either in vivo or ex vivo gene therapy techniques [173-180, 248]. One drawback for the use of adenoviral vectors is that they usually cause a host immune response which deters their use in clinical applications. Another drawback is the fact that there is a loss of transgene expression when a transduced cell divides because the genetic material remains episomal and does not incorporate into the infected cell's genome.

#### 4.1.1.3 Adeno-associated viral vectors

Wild-type adeno-associated viruses (AAVs) are capable of incorporating into the host DNA, offering long term expression. However, a recent report by Gafni, et al., 2004, used luciferase to test the expression of an inducible AAV-2-based vector and found luciferase expression for only 20 days after implantation [249]. Therefore, the use of recombinant AAV-based vectors does not guarantee DNA integration and long-term expression. AAV vectors, unlike adenoviruses, do not normally cause an immune response and are therefore of clinical interest. A recent report adhered AAV-based vectors for VEGF and RANKL to allografts to improve allograft bone remodeling [250]. Unlike wild-type vectors, genetic material delivered via recombinant AAVs does not incorporate into the transduced cell's genome.

#### 4.1.1.4 Retroviral vectors

The important characteristic of retroviral vectors is that transgenes get incorporated into the host cell's DNA. This fact allows for long-term expression of the transgene throughout the life of the cell as well as its progeny. Retroviruses are less clinically applicable due to the inability to control the site of insertion of the transgene into the DNA. Transgene insertion into essential

regions of host DNA can lead to cancer or cell death. Retroviral vectors are therefore normally used in ex vivo gene therapies where the target cell (host) can be controlled and assessed for viability and tumorgenicity. Several recent reports, including some from our laboratory, have shown the effectiveness of retroviral-based gene therapies to induce or improve bone formation [179, 194, 251-253]. The long-term expression of the transgene with this vector necessitated the development of regulatable protein expression systems. Our laboratory reported on the development of a retroviral-based system that causes expression of the transgene only in the presence of Doxycycline [253]. Since then, we have used this vector encoding for BMP4 to improve the healing of calvarial defects in mice [245]. Retroviral vectors are good tools to study the interactions of proteins due to the long-term expression following transduction.

### 4.1.2 Ex Vivo Gene Therapies using Different Cell Types

The process of ex vivo gene therapy involves the genetic manipulation of cells in vitro before they are introduced into the site of desired effect. The cells used in this process must be able to express the transgene and, optimally, should be able to participate in tissue regeneration. Many investigators have identified cell sources from postnatal tissue that show potential for use in bone regeneration applications.

#### 4.1.2.1 Mesenchymal stem cells

Mesenchymal stem cells (MSCs) can be isolated from bone marrow aspirate. These cells have been shown to be able to differentiate into bone [254] and can be used in ex vivo gene therapy approaches for bone regeneration [175, 179]. However, there are very few MSCs present within

bone marrow aspirate. This scarcity of cells necessitates long culture periods to increase the cell number to an applicable level. For this reason, the clinical application of MSCs is limited.

#### 4.1.2.2 Adipose-derived cells

Recently, several groups have shown that cells derived from adult adipose tissue are capable of undergoing osteogenic differentiation [192, 193]. Recently, Peterson et al. (2005) showed the ability of human adipose-derived cells transduced with AdBMP2 to improve healing in long bone defects in nude rats [178]. Adipose-derived cells are of interest clinically because adipose tissue is abundant, easy to collect, and the cells are fairly easy to isolate. However, these adipose-derived cells are a heterogeneous population of cells. Therefore, it is still unclear which cells within the population are directly responsible for bone formation.

#### 4.1.2.3 Skeletal muscle-derived cells

In 2000, our laboratory reported on the use of populations of cells, derived from the muscles of postnatal mice, to enhance bone regeneration [198]. Since then, we have utilized retroviral-mediated gene transfer of BMP2 and BMP4 to enhance bone regeneration within cranial and long bone defects in mice and rats through ex vivo gene therapy [251-253, 255, 256]. We also have combined BMP4 and VEGF gene-based therapies to further enhance bone formation [256].

### 4.1.3 Gene Therapy for Postoperative Resynostosis

In order to test the effects of Noggin on the inhibition of postoperative resynostosis, a treatment strategy was developed to have long-term Noggin exposure at the suturectomy site. A novel retroviral vector was developed using previously established backbones [253] that induced the

expression of both Noggin and green fluorescent protein (GFP) in the infected cell. A retroviral vector was chosen because of its ability to incorporate the transgene into the host cell's genome, allowing for longer-term expression of Noggin. Muscle-derived stem cells were chosen because these cells have been shown to have the ability to survive implantation and express transgenes for an extended period of time [199, 245, 251-253, 255-258]. An ex-vivo approach was used in this study to control the cell type that was transduced and to allow for controlled dosage by standardizing the number of cells that were implanted in the surgery site.

## 4.2 HYPOTHESIS

This study was designed to test the hypothesis that ex vivo Noggin gene therapy would inhibit bone formation and resynostosis in a mouse model of postoperative resynostosis.

## 4.3 MATERIALS AND METHODS

### 4.3.1 Cell Culture

Muscle-derived stem cells (MDSCs) were isolated from the skeletal muscle of postnatal mice as described previously [198, 259]. Cells were cultured in proliferation medium (DMEM supplemented with 10% fetal bovine serum (FBS, Invitrogen), 10% horse serum (HS, Invitrogen), 1% penicillin/streptomycin (Invitrogen), and 1% chick embryo extract (CEE, Accurate Chemical and Scientific Corporation, Westbury, NY) on collagen-coated flasks

(Collagen I, Sigma) as described previously [259]. Cells were grown until a sufficient number was reached to use for transduction.

### 4.3.2 Cell Transduction

Cells were plated at low confluence into an uncoated T25 flask and allowed to attach in proliferation medium. The next day, cells were transduced with a 1:1 ratio of either a retroviral vector to express GFP (CLGFP) or Noggin and GFP (CLNogG) to proliferation medium along with 8µg/ml Polybrene. The retroviral vector construction was described previously [253] (**Figure 18A**) with either of two alterations (**Figure 18B,C**). The cells were transduced for 3 days with 3 changes of the medium containing the retrovirus. Cells were then split and plated into T75 flask and grown for cryo-storage and bioassay. After 2 days in culture, cells were inspected with fluorescence microscopy to estimate transduction efficiency.

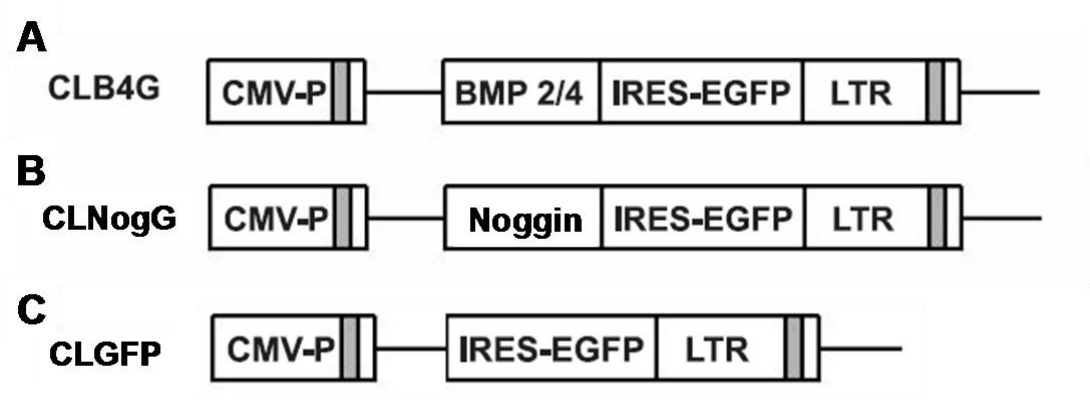


**Figure 18: Structures of retroviral vectors**

Diagram showing the structures of the retroviral vectors used in this study. **A**) The original retroviral vector, as described in Peng et al., 2004 [253] which included a BMP2/4 gene and a gene encoding enhanced green fluorescent protein (EGFP) preceded by an internal ribosome entry site (IRES) allowing for coincident expression of both BMP and GFP genes. **B**) Novel retroviral vector created by cutting out the BMP2/4 gene in **A** and replacing it with the Noggin gene (as developed in Peng et al., 2005 [245]). **C**) Retroviral vector encoding only the GFP gene.

### 4.3.3 Bioassay

In order to test the expression of functional Noggin in our transduced cells, we performed a bioassay as previously described [212, 245]. Briefly, cells were seeded in 6 well plates and allowed to grow to confluence in proliferation medium. After reaching confluence, the medium was changed and the cells grew for an additional 48 hours. At this time, the conditioned medium (CM) was collected and the cells were counted using a Trypan Blue exclusion assay. Functional Noggin expression was quantified using Noggin's ability to inhibit BMP4's induction of alkaline phosphatase (ALP) activity in C2C12 cells. C2C12 cells are a myogenic cell line that is responsive to BMP4 signaling by becoming ALP-positive. Control cells were stimulated with either BMP4 only (50ng/ml), with BMP4 and a known dilution of Noggin, or with proliferation medium only. Serial 2-fold dilutions of CM were added to C2C12 cells at the same time as 50ng/ml of BMP4. The amount of Noggin within each sample can be quantified by determining the number of dilutions that it takes before the CM is unable to inhibit BMP4 activity (cells turn blue after ALP staining).

### 4.3.4 Scaffold Seeding

Cells were seeded onto compressed Gelfoam® scaffolds as previously described [245, 253, 255, 256]. Briefly, the day before surgery, cells were trypsinized and counted. Two millimeter thick compressed Gelfoam® was cut into 3x3mm squares (yielding 3x3x2mm scaffolds) under sterile conditions and each scaffold was placed into a well in a 6 well plate. Cells were resuspended in proliferation medium to a concentration of $4x10^5$cells/25µl. Each 25µl aliquot was added to a Gelfoam® scaffold and allowed to soak into the scaffold (approximately 20 minutes). After the

cells had penetrated into the scaffold, 3ml of medium was added to each well and the construct was allowed to incubate overnight at 37°C. The next day, only constructs that showed very few cells attached to the well or in the medium were used for implantation.

### 4.3.5 Sample

One hundred-eight male C57BL/6J mice, 10 weeks old, were used in this study. The mice were randomly assigned to three groups as follows: Group 1) Suturectomy with no treatment, which served as the surgical control group (n = 36); Group 2) Suturectomy treated with cells expressing green fluorescent protein (GFP) in Gelfoam®, which served as the cell and vehicle control group (n = 36); and Group 3) Suturectomy treated with cells expressing Noggin and GFP in Gelfoam®, which served as the treatment group (n=36).

### 4.3.6 Surgical Technique

As seen in the data presented in Chapter 3 of this work, we have developed a novel model for postoperative resynostosis in the adult mouse. At 10 weeks of age, all mice were anesthetized with 4% isofluorane via inhalation. Anesthesia was maintained using 2% isofluorane via a nosecone. The scalps were shaved and prepared for surgery. Under sterile conditions, the calvaria were exposed via a midline scalp incision, and the skin was reflected laterally to expose the midline sutures. The fused interfrontal sutures were identified and the overlying periosteum was removed. A 0.5mm cutting burr fixed to a hand engine (2000rpm) was used to remove a region of the posterior interfrontal suture approximately 1mm in anteroposterior length, for a

final defect approximately 0.5mm x 1.0mm in size. Care was taken to avoid damage to the underlying dura mater and sagittal sinus.

In mice in the suturectomy control group (Group 1), the suturectomy was performed with no further treatment and the skin was reapproximated and closed using with 4-0 silk suture. In mice in the cell/vehicle control group (Group 2), a Gelfoam® scaffold loaded with $4x10^5$ GFP-expressing cells was used to cover the suturectomy site. In mice in the experimental group (Group 3), the suturectomy site was covered with a Gelfoam® scaffold loaded with $4x10^5$ cells expressing Noggin and GFP. In mice in Groups 2 and 3, the skin was reapproximated along the midline to cover the implant and the skin was closed using 4-0 silk suture. Animals from each group were killed 4, 8, and 12 weeks after surgery, heads were removed, and skulls were fixed in 10% neutral buffered formalin for 24 hrs. Following fixation, skulls were removed from fixative and placed in 70% ethanol for storage.

### 4.3.7 Radiographic Analysis

Each sample was processed for radiographic analysis the same way. The cranial base and brain were removed prior to scanning. Radiographs were taken at 5x magnification with a Faxitron (MX-20, Faxitron X-ray Corporation) set to 35kV and 250sec exposure on Kodak X-OMAT V film. Developed x-ray films were scanned with a Microtek ScanMaker 9800XL set for radiographic scanning at 1200dpi. The images generated were then imported into Northern Eclipse software (Empix Imaging) for digital measurement of defect area.

### 4.3.8 µCT

The animals in each group that were to be killed at the 12 week time point were serially scanned on a VivaCT40 scanner (Scanco Medical, USA) 4, 8, and 12 weeks after surgery (55kVp, 142µA, scan length: 3.12mm, scan time: 5 minutes, voxel size: 30µm). Each scan produced 104 images (**Figure 19A**) that encompassed the entire region of interest. On each image where there was a visible defect, the margins of the defect were traced (**Figure 19B**) and the total defect volume was calculated using the VivaCT software.

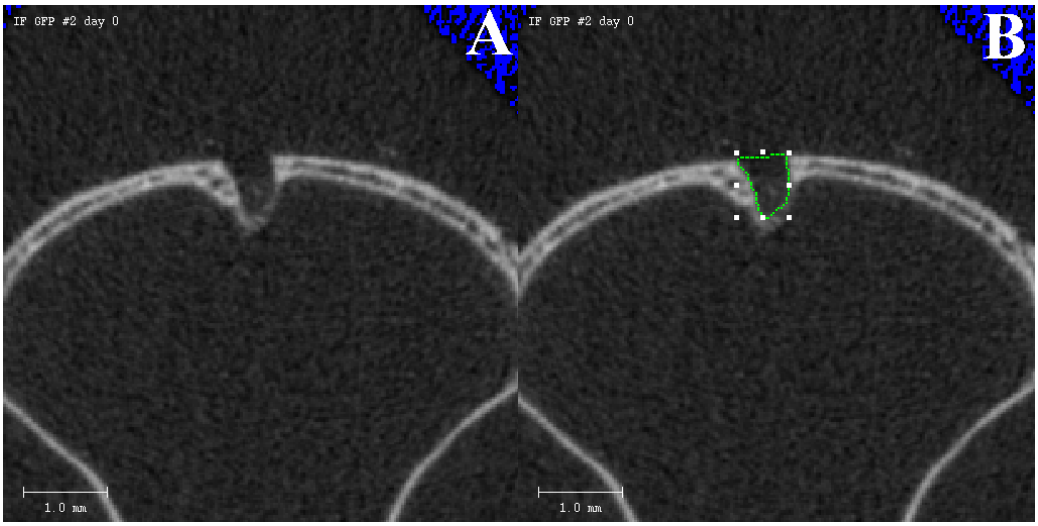


**Figure 19: 2D µCT scan of live mouse with defect**

**A**) Photograph showing a single 2-dimensional slice that is used to measure defect volume. **B**) Image showing a representative tracing of the margin of the defect in the slice shown in A. Each scan for this study generated 104 such images that were used to generate the 3-dimensional reconstructions.

### 4.3.9 Histology

Samples were decalcified in 10% EDTA for 7 days, dehydrated in serial alcohols, and processed for paraffin embedding. Paraffin blocks were cut on a microtome at 5µm thickness every 75µm in the coronal plane from the frontonasal suture, through the frontal bones, to the bregma. Slides were stained with hematoxylin and eosin for qualitative histological analysis.

### 4.3.10 Statistical Analysis

Means and standard deviations for 2-dimensional defect areas were calculated and compared among conditions using a 3 x 1 (surgical group by time) one way analysis of variance. Intergroup differences were assessed using the LSD multiple comparisons test (SPSS v12.0.1). Means and standard deviations for 3-dimensional defect volumes were calculated and compared among conditions using a 3 x 4 (surgical group by time) multiple comparisons test to assess group and age interactions. One way analysis of variance was performed to assess group differences at each time point (3 x 1 surgical group by time). Mean differences were considered significantly different if $p < 0.05$.

## 4.4 RESULTS

### 4.4.1 Noggin Expression

Qualitative microscopic analysis showed viable cells following transduction (**Figure 20A**). We found variable levels of GFP expression among cells within the population, but greater than 90% transduction efficiency (**Figure 20B**).

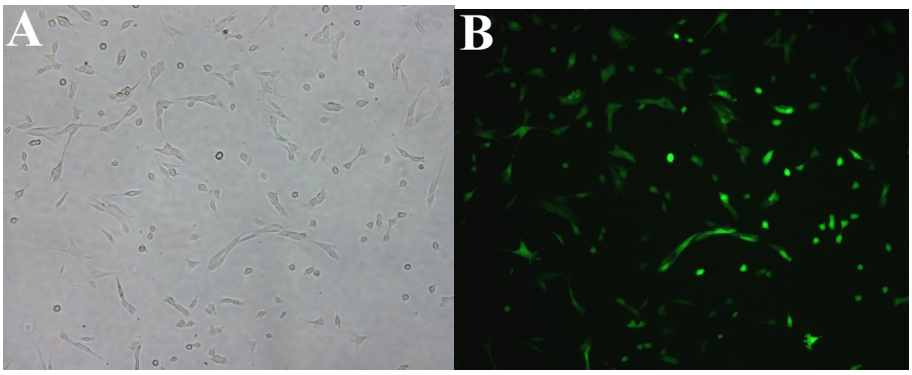


**Figure 20: Photomicrographs showing transduction efficiency**

**A**) Phase contrast image of MDSCs transduced with the CLNogG retroviral vector. **B**) Fluorescent image of the same field as **A** showing expression of GFP after transduction with CLNogG retroviral vector. Note that there was nearly 100% transduction efficiency after the three day exposure to retroviral vector.

Cell counts for the CM samples used for the bioassay showed that, in a confluent well of a 6 well plate, there were approximately $5x10^6$ cells. By testing the CM collected from these confluent wells, we found that the CM from a single well had approximately 125ng/ml of Noggin (**Figure 21**). Adjusting for cell number, media volume, and collection time, we determined that these cells produced approximately 35.4ng/$10^6$cells/day.

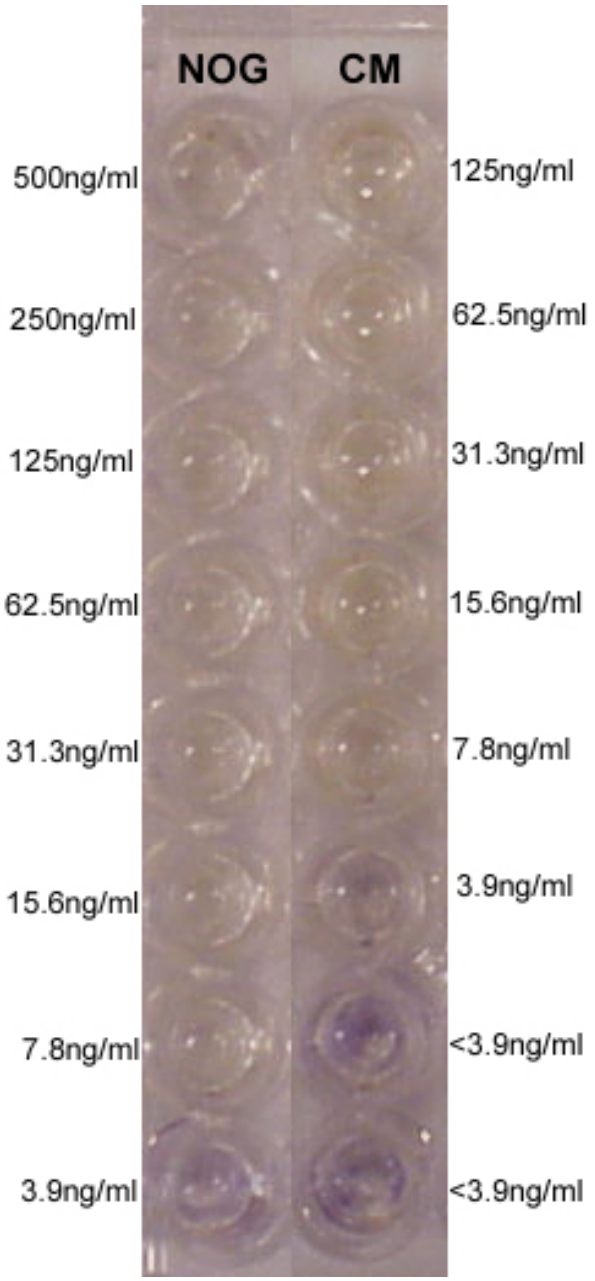


**Figure 21: Noggin concentration as determined by bioasay**

Photograph of lanes of 96 well plate seeded with C2C12 cells. All cells were fed with 50 µl of 50ng/ml BMP4 and 50µl of dilutions of either known amounts of Noggin (NOG, left lane, known concentration shown) or conditioned medium (CM, right lane). Noggin control becomes too dilute to inhibit BMP4 activity at 3.9ng/ml. The CM lane is considered 3.9ng/ml in the first well that turns blue. By doubling the concentration for each well above the first blue well, the initial concentration of the CM is determined.

### 4.4.2 Radiographic Analysis

Radiographs showed that defects in all groups healed over time (**Figure 22**). The Noggin treated defects grossly seemed to be larger than either GFP or control defects at 4 and 8 week time points.

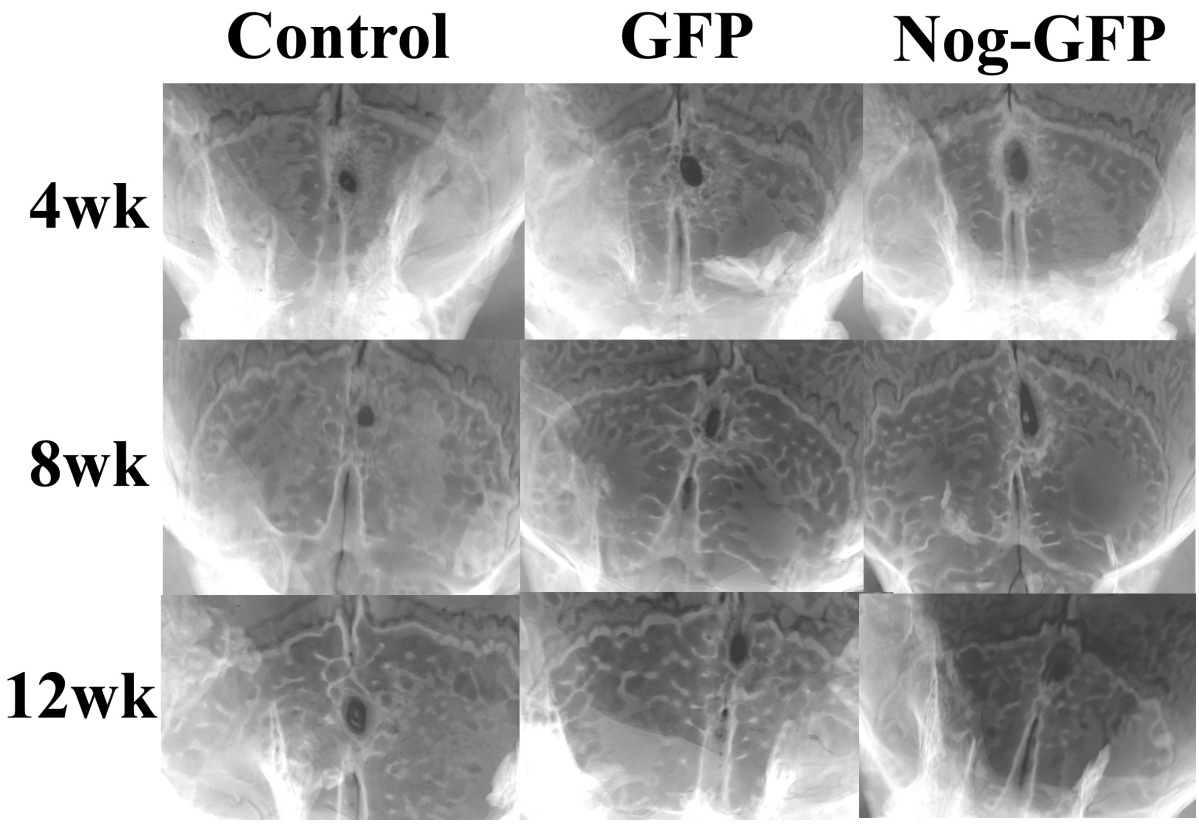


**Figure 22: Radiographs of healing interfrontal defects**

Radiographs taken from animals killed 4, 8, or 12 weeks after interfrontal suturectomy. Notice that the Noggin treated defects tend to be larger than the GFP treated or untreated control defects.

Statistical analysis of defect areas measured from radiographs revealed significant group ($F=5.56;p<0.01$) and age ($F=9.40;p<0.001$) main effects. A significant group x age interaction effect was noted ($F=2.95;p<0.05$), showing that defect area was changing differently among groups over time. Four weeks after surgery, there was a significant difference between the areas of untreated control defects ($0.0929mm^2 \pm 0.06$) compared to defects treated with Noggin expressing cells ($0.1808mm^2 \pm 0.09$; $p<0.05$). The GFP treated defects ($0.1379mm^2 \pm 0.08$) were not significantly different from either untreated control or Noggin treated defects (**Figure 23A**). At 8 weeks after surgery, the Noggin treated defects ($0.1476mm^2 \pm 0.09$) were significantly larger than either untreated control defects ($0.0755mm^2 \pm 0.04$) or GFP treated defects ($0.0699mm^2 \pm 0.03$; $p<0.01$; **Figure 23B**). 12 week data show no significant differences between any of the treatment groups (**Figure 23C**).

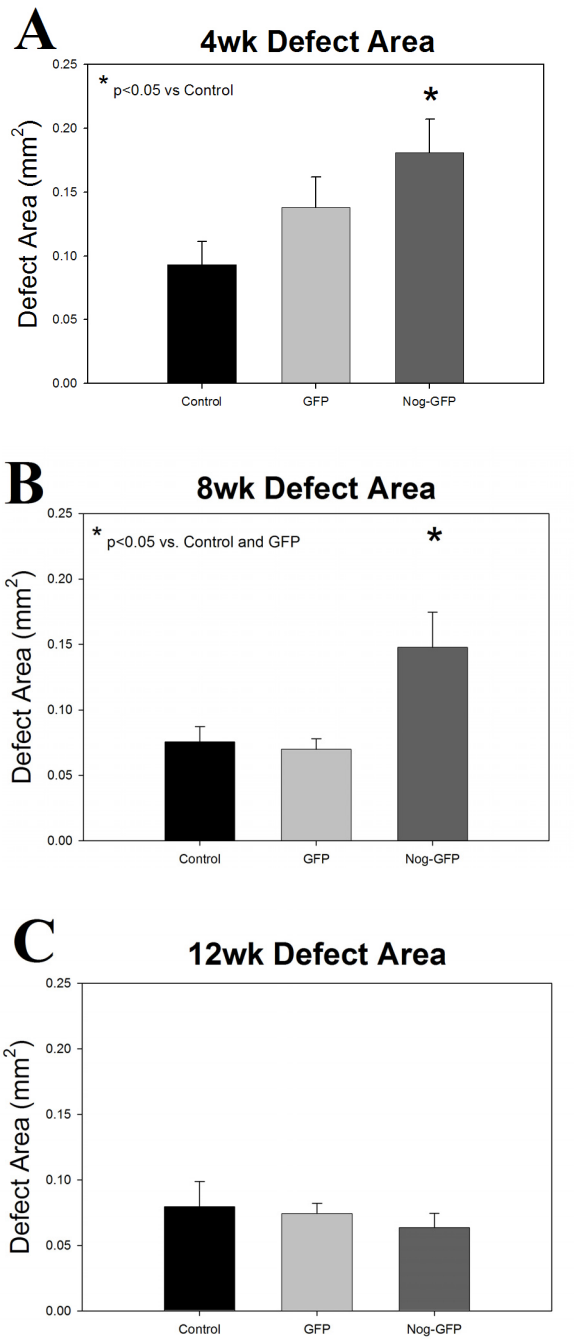


**Figure 23: Defect areas 4, 8, and 12 weeks after surgery**

**A**) Graph of the radiographic data of the 2D defect areas (±SEM) of defects from the three surgical groups 4 weeks after surgery. At this time, the Noggin treated defects (Nog-GFP) were statistically larger than control untreated defects. **B**) Graph of defect areas (±SEM) 8 weeks after surgery showing that Noggin treated defects were significantly larger than both untreated control and GFP treated defects. **C**) Graph of defect areas (±SEM) 12 weeks after surgery showing no differences in the mean areas between the treatment groups.

### 4.4.3 μCT Analysis

Longitudinal 3D μCT reconstructions showed that all defects in all groups healed over time (**Figure 24**). One animal in the control, untreated group showed evidence of an infection when it was killed 12 weeks postoperatively and all postoperative measurements from this animal were excluded from the study. No animals in any group showed complete healing of the interfrontal suturectomy over course of the study.

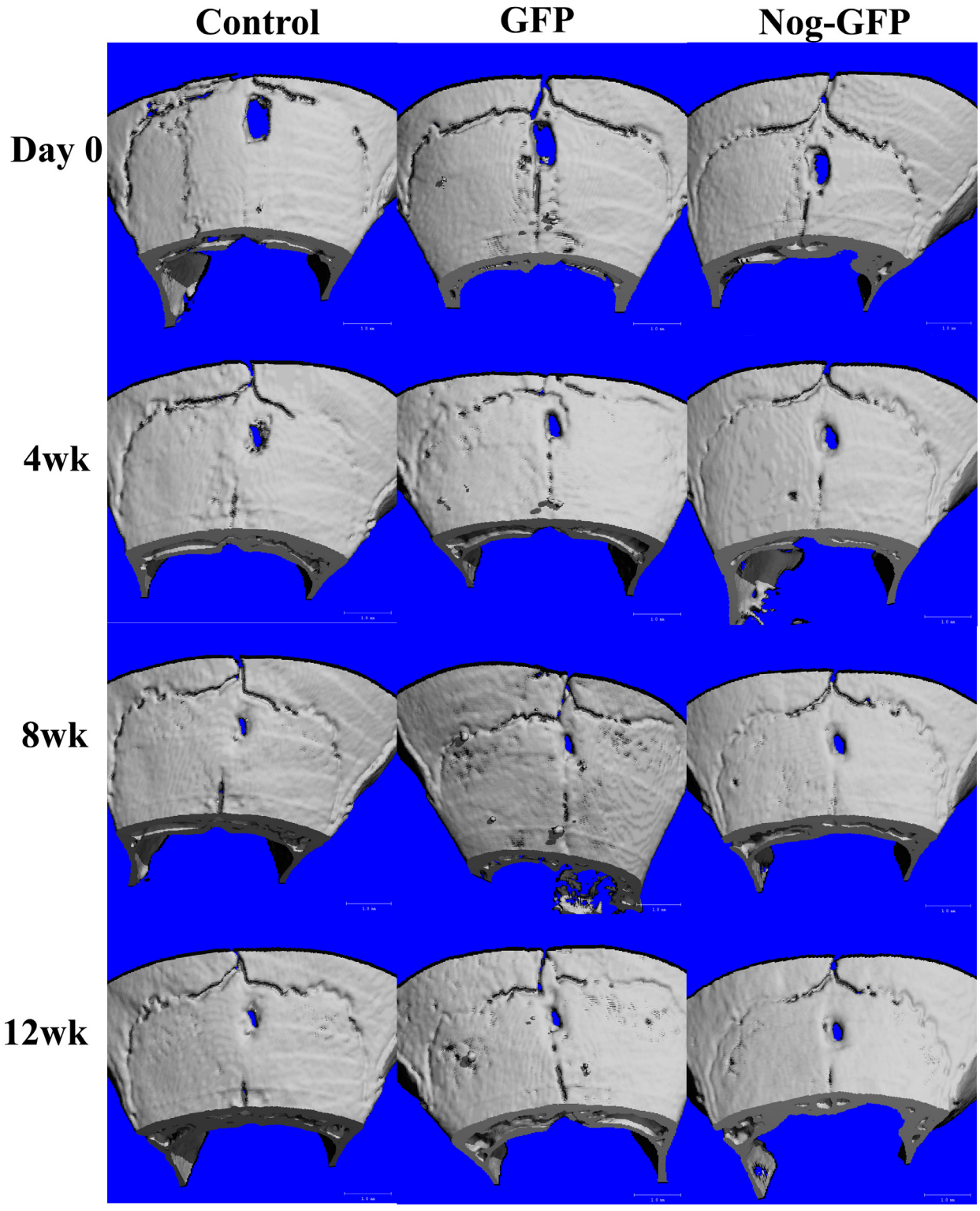


**Figure 24: 3D µCT reconstructions showing longitudinal defect healing in live animals**

Two-way ANOVA (3 x 4 group by time) on defect volumes measured from μCT scans revealed significant group ($F=20.85;p<0.001$) and age ($F=143.950;p<0.001$) main effects (**Table 1**). A significant group x age interaction effect was noted ($F=3.15;p<0.01$), showing that defect volumes were changing differently among groups over time.

**Table 1. Sources of Variability for 3 x 4 2-way ANOVA (Day 0, 4, 8, and 12 Weeks Postoperatively)**

| Sources of Variability | Sum of Squares | Mean Square | F | Sig. |
|---|---|---|---|---|
| Group | .045 | .023 | 20.850 | .000 |
| Time | .468 | .156 | 143.950 | .000 |
| Group x Time | .020 | .003 | 3.149 | .007 |
| Error | .139 | .001 | | |

Immediately postoperatively (Day 0), there was no significant volume differences among the treatment groups (**Table 2**, **Figure 25**, $F=0.029$;NS). Four weeks after surgery, there were significant differences between the volumes of all groups (**Table 2**, **Figure 25**, $F=14.73;p<0.001$). Eight weeks after surgery, volumes of Noggin and GFP treated defects were significantly larger than control defect volumes ($p<0.05$), but not different between Noggin and GFP treated defects (**Table 2**, **Figure 25**). By 12 weeks after surgery, Noggin treated defects were significantly larger than either GFP or untreated control defects ($p<0.01$) while GFP and control defects were not significantly different (**Table 2**, **Figure 25**).

**Table 2. Means and Standard Deviations of Defect Volumes**

| Group | Day 0 Mean Volume ±SD ($mm^3$) | 4wk Mean Volume ±SD ($mm^3$) | 8wk Mean Volume ±SD ($mm^3$) | 12wk Mean Volume ±SD ($mm^3$) |
|---|---|---|---|---|
| Control (n=11) | .1970 ± .0388 | .0469 ± .0220 | .0425 ± .0216 | .0287 ± .0200 |
| GFP (n=12) | .2009 ± .0468 | .0949 ± .0295‡ | .0709 ± .0275‡ | .0460 ± .0178 |
| NOG (n=12) | .1980 ± .0367 | .1307 ± .0519*† | .0893 ± .0296* | .0744 ± .0307*† |

*=Nog vs. control, †=Nog vs. GFP, ‡=GFP vs. control

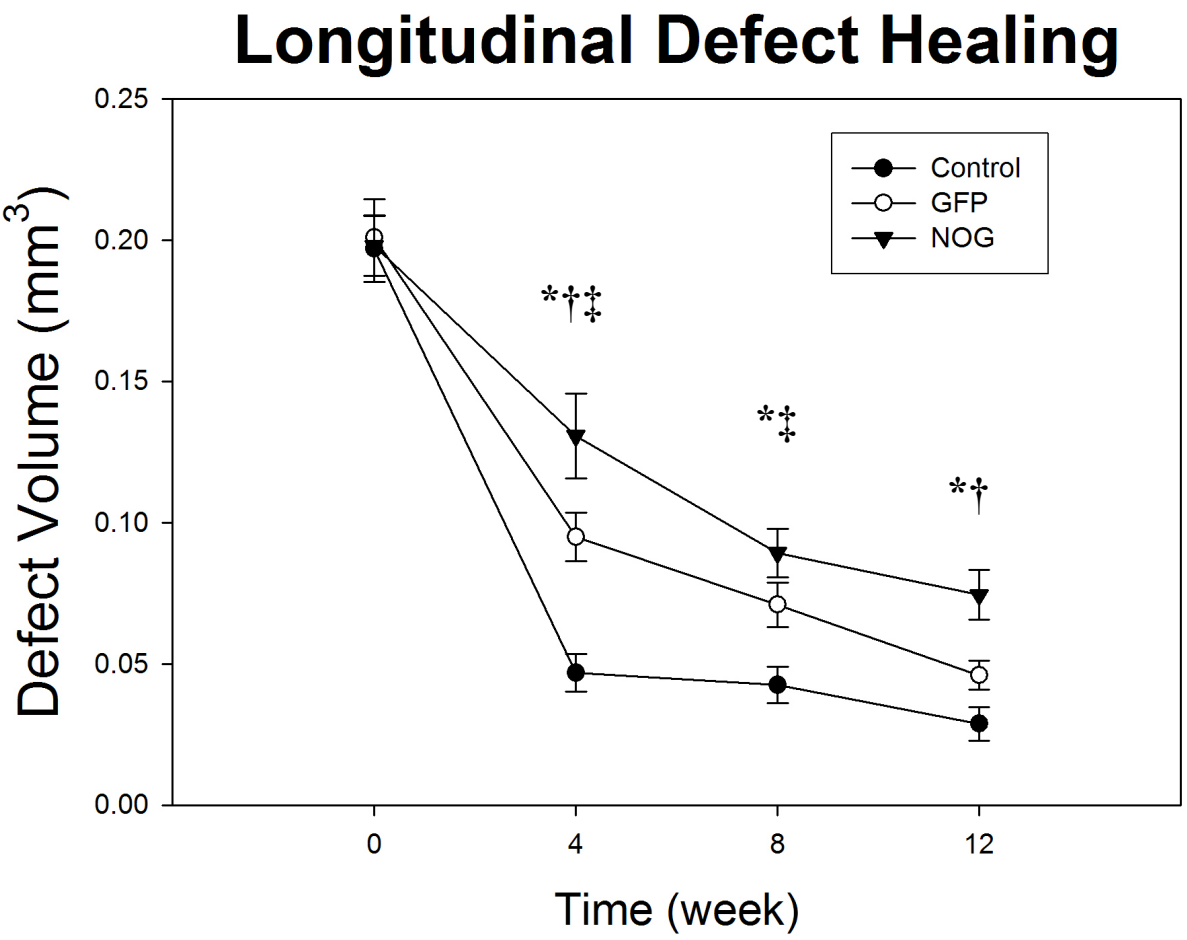


**Figure 25: Defect volumes over time**

Graph showing defect volume changes (±SEM) measured from longitudinal µCT scans at different postoperative time points (see **Table 2**). All groups healed over time. Noggin treated defects were significantly larger than control defects at all time points after surgery (*). Noggin treated defects were significantly larger than GFP treated defects 4 and 12 weeks after surgery (†). GFP treated defects were significantly larger than control defects both 4 and 8 weeks after surgery (‡).

Over the first 4 weeks of the study, the untreated control group showed significant healing (approximately 76% of the original defect size). Between 4 and 12 weeks postoperatively, these defects only healed an additional 9% of the original defect size (for a total of approximately 85% healing). Because of this difference in healing rates, the data seemed to show two distinct phases of defect healing. The first phase was characterized by rapid healing of the defects and occurred within the first 4 weeks following surgery. The second phase was characterized by small, incremental healing of the defect volume and occurred between 4 and 12 weeks after surgery. A 3 x 2 (surgical group by age) 2-way ANOVA to compare changes in defect volume between day 0 and 4 weeks postoperatively among the treatment groups showed significant group and age main effects (**Table 3**). There was also a significant group x age effect (**Table 3**). Among 4, 8, and 12 week measurements, there were significant group and age main effects, but there was no group x age effect noted (**Table 4**).

**Table 3. Sources of Variability for 3 x 2 2way ANOVA (Day 0 and 4 Weeks Postoperativley)**

| Sources of Variability | Sum of Squares | Mean Square | F | Sig. |
|---|---|---|---|---|
| Group | .021 | .010 | 6.820 | .002 |
| Time | .203 | .203 | 132.449 | .000 |
| Group x Time | .020 | .010 | 6.433 | .003 |
| Error | .098 | .002 | | |

**Table 4. Sources of Variability for 3 x 3 2way ANOVA (4, 8, and 12 Weeks Postoperativley)**

| Sources of Variability | Sum of Squares | Mean Square | F | Sig. |
|---|---|---|---|---|
| Group | .059 | .030 | 33.771 | .000 |
| Time | .030 | .015 | 16.885 | .000 |
| Group x Time | .006 | .002 | 1.714 | .153 |
| Error | .085 | .001 | | |

### 4.4.4 Histological Analysis

Qualitative analysis of cross sectional histological slides from animals killed 4, 8, and 12 weeks after surgery showed healing in all bone defects in all groups (**Figure 26**). The bony tissue within the defect was disorganized 4 weeks after surgery, and progressively became more organized. Sections were identified within each sample that showed remaining defects filled with fibrous tissue at each time point after surgery (**Figure 26**).

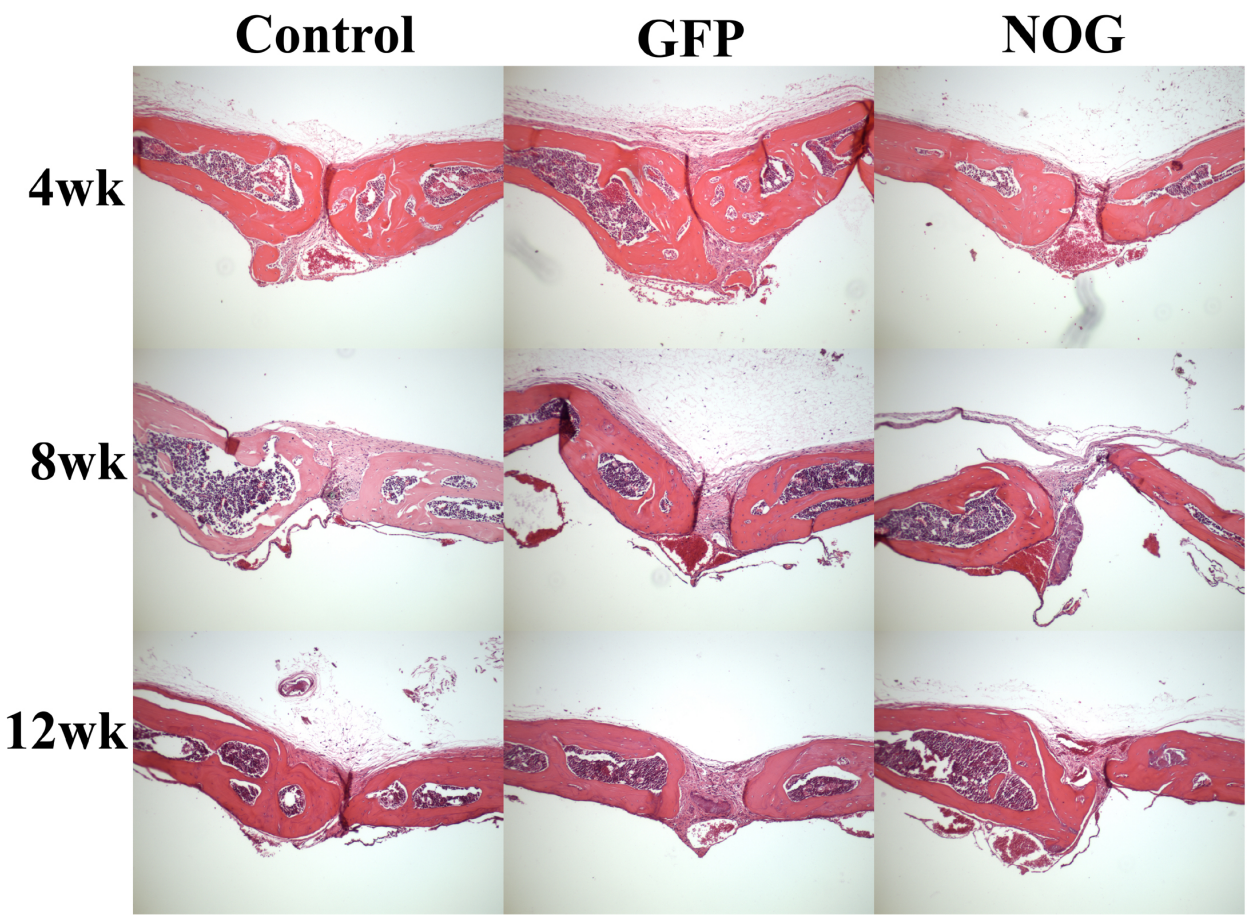


**Figure 26: Histology of suturectomy site healing**

Histophotomicrographs of interfrontal suturectomy sites from untreated (control), GFP treated (GFP), or Noggin treated (NOG) animals. Notice that defects in all groups showed healing within the defect.

## 4.5 DISCUSSION

Craniosynostosis is the term given to the premature fusion of cranial sutures. Such early suture fusion inhibits the normal growth of the brain, causes increased intracranial pressure, and necessitates surgical intervention. Although the surgical techniques currently employed normally lead to increased intracranial volume, decreased intracranial pressure, and improved craniofacial growth, the occurrence of resynostosis of the suturectomy sites can negatively affect postoperative outcomes.

We believe that a molecular adjunct to surgical intervention that targets potent bone forming growth factors expressed during normal bone healing would function to inhibit bone formation and improve postoperative outcomes.

This study was designed to test the hypothesis that postoperative treatment of a suturectomy site with Noggin, a BMP antagonist, would inhibit bone formation within the suturectomy site.

To test this hypothesis, we used an ex vivo gene therapy approach to transduce muscle-derived stem cells to constitutively express Noggin. These cells were implanted onto a mouse interfrontal suturectomy site within a gelatin scaffold. Defect healing was assessed using radiographic, μCT, and histological analyses.

Radiographic analysis showed that Noggin treated defects were significantly larger than untreated control defects 4 and 8 weeks postoperatively. The difference observed at these earlier time points were not apparent 12 weeks after surgery. The GFP treated defects tended to be larger than the untreated control defects 4 weeks after surgery, but this difference diminished by

8 weeks after surgery. Although we expected the GFP treated defects to heal similarly to the untreated control defects, we assume that the inhibition that was observed in the GFP group came from some immune response that the mice had to the implantation of cells within a gelatin scaffold. In spite of this response that we assume was also present in the Noggin treated groups, the data suggest that only through the addition of Noggin was bone formation significantly inhibited. Twelve weeks after surgery, all of the defects were relatively the same size in all groups. From this radiographic data, we would conclude that ex vivo Noggin gene therapy inhibited bone formation for approximately 8 weeks in this model.

Through the use of μCT technology, we were able to assess longitudinal defect healing in a cohort of these animals. Noggin treated defects were significantly larger than untreated control defects at all times after surgery. The GFP treated group healed differently than the untreated control group, evidenced by the statistically larger defects both 4 and 8 weeks after surgery. Finally, Noggin treated defects were significantly larger than the GFP treated defects 4 and 12 weeks after surgery. These data show that both Noggin and GFP treatment significantly inhibited bone formation in this model 4 and 8 weeks after surgery. However, Noggin was more effective than GFP 4 weeks after surgery and was the only treatment group significantly larger than untreated controls 12 weeks after surgery. These data suggest that treatment of small suturectomy sites with transduced cells in a gelatin matrix can inhibit bone formation, but significant longer-term inhibition is only achieved when these cells express Noggin. Therefore, we feel confident that Noggin is effective in inhibiting bone formation in this model of resynostosis.

The longitudinal μCT data also demonstrated a biphasic healing process that occurs in this model of resynostosis. The first phase of rapid healing occured within the first 4 weeks after

surgery. The second phase of slower healing occurred between 4 and 12 weeks. When we compared the defect volumes of the groups based on these phases, we found that Noggin treatment changed the rate of healing in the first phase, and had no effect on healing rate in the second phase, suggesting that the Noggin ex vivo gene therapy approach employed in this study did not have inhibitory effects after 4 weeks postoperatively. However, even though there was no evidence that our Noggin therapy continued to inhibit bone formation after 4 weeks, it did have a lasting effect on total bone formation, evidenced by the significantly larger defects in the Noggin treated group at 12 weeks.

Furthermore, the fact that there was very little defect healing observed after 4 weeks in this model gives insight into the discrepancy between the μCT data and the cross-sectional radiographic data. First, because the radiographic data was collected 4, 8, and 12 weeks after surgery, it only represents the healing that occurred in the second phase of defect healing, not during the first, rapid phase. The μCT data showed that Noggin treatment had its effect during the first phase, not the second phase, making the radiographic data less indicative of Noggin's possible effects. Second, the radiographic data is cross-sectional data, which means that the animals measured at 4 weeks postoperatively are not the same as the animals measured at either 8 or 12 weeks postoperatively. This discrepancy is most evident in the fact that the mean defect area of the untreated control group 12 weeks after surgery was actually larger than the 8 week measurement. The μCT data show continuous healing in all groups over time, which is a more realistic healing pattern. Finally, the radiographic data is less indicative of the true defect size because it changes 3-dimensional data (volume) into 2-dimensional data (area). Radiographs allow for the measurement of the area in which there is no bone on either the ectocortical or endocortical surface. The μCT scans were able to show the true defect margins, whether or not

the defect spanned both cortices (see **Figure 19**). For example, if a defect is cone-chaped, larger on the ectocortical surface and only slightly pierces the endocortex, then the radiograph would show a defect that was the size of the small endocortical defect. Therefore, we feel that traditional radiographic data, at least in this model, is much less reliable than the μCT data.

Though the causes of craniosynostosis are poorly understood, there is one trait that all cases, both syndromic and nonsyndromic, have in common: the overproduction of bone. In all cases, bone forms within the suture, a tissue that is supposed to be devoid of bone until the brain is completely grown. Regardless of the genetic or environmental etiology of the primary craniosynostosis, there is a risk of postoperative resynostosis [38, 52]. We believe that BMP signaling is at least in part responsible for calvarial bone healing and resynostosis following surgery. In fact, BMPs have been shown to be expressed in healing bone defects in the craniofacial skeleton [209].

Noggin has previously been shown to antagonize ectopic bone formation induced by BMPs [211, 212]. A single study has shown evidence that Noggin can inhibit membranous ossification [213]. That study used a bone chamber technique which involves injury to the rat tibia and analyzed the amount of bone that formed within a chamber attached to the injury site [213]. The current study is the first to give evidence that Noggin can inhibit bone healing in normally healing calvarial bone defects. The results presented here suggest that using Noggin to inhibit BMP signaling was effective in the inhibition of postoperative resynostosis in this mouse model. We believe that using Noggin treatment as an adjunct to surgical intervention may be useful to inhibit resynostosis, regardless of the etiology that caused the primary craniosynostosis.

This study is the first to use μCT to analyze the healing of small suturectomy sites in living mice. It is also the first study that addresses the inhibition of postoperative resynostosis using molecular therapies in a mouse model.

This model and similar analytical techniques can be used for continued research to inhibit postoperative resynostosis.

# 5.0 NOGGIN'S EFFECT ON BMP4-INDUCED BONE REGENERATION

## 5.1 INTRODUCTION

Bone is a notoriously regenerative tissue. Normally, in cases of fracture and surgical bone removal, bone has the capacity to heal itself. In many cases, however, bone defects heal with fibrous tissue, rather than with bone, termed a nonunion. Treatment of nonunions usually involves the surgical implantation of a bone graft to enhance healing. A recent review estimates that approximately 1.5 million bone grafting operations are performed each year [138]. Currently, autografting bone from other sites in the patient's body is the gold standard for the treatment of nonunions. Though this technique usually results in healing of nonunions, donor site morbidity, the lack of available harvest sites (especially in the pediatric population), and the high risk of poor outcomes makes autografting suboptimal [139, 140].

Many researchers have chosen to improve bone healing using potent bone-inducing proteins, the bone morphogenetic proteins (BMPs) -2, -4, and -7 [138, 149-151, 159-161, 260]. Although the results in animal experiments are overwhelming, the clinical use of BMPs has only recently begun [138]. It seems obvious that the clinical use of BMPs to assist the healing of many different type of defects will soon be a standard in clinical care.

To understand the applicability of growth factor-based bone enhancement therapies, we must first understand the role of growth factors during normal bone healing. Growth factors and

their antagonists act concurrently during most physiologic processes ranging from normal development and growth to repair or regeneration of damaged tissues. For example, during vertebrate embryogenesis, BMP4 interacts with its antagonist, Noggin, during various inductive events [261]. Such interactions are responsible for the dynamic patterning of Noggin expression in somites [262]. BMPs also have been shown to induce the expression of Noggin in cultured osteoblasts [263]. In vivo studies have revealed coordinated expression of BMPs and Noggin during early skeletogenesis [264] and fracture healing [210]. Tissue engineering and regenerative medicine together constitute a new medical frontier based on the use of interdisciplinary approaches to enhance tissue repair, regeneration, or replacement. Stem cell-based therapy alone or in combination with genetic engineering or gene therapy has become an attractive tissue engineering approach. Indeed, studies have shown that a number of osteogenic BMPs, administered in the form of either proteins or genes, can enhance bone healing and improve bone regeneration [198, 245, 253, 256, 258, 260, 265-267].

Because few efforts have been made to imitate the natural healing process during which the expression of growth factors is accompanied by the expression of their specific antagonists [210], many current therapeutic strategies lead to less than optimal outcomes. There is a paucity of information regarding strategies to control the size and shape of regenerated bone. Especially in the craniofacial region, the size and shape of the reconstructed/regenerated bone must be controlled to maximize function and minimize any interference with surrounding structures (such as nerves, blood vessels, or sensory organs). Toward this aim, researchers recently have developed an inducible gene therapy vector that enables regulated expression of BMP2 or BMP4 [267]. Our studies have demonstrated that MDSCs transduced by a tet-on self-inactivating retroviral vector expressing BMP4 and subcutaneously implanted elicit bone formation only in

the presence of doxycycline (Dox) [253]. We also have reported that these transduced MDSCs can promote regulated bone regeneration in a critical-sized skull defect [245]. Additionally, we have tested the hypothesis that administration of the specific BMP4 antagonist Noggin can further control the bone regeneration induced by stem cells expressing inducible BMP4 [245]. Our results show that the simultaneous administration of Noggin and BMP4 at a ratio of 1:5 (Noggin-expressing cells:BMP4-expressing cells) elicits the physiologic response that occurs naturally during fracture healing [245]. The simultaneous expression of these factors provided us with more stringent control over the inducible therapeutic effects of BMP4, and facilitated the regeneration of bone that more closely resembled the original tissue [245].

## 5.2 HYPOTHESIS

We hypothesized that a high ratio of Noggin expressing cells to BMP4 expressing cells will result in the formation of less ectopic bone and more dense bone within the defect site.

## 5.3 MATERIALS AND METHODS

### 5.3.1 Cell Culture

Muscle-derived stem cells (MDSCs) were isolated from the skeletal muscle of postnatal mice as described previously [198, 259]. MDSCs were cultured in proliferation medium (DMEM supplemented with 10% FBS [Invitrogen], 10% HS [Invitrogen], 1% penicillin/streptomycin

[Invitrogen], and 1% chick embryo extract [CEE, Accurate Chemical and Scientific Corporation, Westbury, NY]) on collagen-coated flasks (Collagen I, Sigma) as described previously [259]. Cells were grown until a sufficient number was reached to use for transduction.

### 5.3.2 Cell Transduction

Three populations of MDSCs were developed in this study from a single population of cells derived from postnatal muscle of C57BL/6J mice. The first population was transduced to express both BMP4 and β-galactosidase (B4 cells) using previously described vectors and protocols [256, 260, 268]. The second population of the same parent MDSCs was transduced to express Noggin and GFP (NOG cells) as described above (**Section 4.2.2**). The third population of MDSCs was transduced to express β-galactosidase only, to serve as a control transduced MDSC population (control). After transduction, proliferation of NOG cells was tested by plating $1x10^4$ cells per well in a 6-well plate and cells were counted using a Trypan Blue exclusion assay 48 hours after seeding. Cell numbers were compared to untransduced (naïve) cells cultured the same way.

### 5.3.3 Scaffold Seeding

Cells were seeded onto compressed Gelfoam® scaffolds as previously described [245, 253, 255, 256]. Briefly, the day before surgery, cells were trypsinized and counted. Two millimeter thick compressed Gelfoam® was cut into 5x5mm squares (yielding 5x5x2mm scaffolds) under sterile conditions and each scaffold was placed into a well in a 6 well plate. All three populations of MDSCs were resuspended in proliferation medium. Cells were mixed together at the correct ratios (**Table 5**), centrifuged, and resuspended to a concentration of $1.5x10^5$cells/25µl. Each 25µl

aliquot was added to a Gelfoam® scaffold and allowed to soak into the scaffold (approximately 20 minutes). After the cells had penetrated into the scaffold, 3ml of medium was added to each well and the construct was allowed to incubate overnight at 37°C. The next day, only constructs that showed very few cells attached to the well or in the medium were used for implantation. Extra cell aliquots were seeded directly onto 6-well plates for imaging 24 hours later.

**Table 5. Cell Number for Each Group of Constructs**

| | # of B4 cells | # of NOG cells | # of control cells |
|---|---|---|---|
| **GROUP 1** 1:2 control:B4 cells | $1 \times 10^5$ | 0 | $5 \times 10^4$ |
| **GROUP 2** 1:2 NOG:B4 cells | $1 \times 10^5$ | $5 \times 10^4$ | 0 |
| **GROUP 3** 1:5 NOG:B4 cells | $1 \times 10^5$ | $2 \times 10^4$ | $3 \times 10^4$ |
| **GROUP 4** 1:10 NOG:B4 cells | $1 \times 10^5$ | $1 \times 10^4$ | $4 \times 10^4$ |
| **GROUP 5** 1:20 NOG:B4 cells | $1 \times 10^5$ | $5 \times 10^3$ | $4.5 \times 10^4$ |

### 5.3.4 Sample

Twenty-two, 10 week old, male C57BL/6J mice (Jackson) were randomly assigned to five groups: **Group 1**) Defects treated with control and BMP4 expressing cells at a 1:2 ratio served as a BMP4 control group (n = 5); **Group 2**) Defects treated with Noggin and BMP4 expressing cells at a 1:2 ratio served as the highest concentration of Noggin expressing cells (n = 5); **Group 3**) Defects treated with Noggin and BMP4 expressing cells at a 1:5 ratio (n=4); **Group 4**) Defects treated with Noggin and BMP4 expressing cells at a 1:10 ratio (n=5); and **Group 5**) Defects treated with Noggin and BMP4 expressing cells at a 1:20 ratio (n=3) served as the lowest concentration of Noggin expressing cells. All animals were killed 6 weeks after surgery. This

protocol was approved by the Animal Research and Care Committee at Children's Hospital of Pittsburgh.

### 5.3.5 Surgical Technique

In each animal in each group, calvarial defects were created along the midline using a 5mm outer diameter round trephine (Fine Science Tools) as previously described [245]. In all animals, the cell/scaffold constructs were placed within the defects and the skin was approximated to cover the construct and sutured together.

### 5.3.6 µCT

Animals in each group were scanned on a VivaCT40 scanner (Scanco Medical, USA) 3 and 6 weeks after surgery (55kVp, 142µA, scan length: 6.36mm, scan time: 10 minutes, voxel size: 30µm). Each scan produced 212 images encompassing the entire 5mm bone defect region. On each image where there was a visible defect, a region of interest (ROI) was defined (**Figure 27A, region #1**) and the bone volume and bone volume mean density within the defect was calculated using the VivaCT software with a threshold set at 192. Mean densities were determined by calibrating the VivaCT using a phantom that has samples of known concentrations of hydroxyapatite (HA). Therefore, mean density was measured in terms of milligrams of HA per cubic centimeter (mgHA/cc). Following these calculations, the images were reopened and the defect ROI was used to define a region above and a region below the defect (**Figure 27B, region #2**). Then, the original defect ROI was deleted to leave only the ectopic bone ROI (**Figure 27C, region #2**). The ectopic bone volume and mean density was determined from this ROI in each

scan. Finally, the defect bone volume and ectopic bone volumes were added together to determine total bone volume and an efficiency measurement was calculated by dividing defect bone volume by total bone volume.

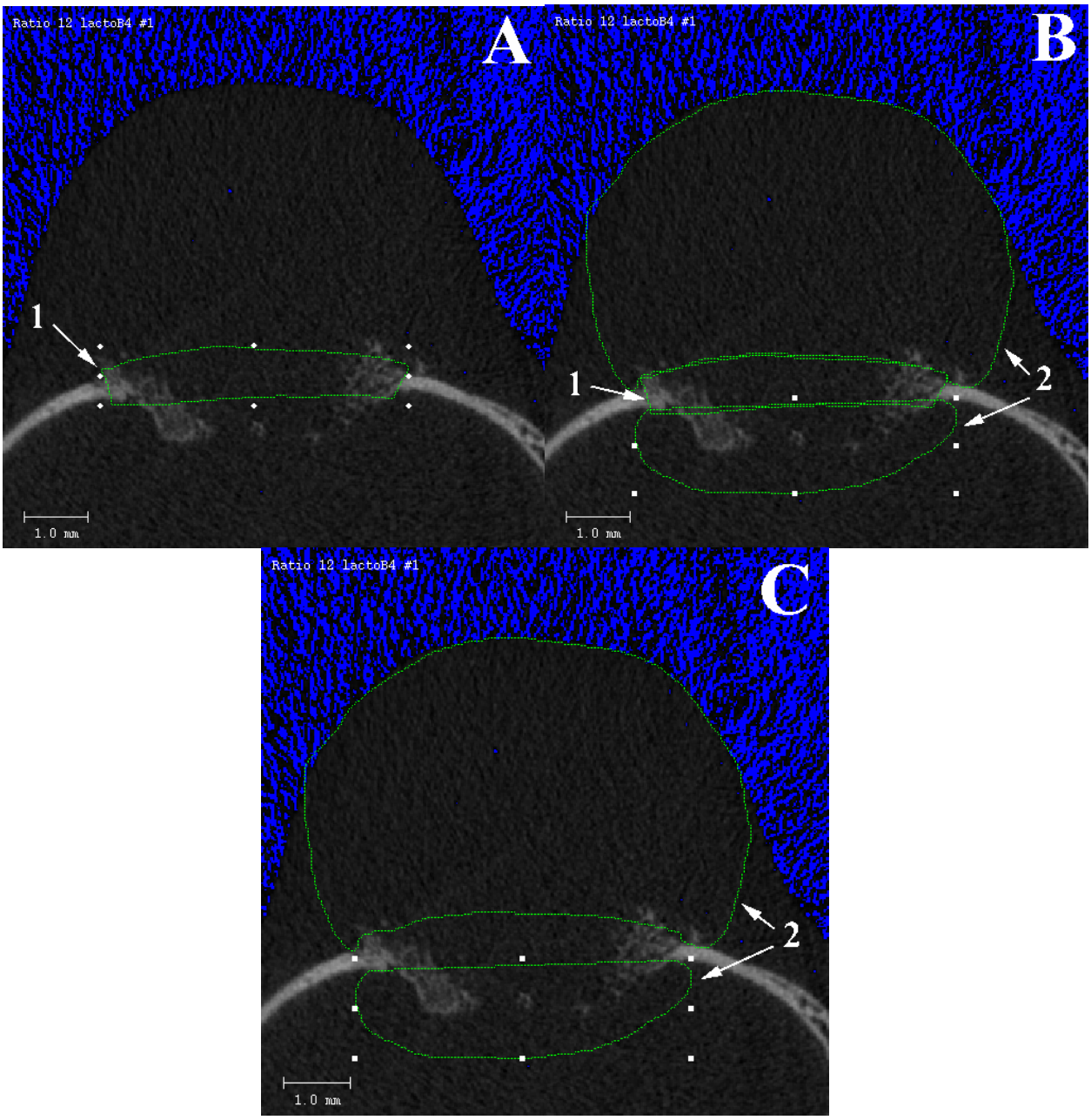


**Figure 27: µCT measurement technique**

**A**) Two-dimensional µCT scan showing the delineation of the defect region of interest (ROI) outlined in yellow (#1). **B**) Scan showing how the defect ROI (#1) was used to define the ectopic ROI (#2). **C**) Scan showing the ectopic ROI (#2) after the defect ROI was removed. ROI #1 was used to measure defect bone volume and defect bone volume mean density. ROI #2 was used to measure ectopic bone volume and ectopic bone volume mean density.

### 5.3.7 Statistical Analysis

Means and standard deviations for defect bone volume (DBV), defect bone volume mean density (DBVMD), ectopic bone volume (EBV), ectopic bone volume mean density (EBVMD), total bone volume (TBV), and treatment efficiency (DBV/TBV) were calculated and compared among groups at each time point using one way analysis of variance (ANOVA). Significant intergroup differences at each age were assessed using the Least Significant Differences multiple comparison test. The relationship between bone volume and bone density, or bone volume and efficiency was also assessed using Pearson product moment correlations. All data were analyzed using SPSS 12.0 for windows (SPSS, Inc., Chicago, IL). Differences were considered significant if $p < 0.05$.

## 5.4 RESULTS

### 5.4.1 Cell Culture

All cell populations survived transduction. A comparison of cell numbers showed no significant difference between the number of NOG cells ($6.67x10^4 \pm 2x10^4$) compared to untransduced cells ($8.33x10^4 \pm 6x10^3$) after 48 hours of culture ($p=0.252$,NS).

### 5.4.2 Scaffold Seeding

After cell aliquots were seeded onto the gelatin scaffolds, extra aliquots were plated into 6-well plates. NOG cells were transduced to simultaneously express both Noggin and GFP while the B4

cells expressed β-galactosidase. Photographs of an extra aliquot from Group 2 (1:2 NOG:B4; **Figure 28A**) showed the presence of a population of GFP-positive NOG cells (**Figure 28B**) within the majority of the cells that were not expressing GFP (**Figure 28C**).

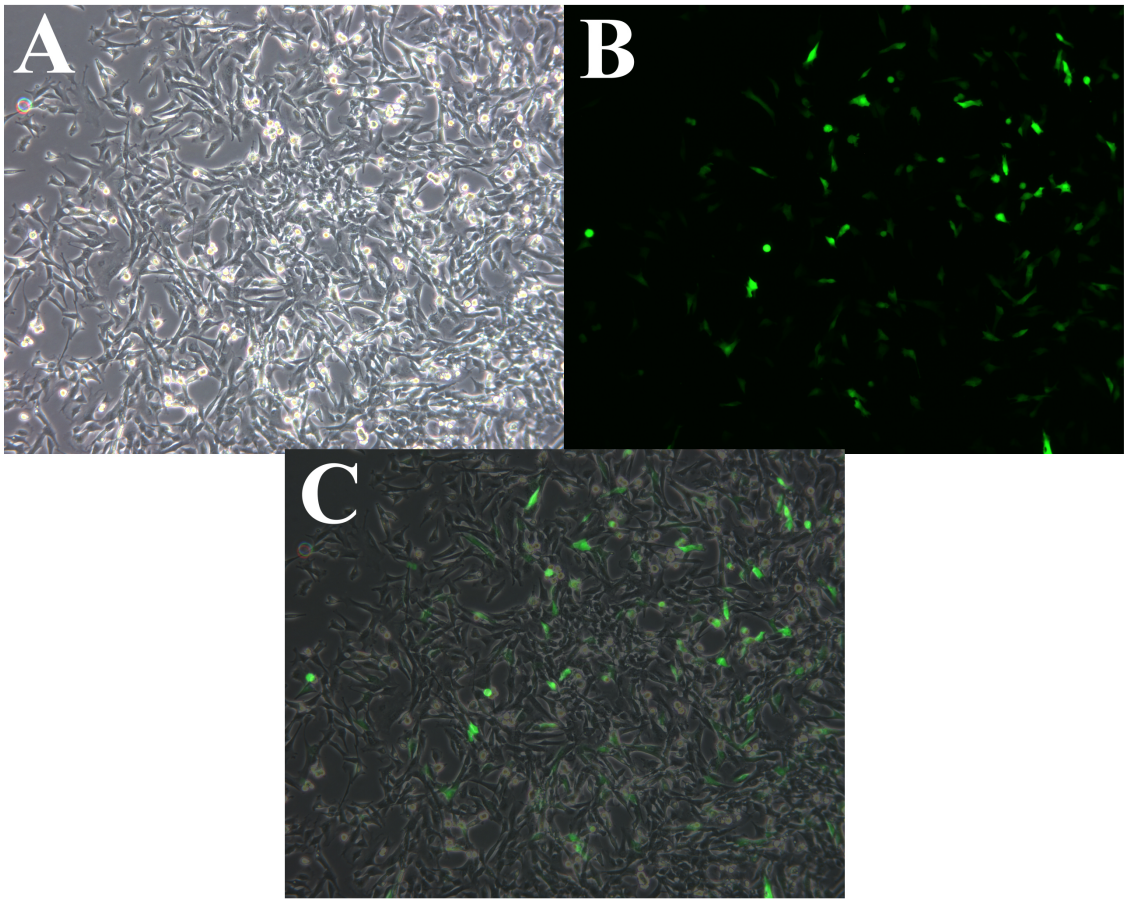


**Figure 28: Micrographs of 1:2 NOG:B4 cell mixture**

**A**) Phase contrast micrograph showing mixed cell culture from an aliquot of cells from Group 2 mixed for scaffold loading and grown in a culture plate for 24 hours. **B**) Fluorescent micrograph showing the presence of GFP-positive cells (NOG cells) within the culture shown in **A**. **C**) Image of merged **A** and **B** images showing that the GFP-positive NOG cells accounted for a subset of the total population (1:2 NOG:B4).

### 5.4.3 μCT analysis

Three and 6 weeks after surgery, μCT scans were taken from animals from each treatment group. All animals scanned showed healing of the defect with radioopaque tissue that resembled bone. There was some overgrowth of the bone around the defect 3 weeks postoperatively (**Figure 29**) that increased in size by 6 weeks (**Figure 30**). Grossly, there appeared to be less bone in the defects treated with 1:2 NOG:B4 cells (Group 2) than in the other treatment groups.

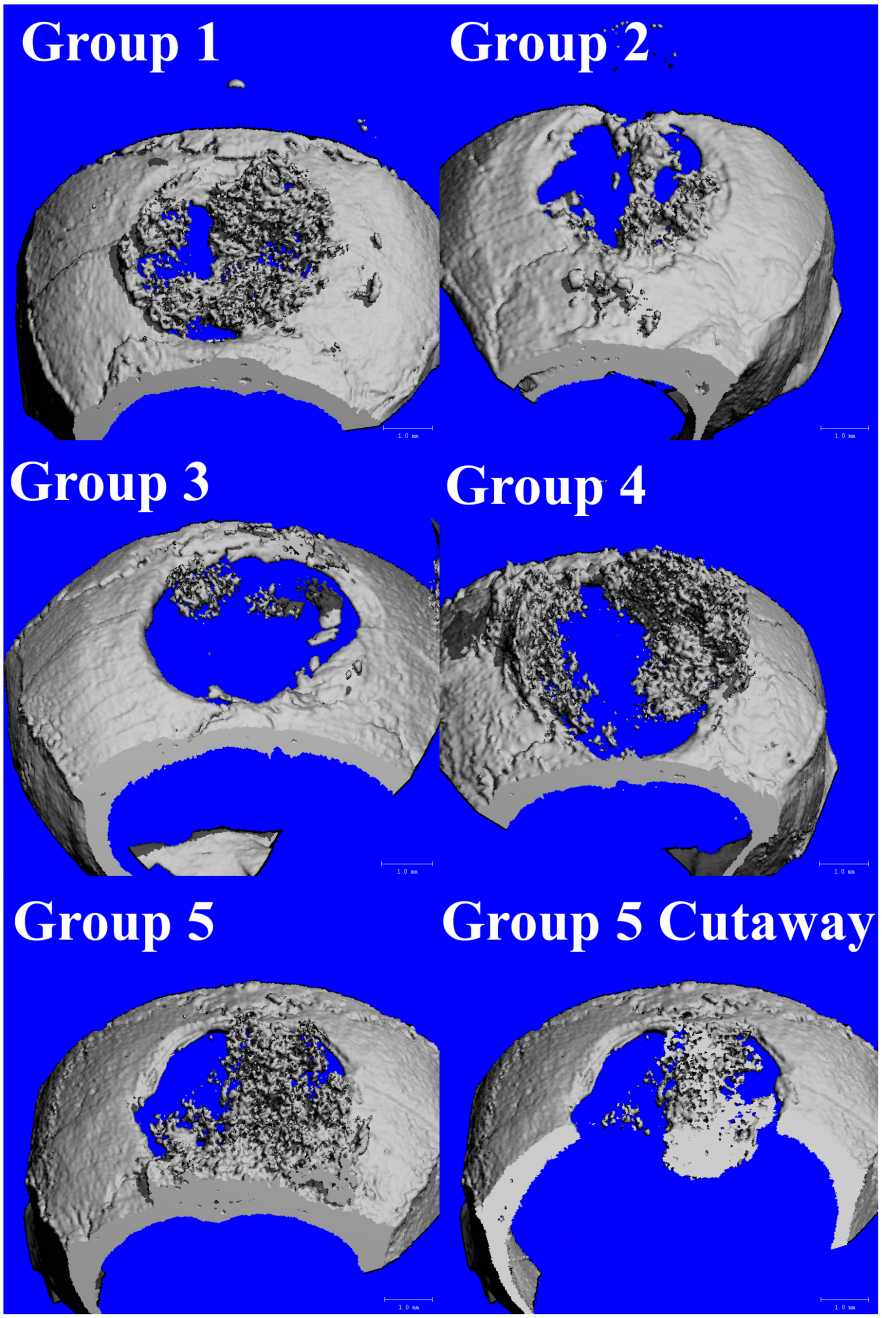


**Figure 29: 3D µCT reconstructions showing bone formation 3 weeks postoperatively**

3D reconstructions show the formation of bone in all treatment groups. Qualitative analysis suggested that there was less bone formed in Groups 2 and 3 (high doses of Noggin) compared to the other groups. Notice that the Group 5 reconstruction does not seem to show marked bone overgrowth on the outside of the skull (Group 5, left), but overgrowth can be seen intracranially, as shown in the cutaway image (right).

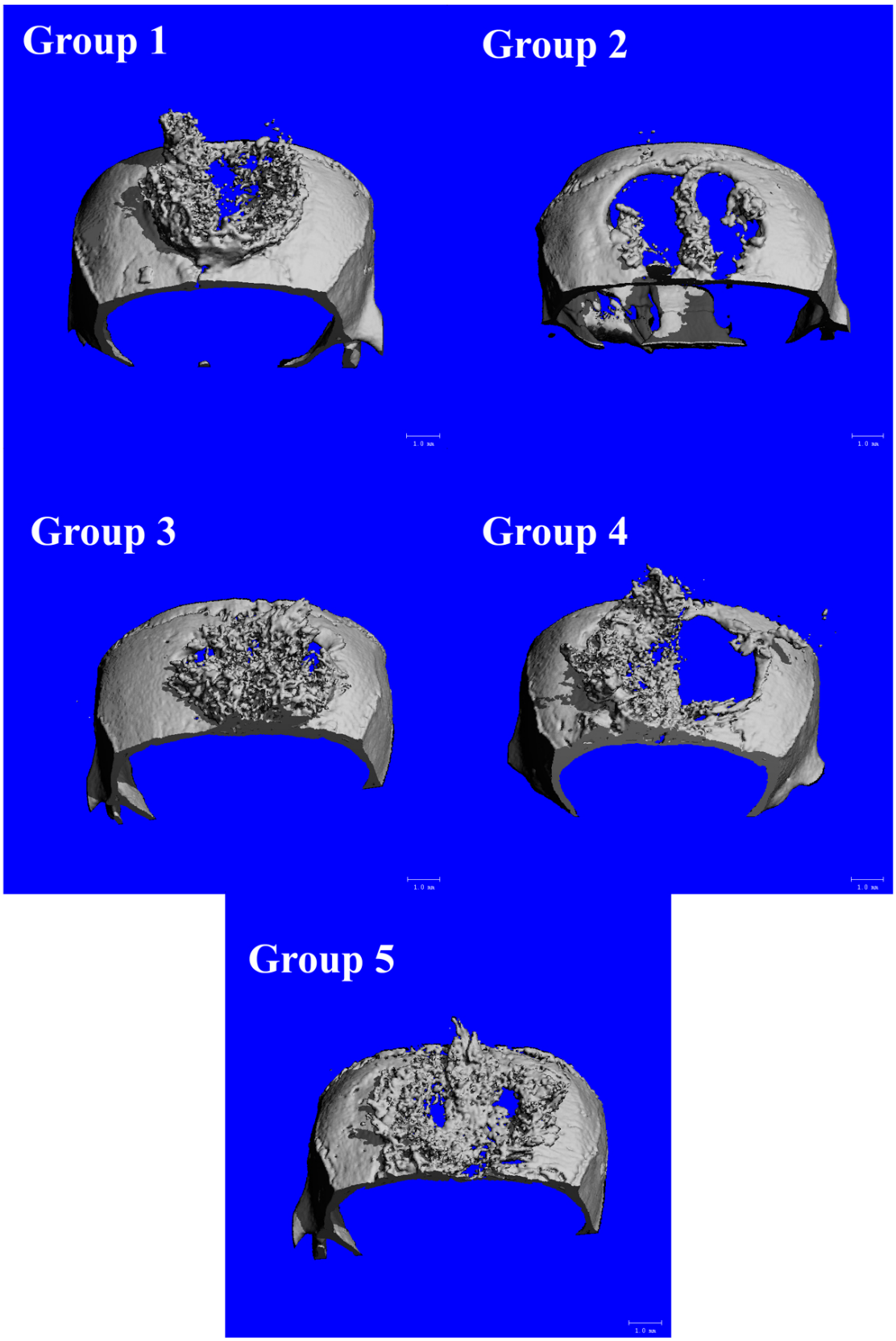


**Figure 30: 3D µCT reconstructions showing bone formation 6 weeks postoperatively**

Analysis of bone volume within the defect (DBV) 3 weeks after surgery (**Figure 29**) showed significant differences among the treatment groups ($F=3.88;p<0.05$). Groups 2 and 3 were found to have the smallest defect bone volumes while Groups 1, 4, and 5 seemed to have similar amounts of bone formation within the defect (**Figure 31)**.

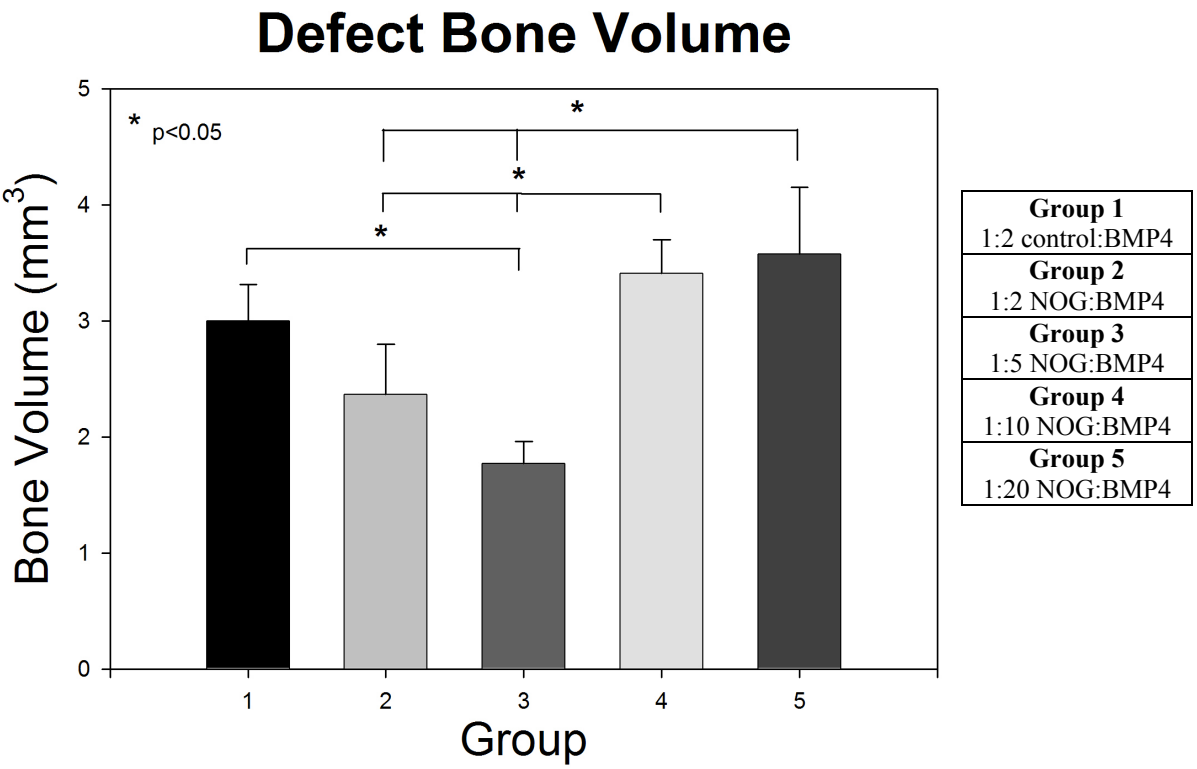


**Figure 31: Defect bone volume (DBV) 3 weeks postoperatively**

Graph depicting the mean volume (±SEM) of bone measured within the defect region. Notice that the groups with the highest concentration of Noggin expressing cells (Groups 2 and 3) had the smallest volume of bone within the defect.

Analysis of mean density of the bone within the defect (DBVMD) 3 weeks postoperatively showed significant differences among the treatment groups ($F=5.09;p<0.01$). Group 5 was found to have the least dense bone within the defect among the groups (**Figure 32**). Group 3 (1:5 NOG:B4) had the highest density of bone within the defect (549.25±38.2mgHA/cc), though it was only significantly higher than Group 4 and Group 5.

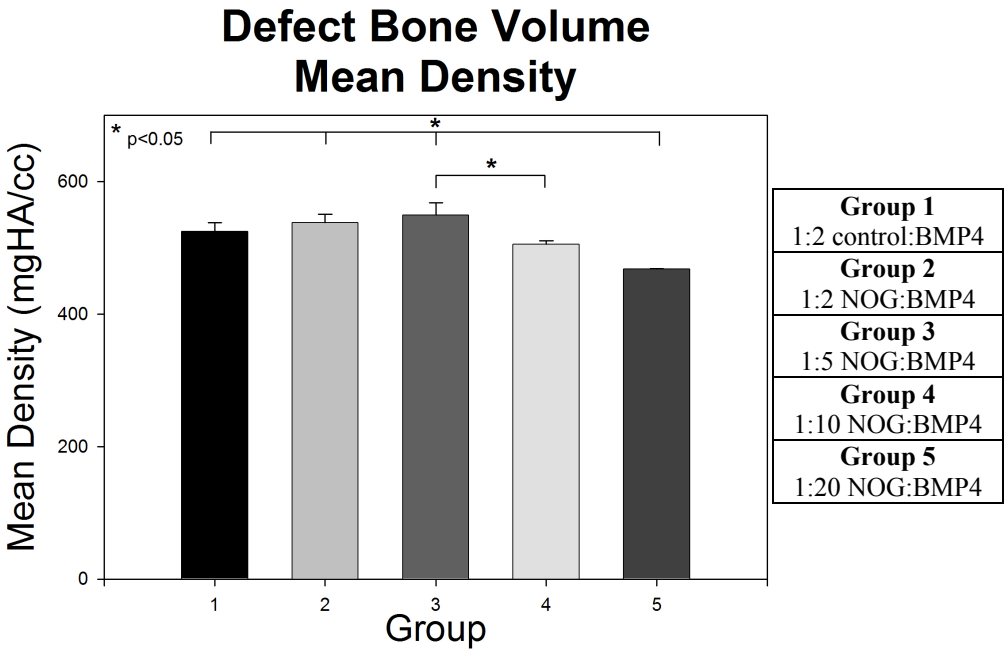


**Figure 32: Bone volume mean density within the defect (DBVMD) 3 weeks postoperatively**

Graph showing the mean density of the bone within the defect (±SEM). Group 5 showed significantly lower density compared to Groups 1, 2, and 3.

There were also significant differences among the groups in the volume of ectopic bone (EBV) that was formed outside of the defect. Similar to the volume of bone within the defect (DBV), Groups 2 and 3 were found to have the smallest volumes of ectopic bone formed (**Figure 33**). Group 5 formed the largest volume of ectopic bone ($3.87\pm0.66mm^3$), though it was not significantly more bone than Groups 1 or 4.

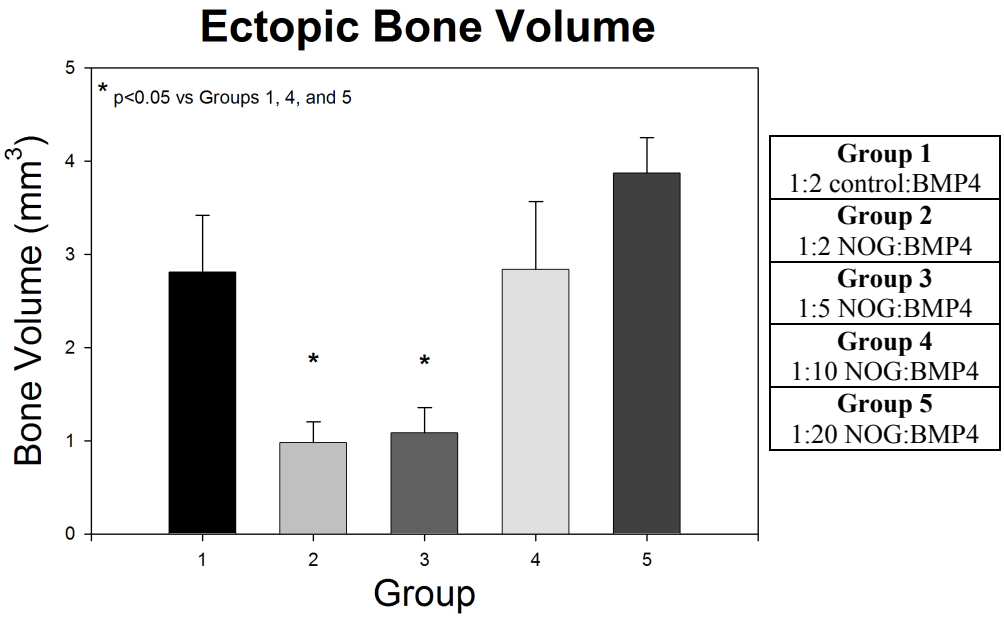


**Figure 33: Ectopic bone volume (EBV) 3 weeks postoperatively**

Graph showing the mean volumes of ectopic bone formed by each group (±SEM). Higher amounts of Noggin (Groups 2 and 3) led to significantly less ectopic bone formation compared to BMP alone (Group 1) or low concentrations of Noggin (Groups 4 and 5).

Mean density for ectopic bone volume was significantly different between the treatment groups ($F=5.74;p<0.01$). The ectopic bone formed by Group 2 was significantly more dense (503.20±24.8mgHA/cc) than the ectopic bone formed in Groups 1, 4, and 5; but it was not significantly more dense than the ectopic bone formed in Group 3 (**Figure 34**).

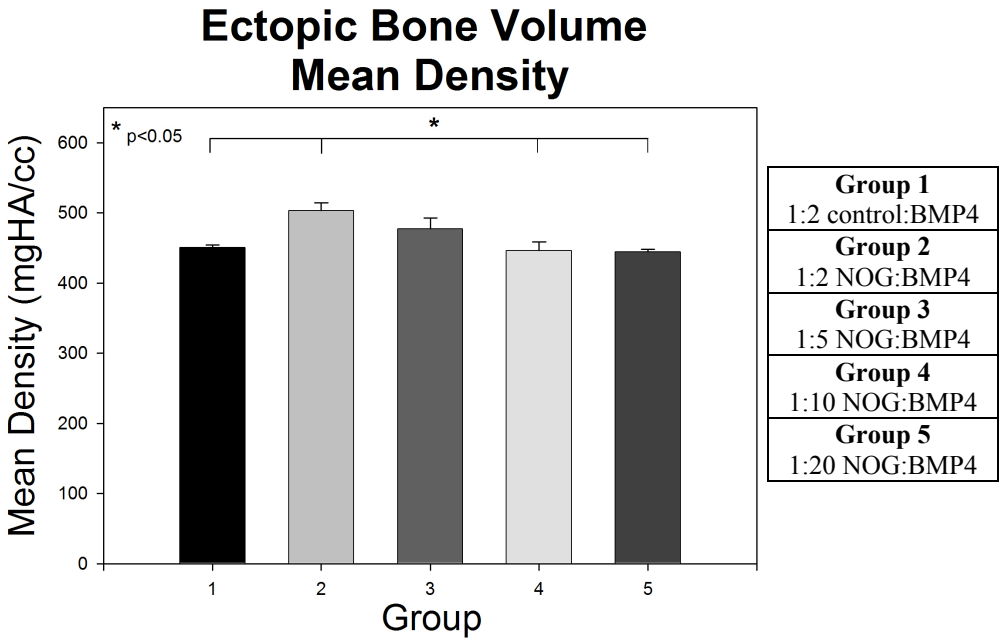


**Figure 34: Ectopic bone volume mean density (EBVMD) 3 weeks postoperatively**

Graph showing mean density of bone formed outside of the defect (±SEM). The highest concentration of Noggin expressing cells tested (Group 2) formed the highest density of ectopic bone.

By adding the DBV and EBV together, we calculated an estimated total bone volume (TBV) that was compared among the 5 treatment groups. Analysis showed that, again, Groups 2 and 3, which had the highest concentrations of Noggin (1:2 and 1:3, respectively), had the smallest total volume of bone formed compared to Groups 1, 4, and 5 (**Figure 35**). The bone volume within the defect (DBV) and the total bone volume (TBV) were used to achieve an efficiency ratio (DBV/TBV). Comparison of the efficiencies of the different treatment groups revealed no significant differences among groups (F=2.23;NS).

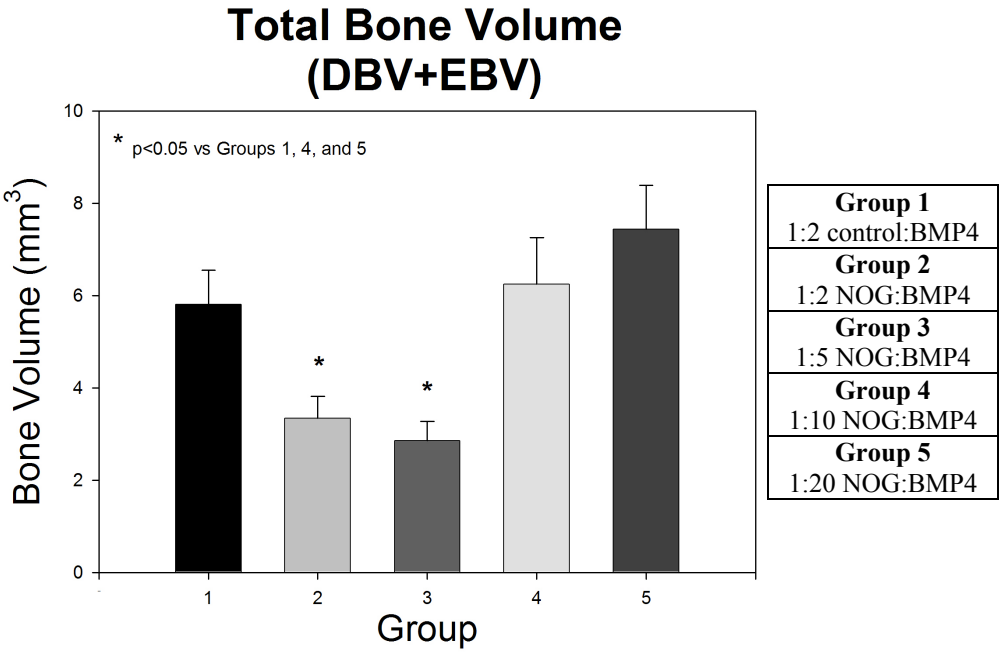


**Figure 35: Total bone volume (DBV+EBV) 3 weeks postoperatively**

Graph showing mean volumes (±SEM) of calculated total bone. Similar to both defect bone volume and ectopic bone volume, high concentrations of Noggin (Groups 2 and 3) significantly inhibited total bone formation.

Six weeks after surgery (**Figure 30**), the comparison among the treatment groups was much different than it was 3 weeks postoperatively. The volume of bone within the defect (DBV) was compared among groups and no significant differences were found (F=1.70;NS). All of the groups had volumes that ranged between 2.3 and 4.6 $mm^3$. Analysis of the mean density of the DBV, however, showed significant differences between the groups (F=10.34;p<0.01). In general, the highest ratios of Noggin to BMP (1:2 and 1:3) led to the formation of denser bone. The bone formed within the defect showed significantly higher density in Group 2 compared to all other groups (**Figure 36**).

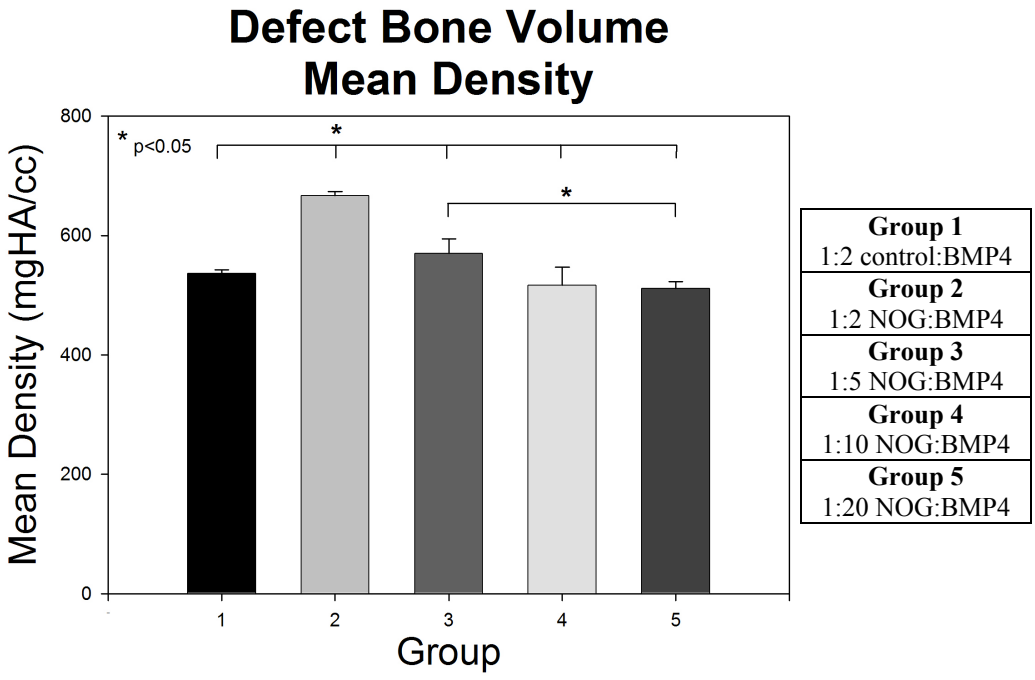


**Figure 36: Mean density of the bone formed within the defect 6 weeks postoperatively**

Graph showing mean density of the defect bone volume (±SEM). Group 2 showed significantly higher bone density within the defect compared to all other groups.

Analysis of the ectopic bone volume 6 weeks postoperatively showed no significant differences among groups (F=2.14;NS), though Group 2 showed the smallest volume of ectopic bone (1.09±0.9mm$^3$) compared to the other groups. Ectopic bone volume mean density was significantly different among the treatment groups 6 weeks postoperatively (F=8.77;p<0.01). The ectopic bone that was formed in animals in Group 2 had significantly higher density compared to the density of the ectopic bone formed in all other treatment groups (**Figure 37**). There were no other differences in ectopic bone mean density between any of the treatment groups.

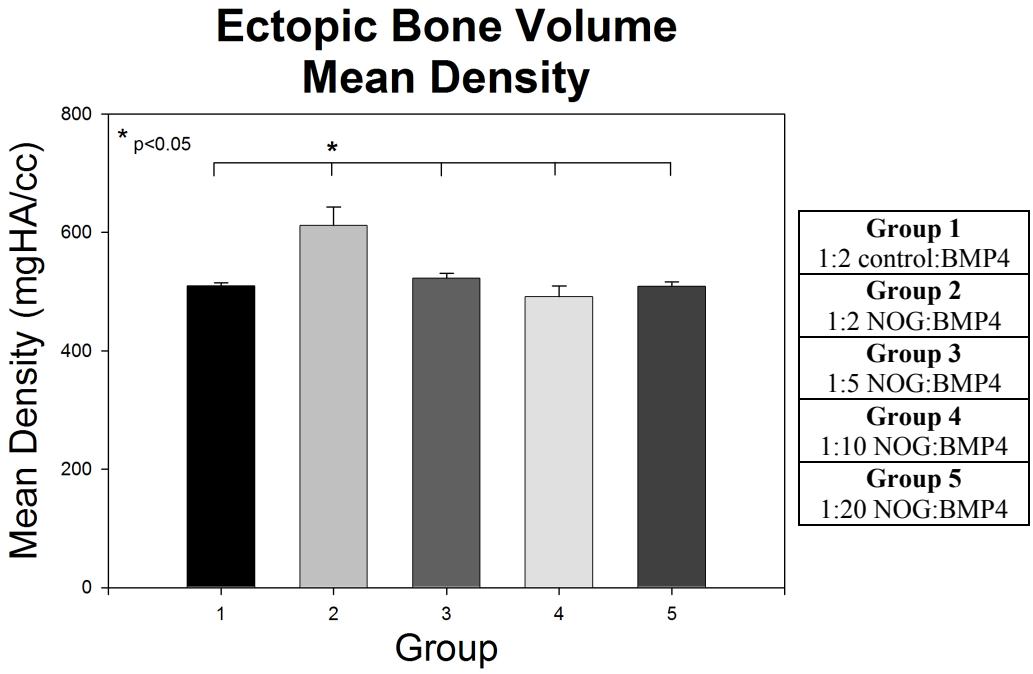


**Figure 37: Mean density of ectopic bone 6 weeks postoperatively**

Graph showing mean density (±SEM) of bone formed outside of the defect region. Group 2 formed significantly higher density ectopic bone compared to other groups.

There were no significant differences in the total bone volume among treatment groups 6 weeks postoperatively (F=2.11;NS). Mean total bone volumes ranged from 3.4mm$^3$ (Group 2) to 15.3mm$^3$ (Group 5). Group 5 showed the largest amount of total bone formation, partially due to a single animal that showed significant bone overgrowth (**Figure 38**).

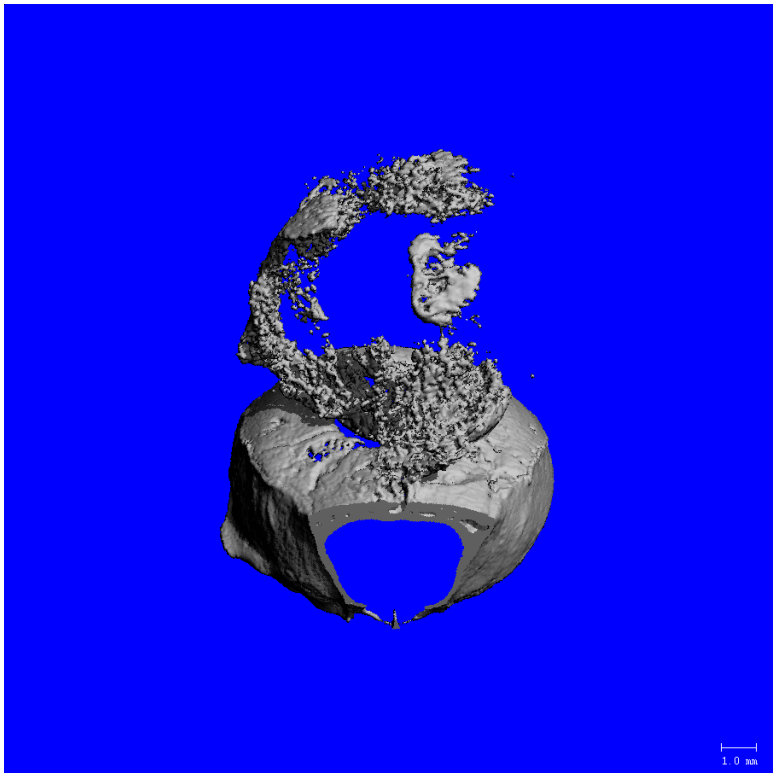


**Figure 38: 3D µCT reconstruction of one animal from Group 5 that showed significant bone overgrowth**

Image depicting the overgrowth of bone that can occur after ex vivo BMP4 gene therapy. High concentrations of Noggin expressing cells mixed with the BMP4 expressing cells inhibited this type of bone overgrowth in this study.

Comparison of the efficiencies of each treatment showed significant differences ($F=5.54;p<0.01$) among the treatment groups. Group 2 showed the highest mean efficiency. Approximately 71% of the bone that had formed 6 weeks postoperatively was located within the defect. This efficiency was significantly better than all other groups (**Figure 39**).

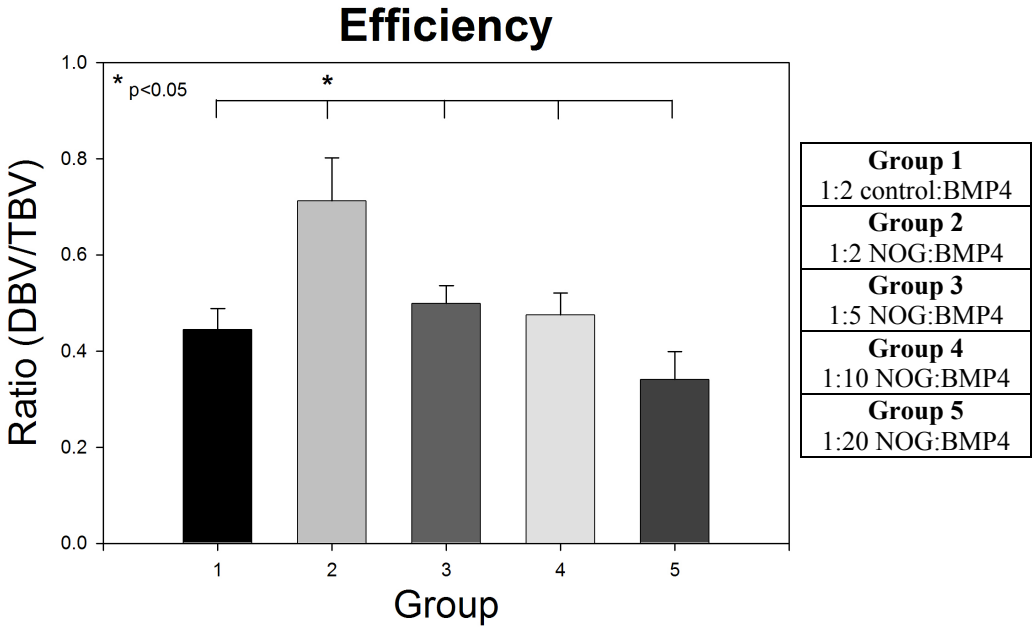


**Figure 39: Efficiency ratings (DBV/TBV) 6 weeks postoperatively**

Graph showing mean efficiency for each group (±SEM). Group 2 (1:2 NOG:B4) was the most efficient treatment, with approximately 71% of the total bone was formed within the defect.

The relationship between bone volume and bone density was assessed at each postoperative time point by comparing the measured defect bone volume (DBV) to the defect bone volume mean density (DBVMD) and by comparing the measured ectopic bone volume (EBV) to the ectopic bone volume mean density (EBVMD). Among the groups tested, we found that, at both 3 and 6 weeks postoperatively, there were negative correlation coefficients ($r=-0.58$ and $r=-0.32$, respectively) between DBV and DBVMD. This correlation was significant ($p<0.01$) only at the 3 week time point (**Figure 40A**). Similar results were found for the ectopic bone

analysis. There was a negative correlation coefficient between EBV and EBVMD at both 3 and 6 weeks postoperatively (r=-0.64 and r=-0.19, respectively) with the correlation being significant ($p<0.01$) 3 weeks postoperatively (**Figure 40B**).

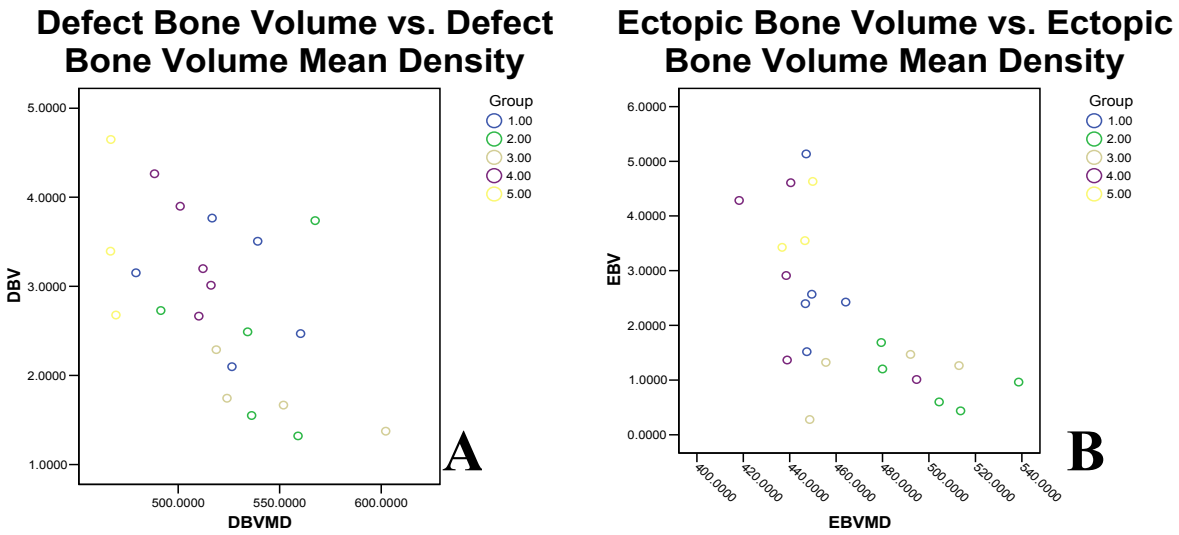


**Figure 40: Scatterplot graphs showing correlations between bone volume and bone density**

**A**) Graph showing a negative correlation between DBV and DBVMD for all animals 3 weeks postoperatively (r=-0.578,p<0.01). **B**) Graph showing a negative correlation between EBV and EBVMD of all animals 3 weeks postoperatively (r=-0.640,p<0.01).

The relationship between total bone volume and either defect bone volume or ectopic bone volume was also tested for all animals at both time points postoperatively. We found that there were significant positive correlations between total bone volume and defect bone volume (r=0.860;p<0.001) and between total bone volume and ectopic bone volume (r=0.983;p<0.001).

## 5.5 DISCUSSION

In all bone regeneration applications, it is important to control the amount of bone that forms following a particular therapy. The necessity for control is most acute in craniofacial reconstruction because of the proximity of bone to vital structures such as blood vessels, nerves, and sensory organs.

We have previously shown that bone healing can be improved through the use of ex vivo gene therapy techniques based on muscle-derived cells expressing BMPs [197, 199, 256, 258]. In an attempt to both elucidate the interaction between vascular endothelial growth factor (VEGF) and BMP and to improve bone healing, combinatorial therapies were developed [256, 269]. These studies were among the first to utilize gene-based approaches to test therapies using combinations of different growth factors.

Peng, et al. reported on the development of an inducible retroviral vector encoding BMP4 expression in 2004 [253]. This vector was developed in part to enable the temporal control of bone formation. When this vector was used to heal calvarial defects in an ex vivo gene-based therapy, it was observed that there was bone formation even without the induction of BMP4 expression and that this "background" bone formation could be inhibited by adding cells that expressed Noggin, a known BMP antagonist [245]. That study also showed that less ectopic bone was formed after BMP expression was induced in the presence of Noggin expressing cells compared to when BMP was expressed in the absence of Noggin expressing cells [245].

Noggin expression has been colocalized with BMP expression during normal bone healing [210]. BMP stimulation has also been shown to increase Noggin expression in osteogenic tissues [129, 270]. Therefore, we believed that the concurrent expression of BMP4 and its antagonist, Noggin, may influence the amount and quality of bone that forms after BMP-

based therapies. The current experiment was designed to test whether the amount and quality of bone could be regulated through biologic means.

The results of this study show a dose response to Noggin. The defects treated with higher ratios of Noggin cells (1:2 and 1:5, Groups 2 and 3, respectively) formed less bone than defects treated with BMP expressing cells only (Group 1) or low ratios of Noggin expressing cells (1:10 and 1:20, Groups 4 and 5, respectively). This trend was observed for the volume of bone within the defect, ectopic bone volume, and total bone volume. These data support the intuitive hypothesis that increased amount of antagonist (Noggin) will cause increased inhibition of agonist (BMP4).

The data also suggest that the therapies that induced less bone produced the bone with the highest density. Both 3 and 6 weeks postoperatively, the groups with smaller bone volumes (both DBV and EBV) demonstrated more dense bone. In fact, 3 weeks postoperatively, there were significant negative correlations between the volume of bone and the density of the bone. This data suggest that more is not necessarily better. Although a vast majority of the research surrounding bone regeneration is interested in creating the most bone in the shortest amount of time, the results from such research may be misleading. For this reason, we believe that the analytical techniques employed in the current study will lead to more accurate interpretation of the effectiveness of bone regeneration techniques.

It is interesting to note that 3 weeks after surgery, Group 2 (1:2 Nog:B4 cells) had significantly denser bone within the defect compared to Group 1 (B4 cells only), but the volume of the bone within the defect was not significantly different. These results are promising in that it was possible to create bone of higher density without significantly decreasing the total volume of

bone that was formed. These data also suggest another means by which Noggin improves BMP induced bone formation, in addition to simply decreasing the volume of bone that formed.

One possible means of improving the density of the bone that forms is through the inhibition of bone resorption. Bone is normally degraded by osteoclasts during remodeling. BMP signaling has been suggested as a positive regulator of bone resorption and in osteoclastic differentiation [271, 272]. It has also been suggested that, because BMPs are notoriously inductive of bone formation, BMPs may act as inhibitors of osteoclastic activity [273]. Because there is still debate regarding the role of BMPs in osteoclastic differentiation and activity, it is difficult to determine whether the increases in bone density observed in the groups with the highest ratios of Noggin expressing cells is caused by the inhibition of osteoclasts.

Overall, extreme caution should be used in the interpretation of the data presented here. It must be noted that the results presented above do not agree with previously published data. Our previous studies showed the presence of a large mass of disorganized trabecular bone much larger than the defect only 3 weeks after surgery [245]. The current study found only minimal bone formation up to 6 weeks postoperatively. We may be able to attribute this difference in the effectiveness of our bone induction to the formation of tumors.

All animals in this study formed large tumors under their skin in the region of the implanted cells. These tumors were not evident during the μCT scanning 3 weeks postoperatively. By 6 weeks after surgery, the tumors were larger than the cranial vault and the animals were killed immediately. The 6 week μCT scans were performed on fixed skulls from these animals.

The cause of the tumors is not understood. The cell population that was used had recently been used by another investigator in our laboratory for a similar ex vivo bone induction study,

with no evidence of tumor formation. It seems logical that the formation of tumors within the implanted tissue would adversely affect the formation of bone, resulting in the differences observed between this study and previous studies by our group.

Regardless of the formation of tumors by 6 weeks postoperatively, we believe that this study supports our hypothesis that the simultaneous implantation of Noggin expressing cells with BMP4 expressing cells can assist in minimizing ectopic bone formation and improve the quality of the bone that forms within the defect. Future studies will involve the use of different cell lines, a focus on Noggin:BMP ratios between 1:1 and 1:5, and the biomechanical testing of the regenerated bone as another measure of the quality of the bone that forms.

This study is the first to attempt to control the amount and quality of bone that is regenerated using BMP-based therapies using a biologically-based strategy. The results, though confounded by the formation of tumors, suggest that combined Noggin and BMP therapies warrant further investigation.

# 6.0 CONCLUSIONS

Many advances have been made in our understanding of bone growth, remodeling, and regeneration. The current task to be undertaken is the translation of this body of knowledge to clinical application. Toward that end, an understanding of molecular biology, cell biology, and gene therapy can be used to advance the field of bone regeneration.

The primary focus of the work presented here was an exploration into biologically-based strategies to control bone formation. The use of currently available strategies to advance bone formation may also be utilized to inhibit bone formation and to improve the quality of therapy in cases of hyperostosis. A series of three studies were designed to assess the ability of Noggin, an extracellular inhibitor of BMPs, to regulate and control bony wound healing in a variety of circumstantes. In the first study, Noggin protein, inhibited bone formation in a rabbit model of human nonsyndromic craniosynostosis. This work also showed that a single application of Noggin protein within a collagen vehicle could inhibit postoperative resynostosis and improve overall craniofacial growth. The second study developed a novel mouse model of postoperative resynostosis to test strategies to control calvarial bone healing. This model was then used to assess the ability of Noggin ex vivo gene therapy to inhibit bone formation within small calvarial defects in mice. In the third study, it was found that a therapy which combined the application of both BMP4 and its antagonist, Noggin, minimized the formation of ectopic bone and improved the quality of bone that forms within the defect.

There were some interesting results that need to be considered. In the second chapter, an initial increase in the defect size was observed in the Noggin treated rabbits. As was discussed, it was hypothesized that this increase was due to the expansion of the calvaria after release of the synostosed suture. It was also speculated that this same expansion occurred in the control groups; but, because healing was occurring as well, no expansion was observed. There could be another reason for the expansion of the Noggin treated defects. The Noggin treatment may have, somehow, recruited more osteoclasts to the defect site and induced resorption of the bone in the defect area. The interaction between BMP signaling and osteoclastogenesis is still being debated, so it is difficult to know whether the inhibition of BMP signaling through Noggin treatment induced bone resorption.

The cause for the inhibition of defect healing by GFP expressing MDSCs is also debatable. In that study, the GFP treated defects were significantly larger than untreated defects both 4 and 8 weeks after surgery, according to the μCT data. It was speculated in the conclusions of Chapter 4 that this inhibition may have been caused by an immune reaction by the normal mice to either the gelatin sponge vehicle or to the MDSCs themselves. Another possible explanation would be that the MDSCs express endogenous inhibitors of bone formation. However, there is a far from a complete understanding of the effects that stem cells have on their environment and the explanation is still speculative. It could also be possible that these cells express many different growth factors that, in this case, inhibited bone formation. Stem cells have also been shown to chemoattract other cell types. By attracting and promoting osteoclastic activity, the MDSCs could have induced bone resorption in the defect area. The field of tissue engineering must constantly be aware that the cellular component is never inert. Though the

intent was to introduce cells that would produce Noggin or GFP in this study, there is no way for us to control the multitude of interactions of which the stem cells are involved.

Another observation that may have broader implications for the field of bone tissue engineering is that a single-dose Noggin treatment had lasting effects on bone healing. Also, in the fourth chapter, the longer-term, ex vivo gene therapy only seemed to affect healing in the first few weeks after surgery. In this same study, it was observed that untreated control defects healed rapidly within the first 4 weeks after surgery. Together, these results suggest that there is a critical time, soon after the defect is created, where treatment may have its effect. Therefore, it may be possible to delay bone healing early in the healing process, resulting in altered bone growth in the longer term. This possibility changes the perceived need for sustained delivery of the therapeutic protein. Through rigorous testing of the long-term results of short-term therapies, we should be able to better understand the bone healing process, leading to the development of more effective biologically-based adjuncts to conventional surgery.

Lastly, by elucidating the interaction between BMP4 and its inhibitor, Noggin, in the fifth chapter, it became apparent that dosage is extremely important. It was hypothesized that the addition of Noggin expressing cells to the BMP4 treatment minimized the formation of ectopic bone and increased the density of the bone that formed within the defect because there was an appropriate dose of BMP4 supplied to the defect site. This data should prove to have broader implications in bone tissue engineering by pointing out that therapies should be developed to improve specific outcomes. These findings suggest that therapies directed toward the most rapid creation of the largest volume of new bone should be avoided. This study has shown that more is not necessarily better by demonstrating that there is a negative correlation between bone volume and bone density. Also, the techniques used to analyze bone formation in this study changed the

way we understand treatment efficiency. Standard radiographic and histological analyses are more useful in the determination of the presence of bone tissue, rather than the quality of the bone tissue. By using new technology, this study was able to directly compare the density of the bone that formed within a defined area, the defect region. Similar analytical techniques should improve our ability to evaluate and compare strategies to improve bone healing.

## 6.1 FUTURE DIRECTIONS

The use of Noggin to control bone formation warrants further investigation. It is believed that the use of a naturally occurring antagonist, such as Noggin, can be readily turned into a clinical reality, especially in cases of single suture, nonsyndromic craniosynostosis. Technologies are being developed for drug delivery to assist in the delivery of Noggin protein for longer durations. Also, there is an acute need for strategies to control the size and shape of the bone that forms following regenerative therapies. To this end, it is important to continue to develop and test both physical (through scaffold manipulation) and biological (through combinatorial therapies) means to control bone formation.

# APPENDIX A

## PAPERS PUBLISHED

**2005**

1. Peng H, Usas A, Hannallah D, Olshanski A, Cooper GM, Huard J. Noggin improves bone healing elicited by muscle stem cells expressing inducible BMP4. Mol Ther. 2005; 12(2): 239-246.

2. Smith TD, Rossie JB, Cooper GM, Mooney MP, Siegel MI. Secondary pneumatization in the maxillary sinus of callitrichid primates: insights from immunohistochemistry and bone cell distribution. Anat Rec Part A. 2005; 285A: 677-689.

3. Peng H, Usas A, Olshanski A, Ho AM, Gearhart B, Cooper GM, Huard J. VEGF improves, whereas sFlt1 inhibits, BMP2-induced bone formation and bone healing through modulation of angiogenesis. J Bone Miner Res. 2005; 20(11): 2017-2027.

4. Losee JE, Feldman E, Ketkar M, Singh D, Kirschner RE, Westesson P, Cooper G, Mooney MP, Bartlett SP. Nonsynostotic occipital plagiocephaly: Radiographic diagnosis of the "sticky suture." Plast Reconstr Surg. 2005; 116(7): 1860-1869.

**2006**

5. Dudas JR, Marra KG, Cooper GM, Penascino VM, Mooney MP, Jiang S, Rubin JP, Losee JE. The osteogenic potential of adipose-derived stem cells for repair of rabbit calvarial defects. Ann Plast Surg. 2006; 56(5):543-548.

6. Noorchashm N, Dudas JR, Ford M, Gastman B, Deleyannis FWB, Vecchione L, Jiang S, Cooper GM, Haralam MA, Losee JE. Conversion furlow palatoplasty: salvage of speech after straight-line palatoplasty and "incomplete IVVP." Ann Plast Surg. 2006; 56(5):505-510.

7. Cooper GM, Singhal VS, Barbano T, Wigginton W, Rabold T, Losken HW, Siegel MI, Mooney MP. Intracranial Volume Changes in Craniosynostotic Rabbits: Effects of Age and Surgical Correction. Plast Reconstr Surg. 2006; 117(6):1886-1890.

8. Weiss KR, Cooper GM, Jadlowiec JA, McGough RL, Huard J. VEGF and BMP Expression in mouse osteosarcoma cells. Clin Orthop Rel Res. 2006; 450: 111-117.

9. Mooney MP, Losken HW, Moursi AM, Bradley JP, Azari K, Acarturk O, Shand J, Cooper GM, Thompson B, Stelnicki EJ, Opperman LA, Siegel MI. Anti-Tgf-β2 antibody therapy inhibits postoperative resynostosis in craniosynostotic rabbits. Paper accepted for publication in PRS.

10. Smith TD, Bhatnagar KP, Rossie JB, Docherty BA, Burrows AM, Cooper GM, Mooney MP, Siegel MI. Scaling of the first ethmoturbinal in nocturnal strepsirrhines: olfactory and respiratory surfaces. Anat Rec. in press.

## BIBLIOGRAPHY


1. Enlow, D.H. 1990. *Handbook of Facial Growth*. Philadelphia: Saunders.

2. Cohen, M.M., Jr. 2000. *Epidemiology of craniosynostosis*. New York: Oxford University Press. 112-118 pp.

3. Jabs, E.W. 2002. Genetic Etiologies of Craniosynostosis. In *Understanding Craniofacial Anomalies: The Etiopathogenesis of Craniosynostoses and Facial Clefting*. M.P. Mooney, and M.I. Siegel, editors. New York: John W. Wiley and Sons. 125-146.

4. Marsh, J.L., and Vannier, M.W. 1985. *Comprehensive Care for Craniofacial Deformities*. St. Louis: C.V. Mosby, Co.

5. Babler, W.J., and Persing, J.A. 1982. Experimental alteration of cranial suture growth: Effects on the neurocranium, basicranium, and midface. In *Factors and Mechanisms Influencing Bone Growth*. B.G. Sarnat, editor. New York: Alan R. Liss, Inc. 333-345.

6. Babler, W. 1989. Relationship of altered cranial suture growth to cranial base and midface. In *Scientific Foundations and Surgical Management of Craniosynostosis*. J.A. Persing, M.T. Edgerton, and J.A. Jane, editors. Baltimore: Williams and Wilkins. 87-95.

7. Burdi, A.R., Kusnetz, A.B., Venes, J.L., and Gebarski, S.S. 1986. The natural history and pathogenesis of the cranial coronal ring articulations: implications in understanding the pathogenesis of the Crouzon craniostenotic defects. *Cleft Palate J* 23:28-39.

8. Hoyte, D.A.N. 1989. The role of the cranial base in normal and abnormal skull development. In *Scientific Foundations and Surgical Treatment of Craniosynostosis*. J.A. Persing, M.T. Edgerton, and J.A. Jane, editors. Baltimore: Williams and Wilkins. 58-76.

9. Mooney, M.P., Losken, H.W., Siegel, M.I., Lalikos, J.F., Losken, A., Burrows, A.M., and Smith, T.D. 1994. Development of a strain of rabbits with congenital simple nonsyndromic coronal suture synostosis. Part II: Somatic and craniofacial growth patterns. *Cleft Palate Craniofac J* 31:8-16.

10. Burrows, A.M., Mooney, M.P., Smith, T.D., Losken, H.W., and Siegel, M.I. 1995. Growth of the cranial vault in rabbits with congenital coronal suture synostosis. *Cleft Palate Craniofac J* 32:235-246.

11. Smith, T.D., Mooney, M.P., Burrows, A.M., Losken, H.W., and Siegel, M.I. 1996. Postnatal changes in the cranial base in rabbits with congenital coronal suture synostosis. *J Craniofac Genet Dev Biol* 16:107-117.

12. Kreiborg, S. 2000. Postnatal growth and development of the craniofacial complex in premature craniosynostosis. In *Craniosynostosis: Diagnosis, Evaluation, and Management*. M.M. Cohen, Jr., and R.E. MacLean, editors. New York: Oxford University Press. 158-176.

13. Vig, K.W.L. 2002. Facial dysmorphology in the craniosynostoses: Clinical implications. In *Understanding Craniofacial Anomalies: The Etiopathogenesis of Craniosynostoses and Facial Clefting*. M.P. Mooney, and M.I. Siegel, editors. New York: John J. Wiley and Sons. 379-390.

14. Richtsmeier, J.T. 2002. Cranial vault dysmorphology and growth in craniosynostosis. In *Understanding Craniofacial Anomalies: The Etiopathogenesis of Craniosynostoses and Facial Clefting*. M.P. Mooney, and M.I. Siegel, editors. New York: John W. Wiley and Sons. 321-342.

15. Hudgins, R.J., Cohen, S.R., Burstein, F.D., and Boydston, W.R. 1998. Multiple suture synostosis and increased intracranial pressure following repair of single suture, nonsyndromal craniosynostosis. *Cleft Palate Craniofac J* 35:167-172.

16. Renier, D. 1989. Intracranial pressure in craniosynostosis: Pre- and postoperative recordings-correlation with functional results. In *Scientific Foundations and Surgical Treatment of Craniosynostosis*. J.A. Persing, M.T. Edgerton, and J.A. Jane, editors. Baltimore: Williams and Wilkins. 263-269.

17. Campbell, J.W., Albright, A.L., Losken, H.W., and Biglan, A.W. 1995. Intracranial hypertension after cranial vault decompression for craniosynostosis. *Pediatr Neurosurg* 22:270-273.

18. Mooney, M.P., Siegel, M.I., Burrows, A.M., Smith, T.D., Losken, H.W., Dechant, J., Cooper, G., Fellows-Mayle, W., Kapucu, M.R., and Kapucu, L.O. 1998. A rabbit model of human familial, nonsyndromic unicoronal suture synostosis. II. Intracranial contents, intracranial volume, and intracranial pressure. *Childs Nerv Syst* 14:247-255.

19. Mooney, M.P., Fellows-Mayle, W., Losken, H.W., Dechant, J., Burrows, A.M., Smith, T.D., Cooper, G.M., Pollack, I., and Siegel, M.I. 1999. Increased intracranial pressure after coronal suturectomy in craniosynostotic rabbits. *J Craniofac Surg* 10:104-110.

20. Camfield, P.R., Camfield, C.S., and Cohen, M.M., Jr. 2000. Neurosurgical aspects of craniosynostosis. In *Craniosynostosis: Diagnosis, Evaluation, and Management*. M.M. Cohen, Jr., and R.E. MacLean, editors. New York: Oxford University Press. 177-183.

21. Fellows-Mayle, W.K., Mooney, M.P., Losken, H.W., Dechant, J., Cooper, G.M., Burrows, A.M., Smith, T.D., Pollack, I.F., and Siegel, M.I. 2000. Age-related changes in intracranial pressure in rabbits with uncorrected familial coronal suture synostosis. *Cleft Palate Craniofac J* 37:370-378.

22. Fellows-Mayle, W.K., Mitchell, R., Losken, H.W., Bradley, J., Siegel, M.I., and Mooney, M.P. 2004. Intracranial pressure changes in craniosynostotic rabbits. *Plast Reconstr Surg* 113:557-565.

23. Gault, D.T., Renier, D., Marchac, D., and Jones, B.M. 1992. Intracranial pressure and intracranial volume in children with craniosynostosis. *Plast Reconstr Surg* 90:377-381.

24. Singhal, V.K., Mooney, M.P., Burrows, A.M., Wigginton, W., Losken, H.W., Smith, T.D., Towbin, R., and Siegel, M.I. 1997. Age related changes in intracranial volume in rabbits with craniosynostosis. *Plast Reconstr Surg* 100:1121-1128; 1129-1130.

25. Mooney, M.P., Burrows, A.M., Wigginton, W., Singhal, V.K., Losken, H.W., Smith, T.D., Dechant, J., Towbin, A., Cooper, G.M., Towbin, R., et al. 1998. Intracranial volume in craniosynostotic rabbits. *J Craniofac Surg* 9:234-239.

26. Chadduck, W.M., Chadduck, J.B., and Boop, F.A. 1992. The subarachnoid spaces in craniosynostosis. *Neurosurgery* 30:867-871.

27. Miller, M.T. 2000. Ocular findings in craniosynostosis. In *Craniosynostosis: Diagnosis, Evaluation, and Management*. M.M. Cohen, Jr., and R.E. MacLean, editors. New York: Oxford University Press. 184-196.

28. Persing, J.A., and Jane, J.A. 2000. Neurosurgical treatment of craniosynostosis. In *Craniosynostosis: Diagnosis, Evaluation, and Management*. M.M. Cohen, Jr., and R.E. MacLean, editors. New York: Oxford University Press. 209-227.

29. Kapp-Simon, K.A., Figueroa, A., Jocher, C.A., and Schafer, M. 1993. Longitudinal assessment of mental development in infants with nonsyndromic craniosynostosis with and without cranial release and reconstruction. *Plast Reconstr Surg* 92:831-839; discussion 840-831.

30. Arnaud, E., Renier, D., and Marchac, D. 1995. Prognosis for mental function in scaphocephaly. *J Neurosurg* 83:476-479.

31. Marchac, D., and Renier, D. 1982. *Craniofacial Surgery for Craniosynostosis*. Boston: Little Brown & Co.

32. Posnick, J.C. 2000. *Craniofacial and Maxillofacial Surgery in Children and Young Adults: Volume 1 and Volume 2*. Philadelphia: W.B. Saunders.

33. Posnick, J.C. 2000. Craniosynostosis and the craniofacial dysostosis syndromes: Current surgical management. In *Craniosynostosis: Diagnosis, Evaluation, and Management*. M.M. Cohen, Jr., and R.E. MacLean, editors. New York: Oxford University Press. 269-291.

34. Persing, J.A., Jane, J.A., and Edgerton, M.A. 1989. Surgical treatment of craniosynostosis. In *Scientific Foundations and Surgical Treatment of Craniosynostosis*. J.A. Persing, M.A. Edgerton, and J.A. Jane, editors. Baltimore: Williams and Wilkins. 87-95.

35. Dufresne, C., and Richtsmeier, J.T. 1995. Interaction of craniofacial dysmorphology, growth, and prediction of surgical outcome. *J Craniofac Surg* 6:270-281.

36. Ousterhout, D.K., and Vargervik, K. 1987. Aesthetic improvement resulting from craniofacial surgery in craniosynostosis syndromes. *J Craniomaxillofac Surg* 15:189-197.

37. Posnick, J.C. 1996. Monobloc and facial bipartition osteotomies: a step-by-step description of the surgical technique. *J Craniofac Surg* 7:229-250; discussion 251.

38. Warren, S.M., and Longaker, M.T. 2001. The pathogenesis of craniosynostosis in the fetus. *Yonsei Med J* 42:646-659.

39. Cohen, M.M., Jr. 2000. Sutural pathology. In *Craniosynostosis: Diagnosis, Evaluation, and Management*. M.M. Cohen, Jr., and R.E. MacLean, editors. New York: Oxford University Press. 95-99.

40. Wilkie, A.O. 1997. Craniosynostosis: genes and mechanisms. *Hum Mol Genet* 6:1647-1656.

41. David, J.D., Poswillo, D., and Simpson, D. 1982. *The Craniosynostoses: Causes, Natural History, and Management*. Berlin: Springer-Verlag.

42. Turvey, T.A., Vig, K.W.L., and R.L., F. 1996. *Facial Clefts and Craniosynostosis: Principles and Management*. Philadelphia: W.B. Saunders.

43. Tessier, P. 2000. Craniofacial surgery in syndromic craniosynostosis. In *Craniosynostosis: Diagnosis, Evaluation, and Management*. M.M. Cohen, Jr., and R.E. MacLean, editors. New York: Oxford University Press. 228-269.

44. Panchal, J., and Uttchin, V. 2003. Management of craniosynostosis. *Plast Reconstr Surg* 111:2032-2048; quiz 2049.

45. Norwood, C.W., Alexander, E., Jr., Davis, C.H., Jr., and Kelly, D.L., Jr. 1974. Recurrent and multiple suture closures after craniectomy for craniosynostosis. *J Neurosurg* 41:715-719.

46. Hassler, W., and Zentner, J. 1990. Radical osteoclastic craniectomy in sagittal synostosis. *Neurosurgery* 27:539-543.

47. Fatah, M.F., Ermis, I., Poole, M.D., and Shun-Shin, G.A. 1992. Prevention of cranial reossification after surgical craniectomy. *J Craniofac Surg* 3:170-172.

48. Drake, D.B., Persing, J.A., Berman, D.E., and Ogle, R.C. 1993. Calvarial deformity regeneration following subtotal craniectomy for craniosynostosis: a case report and theoretical implications. *J Craniofac Surg* 4:85-89; discussion 90.

49. McCarthy, J.G., Glasberg, S.B., Cutting, C.B., Epstein, F.J., Grayson, B.H., Ruff, G., Thorne, C.H., Wisoff, J., and Zide, B.M. 1995. Twenty-year experience with early surgery for craniosynostosis: I. Isolated craniofacial synostosis--results and unsolved problems. *Plast Reconstr Surg* 96:272-283.

50. Pollack, I.F., Losken, H.W., and Biglan, A.W. 1996. Incidence of increased intracranial pressure after early surgical treatment of syndromic craniosynostosis. *Pediatr Neurosurg* 24:202-209.

51. Kirkpatrick, W.N., Koshy, C.E., Waterhouse, N., Fauvel, N.J., Carr, R.J., and Peterson, D.C. 2002. Paediatric transcranial surgery: a review of 114 consecutive procedures. *Br J Plast Surg* 55:561-564.

52. Mommaerts, M.Y., Staels, P.F., and Casselman, J.W. 2001. The faith of a coronal suture grafted onto midline synostosis inducing dura and deprived from tensile stress. *Cleft Palate Craniofac J* 38:533-537.

53. Greene, C.S., Jr. 1998. Pancraniosynostosis after surgery for single sutural craniosynostosis. *Pediatr Neurosurg* 29:127-132.

54. Mooney, M.P., Burrows, A.M., Smith, T.D., Losken, H.W., Opperman, L.A., Dechant, J., Kreithen, A.M., Kapucu, R., Cooper, G.M., Ogle, R.C., et al. 2001. Correction of coronal suture synostosis using suture and dura mater allografts in rabbits with familial craniosynostosis. *Cleft Palate Craniofac J* 38:206-225.

55. Jane, J.A., and Persing, J.A. 1986. Neurosugical treatment of craniosynostosis. In *Craniosynostosis: Diagnosis, Evaluation, and Management*. M.M. Cohen, Jr., editor. New York: Raven Press. 249-320.

56. Babler, W.J., Persing, J.A., Winn, H.R., Jane, J.A., and Rodeheaver, G.T. 1982. Compensatory growth following premature closure of the coronal suture in rabbits. *J Neurosurg* 57:535-542.

57. Anderson, F.M., and Johnson, F.L. 1956. Craniosynostosis; a modification in surgical treatment. *Surgery* 40:961-970.

58. Shillito, J. 1982. Surgical treatment of craniosynostosis. In *Neurological Surgery*. J. Youmans, editor. Philadelphia: W.B. Saunders. 24-256.

59. Losken, H.W., Tschakaloff, A., Mooney, M.P., von Oepen, R., Siegel, M.I., Losken, A., and Swan, J. 1992. The effects of frontal bone advancement with or without biodegradable bone microplates on advancement stability and compensatory craniofacial growth changes in rabbits with experimental coronal immobilization. In *Craniofacial Surgery*. A. Montoya, editor. Bologna, Italy: Monduzzi Editore. 219-233.

60. Moreira-Gonzalez, A., Jackson, I.T., Miyawaki, T., Barakat, K., and DiNick, V. 2003. Clinical outcome in cranioplasty: critical review in long-term follow-up. *J Craniofac Surg* 14:144-153.

61. Williams, J.K., Cohen, S.R., Burstein, F.D., Hudgins, R., Boydston, W., and Simms, C. 1997. A longitudinal, statistical study of reoperation rates in craniosynostosis. *Plast Reconstr Surg* 100:305-310.

62. Roth, D.A., Gold, L.I., Han, V.K., McCarthy, J.G., Sung, J.J., Wisoff, J.H., and Longaker, M.T. 1997. Immunolocalization of transforming growth factor beta 1, beta 2, and beta 3 and insulin-like growth factor I in premature cranial suture fusion. *Plast Reconstr Surg* 99:300-309; discussion 310-306.

63. Cohen, M.M., Jr. 1993. Sutural biology and the correlates of craniosynostosis. *Am J Med Genet* 47:581-616.

64. De Pollack, C., Renier, D., Hott, M., and Marie, P.J. 1996. Increased bone formation and osteoblastic cell phenotype in premature cranial suture ossification (craniosynostosis). *J Bone Miner Res* 11:401-407.

65. Cohen, M.M., Jr. 2000. TGFβ and suture biology. In *Craniosynostosis: Diagnosis, Evaluation, and Management*. M.M. Cohen, Jr., and R.E. MacLean, editors. New York: Oxford University Press. 69-76.

66. Bresnick, S., and Schendel, S. 1995. Crouzon's disease correlates with low fibroblastic growth factor receptor activity in stenosed cranial sutures. *J Craniofac Surg* 6:245-248.

67. Ting, K., Vastardis, H., Mulliken, J.B., Soo, C., Tieu, A., Do, H., Kwong, E., Bertolami, C.N., Kawamoto, H., Kuroda, S., et al. 1999. Human NELL-1 expressed in unilateral coronal synostosis. *J Bone Miner Res* 14:80-89.

68. Lin, K.Y., Nolen, A.A., Gampper, T.J., Jane, J.A., Opperman, L.A., and Ogle, R.C. 1997. Elevated levels of transforming growth factors beta 2 and beta 3 in lambdoid sutures from children with persistent plagiocephaly. *Cleft Palate Craniofac J* 34:331-337.

69. Centrella, M., McCarthy, T.L., and Canalis, E. 1987. Transforming growth factor beta is a bifunctional regulator of replication and collagen synthesis in osteoblast-enriched cell cultures from fetal rat bone. *J Biol Chem* 262:2869-2874.

70. Yousfi, M., Lasmoles, F., and Marie, P.J. 2002. TWIST inactivation reduces CBFA1/RUNX2 expression and DNA binding to the osteocalcin promoter in osteoblasts. *Biochem Biophys Res Commun* 297:641-644.

71. Shevde, N.K., Bendixen, A.C., Maruyama, M., Li, B.L., and Billmire, D.A. 2001. Enhanced activity of osteoblast differentiation factor (PEBP2alphaA2/CBFa1) in affected sutural osteoblasts from patients with nonsyndromic craniosynostosis. *Cleft Palate Craniofac J* 38:606-614.

72. Centrella, M., McCarthy, T.L., and Canalis, E. 1992. Growth factors and cytokines. In *Bone Vol 4: Bone Metabolism and Mineralization*. B.K. Hall, editor. Boca Raton: CRC Press. 47-72.

73. Rosen, D.M., Stempien, S.A., Thompson, A.Y., and Seyedin, S.M. 1988. Transforming growth factor-beta modulates the expression of osteoblast and chondroblast phenotypes in vitro. *J Cell Physiol* 134:337-346.

74. Schmid, C., Steiner, T., and Froesch, E.R. 1983. Insulin-like growth factors stimulate synthesis of nucleic acids and glycogen in cultured calvaria cells. *Calcif Tissue Int* 35:578-585.

75. McCarthy, T.L., Centrella, M., and Canalis, E. 1989. Regulatory effects of insulin-like growth factors I and II on bone collagen synthesis in rat calvarial cultures. *Endocrinology* 124:301-309.

76. Davidovitch, Z., Zwilling, B.S., and Shanfeld, J.L. 1989. Control mechanisms of cartilage and bone. In *Scientific Foundations and Surgical Treatment of Craniosynostosis*. J.A. Persing, M.T. Edgerton, and J.A. Jane, editors. Baltimore: Williams & Wilkins. 38-44.

77. Noda, M. 1989. Transcriptional regulation of osteocalcin production by transforming growth factor-beta in rat osteoblast-like cells. *Endocrinology* 124:612-617.

78. Canalis, E. 1986. Interleukin-1 has independent effects on deoxyribonucleic acid and collagen synthesis in cultures of rat calvariae. *Endocrinology* 118:74-81.

79. Smith, D.D., Gowen, M., and Mundy, G.R. 1987. Effects of interferon-gamma and other cytokines on collagen synthesis in fetal rat bone cultures. *Endocrinology* 120:2494-2499.

80. Lorenzo, J.A. 1991. The role of cytokines in the regulation of local bone resorption. *Crit Rev Immunol* 11:195-213.

81. Opperman, L.A., and Ogle, R.C. 2002. Molecular Studies of Craniosynostosis: Factors Affecting Cranial Suture Morphogenesis and Patency. In *Understanding Craniofacial Anomalies: The Etiopathogenesis of Craniosynostosis and Facial Clefting*. M.P. Mooney, and M.I. Siegel, editors. New York: John W. Wiley and Sons. 497-518.

82. Opperman, L.A., Nolen, A.A., and Ogle, R.C. 1997. TGF-beta 1, TGF-beta 2, and TGF-beta 3 exhibit distinct patterns of expression during cranial suture formation and obliteration in vivo and in vitro. *J Bone Miner Res* 12:301-310.

83. Roth, D.A., Longaker, M.T., McCarthy, J.G., Rosen, D.M., McMullen, H.F., Levine, J.P., Sung, J., and Gold, L.I. 1997. Studies in cranial suture biology: Part I. Increased immunoreactivity for TGF-beta isoforms (beta 1, beta 2, and beta 3) during rat cranial suture fusion. *J Bone Miner Res* 12:311-321.

84. Opperman, L.A., Sweeney, T.M., Redmon, J., Persing, J.A., and Ogle, R.C. 1993. Tissue interactions with underlying dura mater inhibit osseous obliteration of developing cranial sutures. *Dev Dyn* 198:312-322.

85. Opperman, L.A., Passarelli, R.W., Morgan, E.P., Reintjes, M., and Ogle, R.C. 1995. Cranial sutures require tissue interactions with dura mater to resist osseous obliteration in vitro. *J Bone Miner Res* 10:1978-1987.

86. Opperman, L.A., Chhabra, A., Nolen, A.A., Bao, Y., and Ogle, R.C. 1998. Dura mater maintains rat cranial sutures in vitro by regulating suture cell proliferation and collagen production. *J Craniofac Genet Dev Biol* 18:150-158.

87. Bradley, J.P., Levine, J.P., Roth, D.A., McCarthy, J.G., and Longaker, M.T. 1996. Studies in cranial suture biology: IV. Temporal sequence of posterior frontal cranial suture fusion in the mouse. *Plast Reconstr Surg* 98:1039-1045.

88. Roth, D.A., Bradley, J.P., Levine, J.P., McMullen, H.F., McCarthy, J.G., and Longaker, M.T. 1996. Studies in cranial suture biology: part II. Role of the dura in cranial suture fusion. *Plast Reconstr Surg* 97:693-699.

89. Levine, J.H., Moses, H.L., Gold, L.I., and Nanney, L.B. 1993. Spatial and temporal patterns of immunoreactive transforming growth factor beta 1, beta 2, and beta 3 during excisional wound repair. *Am J Pathol* 143:368-380.

90. Opperman, L.A., Adab, K., and Gakunga, P.T. 2000. Transforming growth factor-beta 2 and TGF-beta 3 regulate fetal rat cranial suture morphogenesis by regulating rates of cell proliferation and apoptosis. *Dev Dyn* 219:237-247.

91. Opperman, L.A., Chhabra, A., Cho, R.W., and Ogle, R.C. 1999. Cranial suture obliteration is induced by removal of transforming growth factor (TGF)-beta 3 activity and prevented by removal of TGF-beta 2 activity from fetal rat calvaria in vitro. *J Craniofac Genet Dev Biol* 19:164-173.

92. Massague, J. 1987. The TGF-beta family of growth and differentiation factors. *Cell* 49:437-438.

93. Massague, J. 1990. The transforming growth factor-beta family. *Annu Rev Cell Biol* 6:597-641.

94. Massague, J., Attisano, L., and Wrana, J.L. 1994. The TGF-beta family and its composite receptors. *Trends Cell Biol* 4:172-178.

95. Bonewald, L.F., and Mundy, G.R. 1990. Role of transforming growth factor-beta in bone remodeling. *Clin Orthop Relat Res*:261-276.

96. ten Dijke, P., Iwata, K.K., Goddard, C., Pieler, C., Canalis, E., McCarthy, T.L., and Centrella, M. 1990. Recombinant transforming growth factor type beta 3: biological activities and receptor-binding properties in isolated bone cells. *Mol Cell Biol* 10:4473-4479.

97. Mehrara, B.J., Steinbrech, D.S., Saadeh, P.B., Gittes, G.K., and Longaker, M.T. 1999. Expression of high-affinity receptors for TGF-beta during rat cranial suture fusion. *Ann Plast Surg* 42:502-508.

98. Poisson, E., Sciote, J.J., Koepsel, R., Cooper, G.M., Opperman, L.A., and Mooney, M.P. 2004. Transforming growth factor-beta isoform expression in the perisutural tissues of craniosynostotic rabbits. *Cleft Palate Craniofac J* 41:392-402.

99. Mooney, M.P., Siegel, M.I., and Opperman, L.A. 2002. Animal models of craniosynostosis: experimental, congenital, and transgenic. In *Understanding Craniofacial Anomalies: The Etiopathogenesis fo Craniosynostosis and Facial Clefting*. M.P. Mooney, and M.I. Siegel, editors. New York: John W. Wiley and Sons. 251-272.

100. Mooney, M.P., Smith, T.D., Burrows, A.M., Langdon, H.L., Stone, C.E., Losken, H.W., Caruso, K., and Siegel, M.I. 1996. Coronal suture pathology and synostotic progression in rabbits with congenital craniosynostosis. *Cleft Palate Craniofac J* 33:369-378.

101. Chong, S.L., Mitchell, R., Moursi, A.M., Winnard, P., Losken, H.W., Bradley, J., Ozerdem, O.R., Azari, K., Acarturk, O., Opperman, L.A., et al. 2003. Rescue of coronal suture fusion using transforming growth factor-beta 3 (Tgf-beta 3) in rabbits with delayed-onset craniosynostosis. *Anat Rec A Discov Mol Cell Evol Biol* 274:962-971.

102. Sanford, L.P., Ormsby, I., Gittenberger-de Groot, A.C., Sariola, H., Friedman, R., Boivin, G.P., Cardell, E.L., and Doetschman, T. 1997. TGFbeta2 knockout mice have multiple developmental defects that are non-overlapping with other TGFbeta knockout phenotypes. *Development* 124:2659-2670.

103. Opperman, L.A., Galanis, V., Williams, A.R., and Adab, K. 2002. Transforming growth factor-beta3 (Tgf-beta3) down-regulates Tgf-beta3 receptor type I (Tbetar-I) during rescue of cranial sutures from osseous obliteration. *Orthod Craniofac Res* 5:5-16.

104. Opperman, L.A., Moursi, A.M., Sayne, J.R., and Wintergerst, A.M. 2002. Transforming growth factor-beta 3(Tgf-beta3) in a collagen gel delays fusion of the rat posterior interfrontal suture in vivo. *Anat Rec* 267:120-130.

105. Moursi, A.M., Winnard, P.L., Fryer, D., and Mooney, M.P. 2003. Delivery of transforming growth factor-beta2-perturbing antibody in a collagen vehicle inhibits cranial suture fusion in calvarial organ culture. *Cleft Palate Craniofac J* 40:225-232.

106. Wilkie, A.O., and Wall, S.A. 1996. Craniosynostosis: novel insights into pathogenesis and treatment. *Curr Opin Neurol* 9:146-152.

107. Cohen, M.M., Jr. 2000. Twist and MSX2 mutations. In *Craniosynostosis: Diagnosis, Evaluation, and Management*. M.M. Cohen, Jr., and R.E. MacLean, editors. New York: Oxford University Press. 51-68.

108. Frenkel, S.R., Grande, D.A., Collins, M., and Singh, I.J. 1990. Fibroblast growth factor in chick osteogenesis. *Biomaterials* 11:38-40.

109. Frenkel, S.R., Herskovits, M.S., and Singh, I.J. 1992. Fibroblast growth factor: effects on osteogenesis and chondrogenesis in the chick embryo. *Acta Anat (Basel)* 145:265-268.

110. Mayahara, H., Ito, T., Nagai, H., Miyajima, H., Tsukuda, R., Taketomi, S., Mizoguchi, J., and Kato, K. 1993. In vivo stimulation of endosteal bone formation by basic fibroblast growth factor in rats. *Growth Factors* 9:73-80.

111. Kasperk, C.H., Wergedal, J.E., Mohan, S., Long, D.L., Lau, K.H., and Baylink, D.J. 1990. Interactions of growth factors present in bone matrix with bone cells: effects on DNA synthesis and alkaline phosphatase. *Growth Factors* 3:147-158.

112. Shiang, R., Thompson, L.M., Zhu, Y.Z., Church, D.M., Fielder, T.J., Bocian, M., Winokur, S.T., and Wasmuth, J.J. 1994. Mutations in the transmembrane domain of FGFR3 cause the most common genetic form of dwarfism, achondroplasia. *Cell* 78:335-342.

113. Thomas, J.A., Manchester, D.K., Prescott, K.E., Milner, R., McGavran, L., and Cohen, M.M., Jr. 1996. Hunter-McAlpine craniosynostosis phenotype associated with skeletal anomalies and interstitial deletion of chromosome 17q. *Am J Med Genet* 62:372-375.

114. Johnston, M.C., and Bronsky, P.T. 2002. Craniofacial embryogenesis: Abnormal developmental mechanisns. In *Understanding Craniofacial Anomalies: The Etiopathogenesis of Crainiosynostosis and Facial Clefting*. M.P. Mooney, and M.I. Siegel, editors. New York: John W. Wiley and Sons 61-123.

115. Jabs, E.W., Muller, U., Li, X., Ma, L., Luo, W., Haworth, I.S., Klisak, I., Sparkes, R., Warman, M.L., Mulliken, J.B., et al. 1993. A mutation in the homeodomain of the human MSX2 gene in a family affected with autosomal dominant craniosynostosis. *Cell* 75:443-450.

116. Liu, Y.H., Kundu, R., Wu, L., Luo, W., Ignelzi, M.A., Jr., Snead, M.L., and Maxson, R.E., Jr. 1995. Premature suture closure and ectopic cranial bone in mice expressing Msx2 transgenes in the developing skull. *Proc Natl Acad Sci U S A* 92:6137-6141.

117. Semenza, G.L., Wang, G.L., and Kundu, R. 1995. DNA binding and transcriptional properties of wild-type and mutant forms of the homeodomain protein Msx2. *Biochem Biophys Res Commun* 209:257-262.

118. Cohen, M.M., Jr. 2000. Fibroblasts growth factor receptor mutations. In *Craniosynostosis: Diagnosis, Evaluation, and Management*. M.M. Cohen, Jr., and R.E. MacLean, editors. New York: Oxford University Press. 77-94.

119. Adab, K., Sayne, J.R., Carlson, D.S., and Opperman, L.A. 2002. Tgf-beta1, Tgf-beta2, Tgf-beta3 and Msx2 expression is elevated during frontonasal suture morphogenesis and during active postnatal facial growth. *Orthod Craniofac Res* 5:227-237.

120. Muller, U., Warman, M.L., Mulliken, J.B., and Weber, J.L. 1993. Assignment of a gene locus involved in craniosynostosis to chromosome 5qter. *Hum Mol Genet* 2:119-122.

121. Davidson, D. 1995. The function and evolution of Msx genes: pointers and paradoxes. *Trends Genet* 11:405-411.

122. Couly, G.F., Coltey, P.M., and Le Douarin, N.M. 1993. The triple origin of skull in higher vertebrates: a study in quail-chick chimeras. *Development* 117:409-429.

123. Winograd, J.M., Im, M.J., and Vander Kolk, C.A. 1997. Osteoblastic and osteoclastic activation in coronal sutures undergoing fusion ex vivo. *Plast Reconstr Surg* 100:1103-1112.

124. Orr-Urtreger, A., Bedford, M.T., Burakova, T., Arman, E., Zimmer, Y., Yayon, A., Givol, D., and Lonai, P. 1993. Developmental localization of the splicing alternatives of fibroblast growth factor receptor-2 (FGFR2). *Dev Biol* 158:475-486.

125. Orr-Urtreger, A., Givol, D., Yayon, A., Yarden, Y., and Lonai, P. 1991. Developmental expression of two murine fibroblast growth factor receptors, flg and bek. *Development* 113:1419-1434.

126. Vainio, S., Karavanova, I., Jowett, A., and Thesleff, I. 1993. Identification of BMP-4 as a signal mediating secondary induction between epithelial and mesenchymal tissues during early tooth development. *Cell* 75:45-58.

127. Graham, A., Francis-West, P., Brickell, P., and Lumsden, A. 1994. The signalling molecule BMP4 mediates apoptosis in the rhombencephalic neural crest. *Nature* 372:684-686.

128. Ignelzi, M.A., Jr., Wang, W., and Young, A.T. 2003. Fibroblast growth factors lead to increased Msx2 expression and fusion in calvarial sutures. *J Bone Miner Res* 18:751-759.

129. Warren, S.M., Brunet, L.J., Harland, R.M., Economides, A.N., and Longaker, M.T. 2003. The BMP antagonist noggin regulates cranial suture fusion. *Nature* 422:625-629.

130. Smith, W.C., and Harland, R.M. 1992. Expression cloning of noggin, a new dorsalizing factor localized to the Spemann organizer in Xenopus embryos. *Cell* 70:829-840.

131. Zimmerman, L.B., De Jesus-Escobar, J.M., and Harland, R.M. 1996. The Spemann organizer signal noggin binds and inactivates bone morphogenetic protein 4. *Cell* 86:599-606.

132. Balemans, W., and Van Hul, W. 2002. Extracellular regulation of BMP signaling in vertebrates: a cocktail of modulators. *Dev Biol* 250:231-250.

133. Rice, D.P., Rice, R., and Thesleff, I. 2003. Molecular mechanisms in calvarial bone and suture development, and their relation to craniosynostosis. *Eur J Orthod* 25:139-148.

134. Alsberg, E., Anderson, K.W., Albeiruti, A., Rowley, J.A., and Mooney, D.J. 2002. Engineering growing tissues. *Proc Natl Acad Sci U S A* 99:12025-12030.

135. Alsberg, E., Hill, E.E., and Mooney, D.J. 2001. Craniofacial tissue engineering. *Crit Rev Oral Biol Med* 12:64-75.

136. Boyan, B.D., Lohmann, C.H., Romero, J., and Schwartz, Z. 1999. Bone and cartilage tissue engineering. *Clin Plast Surg* 26:629-645, ix.

137. Mooney, M.P., Moursi, A.M., Opperman, L.A., and Siegel, M.I. 2004. Cytokine therapy for craniosynostosis. *Expert Opin Biol Ther* 4:279-299.

138. Einhorn, T.A. 2003. Clinical applications of recombinant human BMPs: early experience and future development. *J Bone Joint Surg Am* 85-A Suppl 3:82-88.

139. Silber, J.S., Anderson, D.G., Daffner, S.D., Brislin, B.T., Leland, J.M., Hilibrand, A.S., Vaccaro, A.R., and Albert, T.J. 2003. Donor site morbidity after anterior iliac crest bone harvest for single-level anterior cervical discectomy and fusion. *Spine* 28:134-139.

140. Summers, B.N., and Eisenstein, S.M. 1989. Donor site pain from the ilium. A complication of lumbar spine fusion. *J Bone Joint Surg Br* 71:677-680.

141. Sammarco, V.J., and Chang, L. 2002. Modern issues in bone graft substitutes and advances in bone tissue technology. *Foot Ankle Clin* 7:19-41.

142. Eppley, B.L., Pietrzak, W.S., and Blanton, M.W. 2005. Allograft and alloplastic bone substitutes: a review of science and technology for the craniomaxillofacial surgeon. *J Craniofac Surg* 16:981-989.

143. Giannoudis, P.V., Dinopoulos, H., and Tsiridis, E. 2005. Bone substitutes: an update. *Injury* 36 Suppl 3:S20-27.

144. Rezwan, K., Chen, Q.Z., Blaker, J.J., and Boccaccini, A.R. 2006. Biodegradable and bioactive porous polymer/inorganic composite scaffolds for bone tissue engineering. *Biomaterials* 27:3413-3431.

145. Urist, M.R. 1965. Bone: formation by autoinduction. *Science* 150:893-899.

146. Khouri, R.K., Brown, D.M., Koudsi, B., Deune, E.G., Gilula, L.A., Cooley, B.C., and Reddi, A.H. 1996. Repair of calvarial defects with flap tissue: role of bone morphogenetic proteins and competent responding tissues. *Plast Reconstr Surg* 98:103-109.

147. Heckman, J.D., Boyan, B.D., Aufdemorte, T.B., and Abbott, J.T. 1991. The use of bone morphogenetic protein in the treatment of non-union in a canine model. *J Bone Joint Surg Am* 73:750-764.

148. Bostrom, M., Lane, J.M., Tomin, E., Browne, M., Berberian, W., Turek, T., Smith, J., Wozney, J., and Schildhauer, T. 1996. Use of bone morphogenetic protein-2 in the rabbit ulnar nonunion model. *Clin Orthop*:272-282.

149. Lindholm, T.C., Lindholm, T.S., Alitalo, I., and Urist, M.R. 1988. Bovine bone morphogenetic protein (bBMP) induced repair of skull trephine defects in sheep. *Clin Orthop* 227:265-268.

150. Nilsson, O.S., Urist, M.R., Dawson, E.G., Schmalzried, T.P., and Finerman, G.A. 1986. Bone repair induced by bone morphogenetic protein in ulnar defects in dogs. *J Bone Joint Surg Br* 68:635-642.

151. Boyne, P.J. 2001. Application of bone morphogenetic proteins in the treatment of clinical oral and maxillofacial osseous defects. *J Bone Joint Surg Am* 83-A Suppl 1:S146-150.

152. Danesh-Meyer, M.J. 2000. Tissue engineering in periodontics using rhBMP-2. *J N Z Soc Periodontol*:10-14.

153. Marukawa, E., Asahina, I., Oda, M., Seto, I., Alam, M.I., and Enomoto, S. 2001. Bone regeneration using recombinant human bone morphogenetic protein-2 (rhBMP-2) in alveolar defects of primate mandibles. *Br J Oral Maxillofac Surg* 39:452-459.

154. Pluhar, G.E., Manley, P.A., Heiner, J.P.J.R.V., Seeherman, H.J., and Markel, M.D. 2001. The effect of recombinant human bone morphogenetic protein-2 on femoral reconstruction with an intercalary allograft in a dog model. *J Orthop Res* 19:308-317.

155. Cook, S.D., Baffes, G.C., Wolfe, M.W., Sampath, T.K., Rueger, D.C., and Whitecloud, T.S., 3rd. 1994. The effect of recombinant human osteogenic protein-1 on healing of large segmental bone defects. *J Bone Joint Surg Am* 76:827-838.

156. Yasko, A.W., Lane, J.M., Fellinger, E.J., Rosen, V., Wozney, J.M., and Wang, E.A. 1992. The healing of segmental bone defects, induced by recombinant human bone morphogenetic protein (rhBMP-2). A radiographic, histological, and biomechanical study in rats. *J Bone Joint Surg Am* 74:659-670.

157. Zellin, G., and Linde, A. 1997. Treatment of segmental defects in long bones using osteopromotive membranes and recombinant human bone morphogenetic protein-2. An experimental study in rabbits. *Scand J Plast Reconstr Surg Hand Surg* 31:97-104.

158. Mayer, M., Hollinger, J., Ron, E., and Wozney, J. 1996. Maxillary alveolar cleft repair in dogs using recombinant human bone morphogenetic protein-2 and a polymer carrier. *Plast Reconstr Surg* 98:247-259.

159. Hollinger, J.O., Schmitt, J.M., Buck, D.C., Shannon, R., Joh, S.P., Zegzula, H.D., and Wozney, J. 1998. Recombinant human bone morphogenetic protein-2 and collagen for bone regeneration. *J Biomed Mater Res* 43:356-364.

160. Zegzula, H.D., Buck, D.C., Brekke, J., Wozney, J.M., and Hollinger, J.O. 1997. Bone formation with use of rhBMP-2 (recombinant human bone morphogenetic protein-2). *J Bone Joint Surg Am* 79:1778-1790.

161. Johnson, E.E., Urist, M.R., and Finerman, G.A. 1988. Bone morphogenetic protein augmentation grafting of resistant femoral nonunions. A preliminary report. *Clin Orthop*:257-265.

162. Johnson, E.E., Urist, M.R., and Finerman, G.A. 1988. Repair of segmental defects of the tibia with cancellous bone grafts augmented with human bone morphogenetic protein. A preliminary report. *Clin Orthop*:249-257.

163. Johnson, E.E., Urist, M.R., and Finerman, G.A. 1990. Distal metaphyseal tibial nonunion. Deformity and bone loss treated by open reduction, internal fixation, and human bone morphogenetic protein (hBMP). *Clin Orthop*:234-240.

164. Geiger, M., Li, R.H., and Friess, W. 2003. Collagen sponges for bone regeneration with rhBMP-2. *Adv Drug Deliv Rev* 55:1613-1629.

165. Jingushi, S., Urabe, K., Okazaki, K., Hirata, G., Sakai, A., Ikenoue, T., and Iwamoto, Y. 2002. Intramuscular bone induction by human recombinant bone morphogenetic protein-

2 with beta-tricalcium phosphate as a carrier: in vivo bone banking for muscle-pedicle autograft. *J Orthop Sci* 7:490-494.

166. Li, R.H., Bouxsein, M.L., Blake, C.A., D'Augusta, D., Kim, H., Li, X.J., Wozney, J.M., and Seeherman, H.J. 2003. rhBMP-2 injected in a calcium phosphate paste (alpha-BSM) accelerates healing in the rabbit ulnar osteotomy model. *J Orthop Res* 21:997-1004.

167. Kim, H.D., and Valentini, R.F. 2002. Retention and activity of BMP-2 in hyaluronic acid-based scaffolds in vitro. *J Biomed Mater Res* 59:573-584.

168. Minamide, A., Kawakami, M., Hashizume, H., Sakata, R., and Tamaki, T. 2001. Evaluation of carriers of bone morphogenetic protein for spinal fusion. *Spine* 26:933-939.

169. Friedlaender, G.E., Perry, C.R., Cole, J.D., Cook, S.D., Cierny, G., Muschler, G.F., Zych, G.A., Calhoun, J.H., LaForte, A.J., and Yin, S. 2001. Osteogenic protein-1 (bone morphogenetic protein-7) in the treatment of tibial nonunions. *J Bone Joint Surg Am* 83-A Suppl 1:S151-158.

170. Burkus, J.K., Gornet, M.F., Dickman, C.A., and Zdeblick, T.A. 2002. Anterior lumbar interbody fusion using rhBMP-2 with tapered interbody cages. *J Spinal Disord Tech* 15:337-349.

171. Govender, S., Csimma, C., Genant, H.K., Valentin-Opran, A., Amit, Y., Arbel, R., Aro, H., Atar, D., Bishay, M., Borner, M.G., et al. 2002. Recombinant human bone morphogenetic protein-2 for treatment of open tibial fractures: a prospective, controlled, randomized study of four hundred and fifty patients. *J Bone Joint Surg Am* 84-A:2123-2134.

172. Musgrave, D.S., Bosch, P., Ghivizzani, S., Robbins, P.D., Evans, C.H., and Huard, J. 1999. Adenovirus-mediated direct gene therapy with bone morphogenetic protein-2 produces bone. *Bone* 24:541-547.

173. Abdelaal, M.M., Tholpady, S.S., Kessler, J.D., Morgan, R.F., and Ogle, R.C. 2004. BMP-9-transduced prefabricated muscular flaps for the treatment of bony defects. *J Craniofac Surg* 15:736-741; discussion 742-734.

174. Bertone, A.L., Pittman, D.D., Bouxsein, M.L., Li, J., Clancy, B., and Seeherman, H.J. 2004. Adenoviral-mediated transfer of human BMP-6 gene accelerates healing in a rabbit ulnar osteotomy model. *J Orthop Res* 22:1261-1270.

175. Blum, J.S., Barry, M.A., Mikos, A.G., and Jansen, J.A. 2003. In vivo evaluation of gene therapy vectors in ex vivo-derived marrow stromal cells for bone regeneration in a rat critical-size calvarial defect model. *Hum Gene Ther* 14:1689-1701.

176. Dunn, C.A., Jin, Q., Taba, M., Jr., Franceschi, R.T., Bruce Rutherford, R., and Giannobile, W.V. 2005. BMP gene delivery for alveolar bone engineering at dental implant defects. *Mol Ther* 11:294-299.

177. Kang, Q., Sun, M.H., Cheng, H., Peng, Y., Montag, A.G., Deyrup, A.T., Jiang, W., Luu, H.H., Luo, J., Szatkowski, J.P., et al. 2004. Characterization of the distinct orthotopic bone-forming activity of 14 BMPs using recombinant adenovirus-mediated gene delivery. *Gene Ther* 11:1312-1320.

178. Peterson, B., Zhang, J., Iglesias, R., Kabo, M., Hedrick, M., Benhaim, P., and Lieberman, J.R. 2005. Healing of critically sized femoral defects, using genetically modified mesenchymal stem cells from human adipose tissue. *Tissue Eng* 11:120-129.

179. Zhang, X.S., Linkhart, T.A., Chen, S.T., Peng, H., Wergedal, J.E., Guttierez, G.G., Sheng, M.H., Lau, K.H., and Baylink, D.J. 2004. Local ex vivo gene therapy with bone marrow stromal cells expressing human BMP4 promotes endosteal bone formation in mice. *J Gene Med* 6:4-15.

180. Zhao, M., Zhao, Z., Koh, J.T., Jin, T., and Franceschi, R.T. 2005. Combinatorial gene therapy for bone regeneration: Cooperative interactions between adenovirus vectors expressing bone morphogenetic proteins 2, 4, and 7. *J Cell Biochem* 95:1-16.

181. Abe, N., Lee, Y.P., Sato, M., Zhang, X., Wu, J., Mitani, K., and Lieberman, J.R. 2002. Enhancement of bone repair with a helper-dependent adenoviral transfer of bone morphogenetic protein-2. *Biochem Biophys Res Commun* 297:523-527.

182. Chang, S.C., Chuang, H., Chen, Y.R., Yang, L.C., Chen, J.K., Mardini, S., Chung, H.Y., Lu, Y.L., Ma, W.C., and Lou, J. 2004. Cranial repair using BMP-2 gene engineered bone marrow stromal cells. *J Surg Res* 119:85-91.

183. Chang, S.C., Chuang, H.L., Chen, Y.R., Chen, J.K., Chung, H.Y., Lu, Y.L., Lin, H.Y., Tai, C.L., and Lou, J. 2003. Ex vivo gene therapy in autologous bone marrow stromal stem cells for tissue-engineered maxillofacial bone regeneration. *Gene Ther* 10:2013-2019.

184. Chang, S.C., Wei, F.C., Chuang, H., Chen, Y.R., Chen, J.K., Lee, K.C., Chen, P.K., Tai, C.L., and Lou, J. 2003. Ex vivo gene therapy in autologous critical-size craniofacial bone regeneration. *Plast Reconstr Surg* 112:1841-1850.

185. Sugiyama, O., An, D.S., Kung, S.P., Feeley, B.T., Gamradt, S., Liu, N.Q., Chen, I.S., and Lieberman, J.R. 2005. Lentivirus-mediated gene transfer induces long-term transgene expression of BMP-2 in vitro and new bone formation in vivo. *Mol Ther* 11:390-398.

186. Herbertson, A., and Aubin, J.E. 1995. Dexamethasone alters the subpopulation make-up of rat bone marrow stromal cell cultures. *J Bone Miner Res* 10:285-294.

187. Simmons, D.J., Seitz, P., Kidder, L., Klein, G.L., Waeltz, M., Gundberg, C.M., Tabuchi, C., Yang, C., and Zhang, R.W. 1991. Partial characterization of rat marrow stromal cells. *Calcif Tissue Int* 48:326-334.

188. Ogawa, R., Mizuno, H., Watanabe, A., Migita, M., Shimada, T., and Hyakusoku, H. 2004. Osteogenic and chondrogenic differentiation by adipose-derived stem cells harvested from GFP transgenic mice. *Biochem Biophys Res Commun* 313:871-877.

189. Ogawa, R., Mizuno, H., Watanabe, A., Migita, M., Hyakusoku, H., and Shimada, T. 2004. Adipogenic differentiation by adipose-derived stem cells harvested from GFP transgenic mice-including relationship of sex differences. *Biochem Biophys Res Commun* 319:511-517.

190. Zuk, P.A., Zhu, M., Mizuno, H., Huang, J., Futrell, J.W., Katz, A.J., Benhaim, P., Lorenz, H.P., and Hedrick, M.H. 2001. Multilineage cells from human adipose tissue: implications for cell-based therapies. *Tissue Eng* 7:211-228.

191. Jaiswal, R.K., Jaiswal, N., Bruder, S.P., Mbalaviele, G., Marshak, D.R., and Pittenger, M.F. 2000. Adult human mesenchymal stem cell differentiation to the osteogenic or adipogenic lineage is regulated by mitogen-activated protein kinase. *J Biol Chem* 275:9645-9652.

192. Huang, J.I., Beanes, S.R., Zhu, M., Lorenz, H.P., Hedrick, M.H., and Benhaim, P. 2002. Rat extramedullary adipose tissue as a source of osteochondrogenic progenitor cells. *Plast Reconstr Surg* 109:1033-1041; discussion 1042-1033.

193. Zuk, P.A., Zhu, M., Ashjian, P., De Ugarte, D.A., Huang, J.I., Mizuno, H., Alfonso, Z.C., Fraser, J.K., Benhaim, P., and Hedrick, M.H. 2002. Human adipose tissue is a source of multipotent stem cells. *Mol Biol Cell* 13:4279-4295.

194. Edwards, P.C., Ruggiero, S., Fantasia, J., Burakoff, R., Moorji, S.M., Paric, E., Razzano, P., Grande, D.A., and Mason, J.M. 2005. Sonic hedgehog gene-enhanced tissue engineering for bone regeneration. *Gene Ther* 12:75-86.

195. Krebsbach, P.H., Gu, K., Franceschi, R.T., and Rutherford, R.B. 2000. Gene therapy-directed osteogenesis: BMP-7-transduced human fibroblasts form bone in vivo. *Hum Gene Ther* 11:1201-1210.

196. Rutherford, R.B., Moalli, M., Franceschi, R.T., Wang, D., Gu, K., and Krebsbach, P.H. 2002. Bone morphogenetic protein-transduced human fibroblasts convert to osteoblasts and form bone in vivo. *Tissue Eng* 8:441-452.

197. Musgrave, D.S., Pruchnic, R., Wright, V., Bosch, P., Ghivizzani, S.C., Robbins, P.D., and Huard, J. 2001. The effect of bone morphogenetic protein-2 expression on the early fate of skeletal muscle-derived cells. *Bone* 28:499-506.

198. Lee, J.Y., Qu-Petersen, Z., Cao, B., Kimura, S., Jankowski, R., Cummins, J., Usas, A., Gates, C., Robbins, P., Wernig, A., et al. 2000. Clonal isolation of muscle-derived cells capable of enhancing muscle regeneration and bone healing. *J Cell Biol* 150:1085-1100.

199. Lee, J.Y., Musgrave, D., Pelinkovic, D., Fukushima, K., Cummins, J., Usas, A., Robbins, P., Fu, F.H., and Huard, J. 2001. Effect of bone morphogenetic protein-2-expressing muscle-derived cells on healing of critical-sized bone defects in mice. *J Bone Joint Surg Am* 83-A:1032-1039.

200. Aikawa, T., Shirasuna, K., Iwamoto, M., Watatani, K., Nakamura, T., Okura, M., Yoshioka, H., and Matsuya, T. 1996. Establishment of bone morphogenetic protein 2 responsive chondrogenic cell line. *J Bone Miner Res* 11:544-553.

201. Asakura, A., Komaki, M., and Rudnicki, M. 2001. Muscle satellite cells are multipotential stem cells that exhibit myogenic, osteogenic, and adipogenic differentiation. *Differentiation* 68:245-253.

202. Levy, M.M., Joyner, C.J., Virdi, A.S., Reed, A., Triffitt, J.T., Simpson, A.H., Kenwright, J., Stein, H., and Francis, M.J. 2001. Osteoprogenitor cells of mature human skeletal muscle tissue: an in vitro study. *Bone* 29:317-322.

203. Bosch, P., Musgrave, D.S., Lee, J.Y., Cummins, J., Shuler, T., Ghivizzani, T.C., Evans, T., Robbins, T.D., and Huard. 2000. Osteoprogenitor cells within skeletal muscle. *J Orthop Res* 18:933-944.

204. Peng, H., and Huard, J. 2003. Stem cells in the treatment of muscle and connective tissue diseases. *Curr Opin Pharmacol* 3:329-333.

205. Corsi, K., Li, G.H., Peng, H., and Huard, J. 2004. Muscle-based gene therapy and tissue engineering for cartilage and bone healing. *Current Genomics* 5:7-17.

206. Cohen, M.M., Jr. 2002. Malformations of the craniofacial region: evolutionary, embryonic, genetic, and clinical perspectives. *Am J Med Genet* 115:245-268.

207. Pang, E.K., Im, S.U., Kim, C.S., Choi, S.H., Chai, J.K., Kim, C.K., Han, S.B., and Cho, K.S. 2004. Effect of recombinant human bone morphogenetic protein-4 dose on bone formation in a rat calvarial defect model. *J Periodontol* 75:1364-1370.

208. Onishi, T., Ishidou, Y., Nagamine, T., Yone, K., Imamura, T., Kato, M., Sampath, T.K., ten Dijke, P., and Sakou, T. 1998. Distinct and overlapping patterns of localization of bone morphogenetic protein (BMP) family members and a BMP type II receptor during fracture healing in rats. *Bone* 22:605-612.

209. Spector, J.A., Luchs, J.S., Mehrara, B.J., Greenwald, J.A., Smith, L.P., and Longaker, M.T. 2001. Expression of bone morphogenetic proteins during membranous bone healing. *Plast Reconstr Surg* 107:124-134.

210. Yoshimura, Y., Nomura, S., Kawasaki, S., Tsutsumimoto, T., Shimizu, T., and Takaoka, K. 2001. Colocalization of noggin and bone morphogenetic protein-4 during fracture healing. *J Bone Miner Res* 16:876-884.

211. Glaser, D.L., Economides, A.N., Wang, L., Liu, X., Kimble, R.D., Fandl, J.P., Wilson, J.M., Stahl, N., Kaplan, F.S., and Shore, E.M. 2003. In vivo somatic cell gene transfer of an engineered Noggin mutein prevents BMP4-induced heterotopic ossification. *J Bone Joint Surg Am* 85-A:2332-2342.

212. Hannallah, D., Peng, H., Young, B., Usas, A., Gearhart, B., and Huard, J. 2004. Retroviral delivery of Noggin inhibits the formation of heterotopic ossification induced by BMP-4, demineralized bone matrix, and trauma in an animal model. *J Bone Joint Surg Am* 86-A:80-91.

213. Aspenberg, P., Jeppsson, C., and Economides, A.N. 2001. The bone morphogenetic proteins antagonist Noggin inhibits membranous ossification. *J Bone Miner Res* 16:497-500.

214. Cooper, G.M., Mooney, M.P., Burrows, A.M., Smith, T.D., Dechant, J., Losken, H.W., Marsh, J.L., and Siegel, M.I. 1999. Brain growth rates in craniosynostotic rabbits. *Cleft Palate Craniofac J* 36:314-321.

215. Mooney, M.P., Losken, H.W., Siegel, M.I., Lalikos, J.F., Losken, A., Smith, T.D., and Burrows, A.M. 1994. Development of a strain of rabbits with congenital simple nonsyndromic coronal suture synostosis. Part I: Breeding demographics, inheritance pattern, and craniofacial anomalies. *Cleft Palate Craniofac J* 31:1-7.

216. Mooney, M.P., Aston, C.E., Siegel, M.I., Losken, H.W., Smith, T.D., Burrows, A.M., Wenger, S.L., Caruso, K., Siegel, B., and Ferrell, R.E. 1996. Craniosynostosis with autosomal dominant transmission in New Zealand white rabbits. *J Craniofac Genet Dev Biol* 16:52-63.

217. Masoud, I., Shapiro, F., and Moses, A. 1986. Longitudinal roentgencephalometric study of the growth of the New Zealand white rabbit: cumulative and biweekly incremental growth rates for skull and mandible. *J Craniofac Genet Dev Biol* 6:259-287.

218. Alberius, P., and Selvik, G. 1986. Long-term analysis of calvarial growth in rabbits. *Anat Anz* 162:153-170.

219. Harel, S., Watanabe, K., Linke, I., and Schain, R.J. 1972. Growth and development of the rabbit brain. *Biol Neonate* 21:381-399.

220. Most, D., Levine, J.P., Chang, J., Sung, J., McCarthy, J.G., Schendel, S.A., and Longaker, M.T. 1998. Studies in cranial suture biology: up-regulation of transforming growth factor-beta1 and basic fibroblast growth factor mRNA correlates with posterior frontal cranial suture fusion in the rat. *Plast Reconstr Surg* 101:1431-1440.

221. Greenwald, J.A., Mehrara, B.J., Spector, J.A., Warren, S.M., Fagenholz, P.J., Smith, L.E., Bouletreau, P.J., Crisera, F.E., Ueno, H., and Longaker, M.T. 2001. In vivo modulation of FGF biological activity alters cranial suture fate. *Am J Pathol* 158:441-452.

222. Gabbay, J.S., Heller, J., Spoon, D.B., Mooney, M., Acarturk, O., Askari, M., Wasson, K.L., and Bradley, J.P. 2006. Noggin Underexpression and Runx-2 Overexpression in a Craniosynostosis Rabbit Model. *Ann Plast Surg* 56:306-311.

223. Groppe, J., Greenwald, J., Wiater, E., Rodriguez-Leon, J., Economides, A.N., Kwiatkowski, W., Affolter, M., Vale, W.W., Belmonte, J.C., and Choe, S. 2002. Structural basis of BMP signalling inhibition by the cystine knot protein Noggin. *Nature* 420:636-642.

224. Schmitz, J.P., and Hollinger, J.O. 1986. The critical size defect as an experimental model for craniomandibulofacial nonunions. *Clin Orthop*:299-308.

225. Hollinger, J.O., and Kleinschmidt, J.C. 1990. The critical size defect as an experimental model to test bone repair materials. *J Craniofac Surg* 1:60-68.

226. Mooney, M.P., and Siegel, M.I. 2005. Animal models for bone tissue engineering. In *Encyclopedia of Biomaterials and Biomedical Engineering*. G. Wnek, and G. Bowlin, editors. New York: Marcel Dekker. 1-19.

227. Krebsbach, P.H., Mankani, M.H., Satomura, K., Kuznetsov, S.A., and Robey, P.G. 1998. Repair of craniotomy defects using bone marrow stromal cells. *Transplantation* 66:1272-1278.

228. Babler, W.J., Persing, J.A., Persson, K.M., Winn, H.R., Jane, J.A., and Rodeheaver, G.T. 1982. Skull growth after coronal suturectomy, periostectomy, and dural transection. *J Neurosurg* 56:529-535.

229. Spector, J.A., Greenwald, J.A., Warren, S.M., Bouletreau, P.J., Crisera, F.E., Mehrara, B.J., and Longaker, M.T. 2002. Co-culture of osteoblasts with immature dural cells causes an increased rate and degree of osteoblast differentiation. *Plast Reconstr Surg* 109:631-642; discussion 643-644.

230. Spector, J.A., Greenwald, J.A., Warren, S.M., Bouletreau, P.J., Detch, R.C., Fagenholz, P.J., Crisera, F.E., and Longaker, M.T. 2002. Dura mater biology: autocrine and paracrine effects of fibroblast growth factor 2. *Plast Reconstr Surg* 109:645-654.

231. Greenwald, J.A., Mehrara, B.J., Spector, J.A., Chin, G.S., Steinbrech, D.S., Saadeh, P.B., Luchs, J.S., Paccione, M.F., Gittes, G.K., and Longaker, M.T. 2000. Biomolecular mechanisms of calvarial bone induction: immature versus mature dura mater. *Plast Reconstr Surg* 105:1382-1392.

232. Greenwald, J.A., Mehrara, B.J., Spector, J.A., Fagenholz, P.J., Saadeh, P.B., Steinbrech, D.S., Gittes, G.K., and Longaker, M.T. 2000. Immature versus mature dura mater: II. Differential expression of genes important to calvarial reossification. *Plast Reconstr Surg* 106:630-638; discussion 639.

233. Gosain, A.K., Santoro, T.D., Song, L.S., Capel, C.C., Sudhakar, P.V., and Matloub, H.S. 2003. Osteogenesis in calvarial defects: contribution of the dura, the pericranium, and the surrounding bone in adult versus infant animals. *Plast Reconstr Surg* 112:515-527.

234. Mooney, M.P., Losken, H.W., Tschakaloff, A., Siegel, M.I., Losken, A., and Lalikos, J.F. 1993. Congenital bilateral coronal suture synostosis in a rabbit and craniofacial growth comparisons with experimental models. *Cleft Palate Craniofac J* 30:121-128.

235. Levine, J.P., Bradley, J.P., Roth, D.A., McCarthy, J.G., and Longaker, M.T. 1998. Studies in cranial suture biology: regional dura mater determines overlying suture biology. *Plast Reconstr Surg* 101:1441-1447.

236. Nussenbaum, B., and Krebsbach, P.H. 2006. The role of gene therapy for craniofacial and dental tissue engineering. *Adv Drug Deliv Rev* 58:577-591.

237. Schmitz, J.P., Schwartz, Z., Hollinger, J.O., and Boyan, B.D. 1990. Characterization of rat calvarial nonunion defects. *Acta Anat (Basel)* 138:185-192.

238. Brinker, M.R. 2003. Nonunions: Evaluation and Treatment. In *Skeletal Trauma: Basic Science, Management, and Reconstruction*. B.D. Browner, J.B. Jupiter, A.M. Levine, P.G. Trafton, N.E. Green, and M.F. Swiontkowski, editors. New York: Saunders. 507.

239. Gosain, A.K., Song, L., Yu, P., Mehrara, B.J., Maeda, C.Y., Gold, L.I., and Longaker, M.T. 2000. Osteogenesis in cranial defects: reassessment of the concept of critical size and the expression of TGF-beta isoforms. *Plast Reconstr Surg* 106:360-371; discussion 372.

240. Dayoub, H., Dumont, R.J., Li, J.Z., Dumont, A.S., Hankins, G.R., Kallmes, D.F., and Helm, G.A. 2003. Human mesenchymal stem cells transduced with recombinant bone morphogenetic protein-9 adenovirus promote osteogenesis in rodents. *Tissue Eng* 9:347-356.

241. Li, J.Z., Hankins, G.R., Kao, C., Li, H., Kammauff, J., and Helm, G.A. 2003. Osteogenesis in rats induced by a novel recombinant helper-dependent bone morphogenetic protein-9 (BMP-9) adenovirus. *J Gene Med* 5:748-756.

242. Tarkka, T., Sipola, A., Jamsa, T., Soini, Y., Yla-Herttuala, S., Tuukkanen, J., and Hautala, T. 2003. Adenoviral VEGF-A gene transfer induces angiogenesis and promotes bone formation in healing osseous tissues. *J Gene Med* 5:560-566.

243. Cowan, C.M., Shi, Y.Y., Aalami, O.O., Chou, Y.F., Mari, C., Thomas, R., Quarto, N., Contag, C.H., Wu, B., and Longaker, M.T. 2004. Adipose-derived adult stromal cells heal critical-size mouse calvarial defects. *Nat Biotechnol* 22:560-567.

244. Canalis, E., Economides, A.N., and Gazzerro, E. 2003. Bone morphogenetic proteins, their antagonists, and the skeleton. *Endocr Rev* 24:218-235.

245. Peng, H., Usas, A., Hannallah, D., Olshanski, A., Cooper, G.M., and Huard, J. 2005. Noggin improves bone healing elicited by muscle stem cells expressing inducible BMP4. *Mol Ther* 12:239-246.

246. Ono, I., Yamashita, T., Jin, H.Y., Ito, Y., Hamada, H., Akasaka, Y., Nakasu, M., Ogawa, T., and Jimbow, K. 2004. Combination of porous hydroxyapatite and cationic liposomes as a vector for BMP-2 gene therapy. *Biomaterials* 25:4709-4718.

247. Huang, Y.C., Simmons, C., Kaigler, D., Rice, K.G., and Mooney, D.J. 2005. Bone regeneration in a rat cranial defect with delivery of PEI-condensed plasmid DNA encoding for bone morphogenetic protein-4 (BMP-4). *Gene Ther* 12:418-426.

248. Katsube, K., Bishop, A.T., Simari, R.D., Yla-Herttuala, S., and Friedrich, P.F. 2005. Vascular endothelial growth factor (VEGF) gene transfer enhances surgical revascularization of necrotic bone. *J Orthop Res* 23:469-474.

249. Gafni, Y., Pelled, G., Zilberman, Y., Turgeman, G., Apparailly, F., Yotvat, H., Galun, E., Gazit, Z., Jorgensen, C., and Gazit, D. 2004. Gene therapy platform for bone regeneration using an exogenously regulated, AAV-2-based gene expression system. *Mol Ther* 9:587-595.

250. Ito, H., Koefoed, M., Tiyapatanaputi, P., Gromov, K., Goater, J.J., Carmouche, J., Zhang, X., Rubery, P.T., Rabinowitz, J., Samulski, R.J., et al. 2005. Remodeling of cortical bone allografts mediated by adherent rAAV-RANKL and VEGF gene therapy. *Nat Med* 11:291-297.

251. Shen, H.C., Peng, H., Usas, A., Gearhart, B., Cummins, J., Fu, F.H., and Huard, J. 2004. Ex vivo gene therapy-induced endochondral bone formation: comparison of muscle-derived stem cells and different subpopulations of primary muscle-derived cells. *Bone* 34:982-992.

252. Shen, H.C., Peng, H., Usas, A., Gearhart, B., Fu, F.H., and Huard, J. 2004. Structural and functional healing of critical-size segmental bone defects by transduced muscle-derived cells expressing BMP4. *J Gene Med* 6:984-991.

253. Peng, H., Usas, A., Gearhart, B., Young, B., Olshanski, A., and Huard, J. 2004. Development of a self-inactivating tet-on retroviral vector expressing bone morphogenetic protein 4 to achieve regulated bone formation. *Mol Ther* 9:885-894.

254. Pittenger, M.F., Mackay, A.M., Beck, S.C., Jaiswal, R.K., Douglas, R., Mosca, J.D., Moorman, M.A., Simonetti, D.W., Craig, S., and Marshak, D.R. 1999. Multilineage potential of adult human mesenchymal stem cells. *Science* 284:143-147.

255. Peng, H., Usas, A., Gearhart, B., Olshanski, A., Shen, H.C., and Huard, J. 2004. Converse relationship between in vitro osteogenic differentiation and in vivo bone healing elicited

by different populations of muscle-derived cells genetically engineered to express BMP4. *J Bone Miner Res* 19:630-641.

256. Peng, H., Wright, V., Usas, A., Gearhart, B., Shen, H.C., Cummins, J., and Huard, J. 2002. Synergistic enhancement of bone formation and healing by stem cell-expressed VEGF and bone morphogenetic protein-4. *J Clin Invest* 110:751-759.

257. Musgrave, D.S., Bosch, P., Lee, J.Y., Pelinkovic, D., Ghivizzani, S.C., Whalen, J., Niyibizi, C., and Huard, J. 2000. Ex vivo gene therapy to produce bone using different cell types. *Clin Orthop*:290-305.

258. Wright, V., Peng, H., Usas, A., Young, B., Gearhart, B., Cummins, J., and Huard, J. 2002. BMP4-expressing muscle-derived stem cells differentiate into osteogenic lineage and improve bone healing in immunocompetent mice. *Mol Ther* 6:169-178.

259. Qu-Petersen, Z., Deasy, B., Jankowski, R., Ikezawa, M., Cummins, J., Pruchnic, R., Mytinger, J., Cao, B., Gates, C., Wernig, A., et al. 2002. Identification of a novel population of muscle stem cells in mice: potential for muscle regeneration. *J Cell Biol* 157:851-864.

260. Peng, H., Chen, S.T., Wergedal, J.E., Polo, J.M., Yee, J.K., Lau, K.H., and Baylink, D.J. 2001. Development of an MFG-based retroviral vector system for secretion of high levels of functionally active human BMP4. *Mol Ther* 4:95-104.

261. Capdevila, J., and Johnson, R.L. 1998. Endogenous and ectopic expression of noggin suggests a conserved mechanism for regulation of BMP function during limb and somite patterning. *Dev Biol* 197:205-217.

262. Sela-Donenfeld, D., and Kalcheim, C. 2002. Localized BMP4-noggin interactions generate the dynamic patterning of noggin expression in somites. *Dev Biol* 246:311-328.

263. Gazzerro, E., Gangji, V., and Canalis, E. 1998. Bone morphogenetic proteins induce the expression of noggin, which limits their activity in cultured rat osteoblasts. *J Clin Invest* 102:2106-2114.

264. Nifuji, A., and Noda, M. 1999. Coordinated expression of noggin and bone morphogenetic proteins (BMPs) during early skeletogenesis and induction of noggin expression by BMP-7. *J Bone Miner Res* 14:2057-2066.

265. Lee, J.Y., Peng, H., Usas, A., Musgrave, D., Cummins, J., Pelinkovic, D., Jankowski, R., Ziran, B., Robbins, P., and Huard, J. 2002. Enhancement of bone healing based on ex vivo gene therapy using human muscle-derived cells expressing bone morphogenetic protein 2. *Hum Gene Ther* 13:1201-1211.

266. Lieberman, J.R., Daluiski, A., Stevenson, S., Wu, L., McAllister, P., Lee, Y.P., Kabo, J.M., Finerman, G.A., Berk, A.J., and Witte, O.N. 1999. The effect of regional gene therapy

with bone morphogenetic protein-2-producing bone-marrow cells on the repair of segmental femoral defects in rats. *J Bone Joint Surg Am* 81:905-917.

267. Moutsatsos, I.K., Turgeman, G., Zhou, S., Kurkalli, B.G., Pelled, G., Tzur, L., Kelley, P., Stumm, N., Mi, S., Muller, R., et al. 2001. Exogenously regulated stem cell-mediated gene therapy for bone regeneration. *Mol Ther* 3:449-461.

268. Kuroda, R., Usas, A., Kubo, S., Corsi, K., Peng, H., Rose, T., Cummins, J., Fu, F.H., and Huard, J. 2006. Cartilage repair using bone morphogenetic protein 4 and muscle-derived stem cells. *Arthritis Rheum* 54:433-442.

269. Peng, H., Usas, A., Olshanski, A., Ho, A.M., Gearhart, B., Cooper, G.M., and Huard, J. 2005. VEGF improves, whereas sFlt1 inhibits, BMP2-induced bone formation and bone healing through modulation of angiogenesis. *J Bone Miner Res* 20:2017-2027.

270. Nakamura, Y., Tensho, K., Nakaya, H., Nawata, M., Okabe, T., and Wakitani, S. 2005. Low dose fibroblast growth factor-2 (FGF-2) enhances bone morphogenetic protein-2 (BMP-2)-induced ectopic bone formation in mice. *Bone* 36:399-407.

271. Itoh, K., Udagawa, N., Katagiri, T., Iemura, S., Ueno, N., Yasuda, H., Higashio, K., Quinn, J.M., Gillespie, M.T., Martin, T.J., et al. 2001. Bone morphogenetic protein 2 stimulates osteoclast differentiation and survival supported by receptor activator of nuclear factor-kappaB ligand. *Endocrinology* 142:3656-3662.

272. Kaneko, H., Arakawa, T., Mano, H., Kaneda, T., Ogasawara, A., Nakagawa, M., Toyama, Y., Yabe, Y., Kumegawa, M., and Hakeda, Y. 2000. Direct stimulation of osteoclastic bone resorption by bone morphogenetic protein (BMP)-2 and expression of BMP receptors in mature osteoclasts. *Bone* 27:479-486.

273. Boyle, W.J., Simonet, W.S., and Lacey, D.L. 2003. Osteoclast differentiation and activation. *Nature* 423:337-342.